Faculty of Health Science
Department of Pharmacy
Drug Transport and Delivery Research Group

Chitosan Lecithin Nanoparticles with New Chemical Entity

Antimicrobial Evaluation

—

Lisa Myrseth Hemmingsen
Master thesis in Pharmacy, May 2015

SUPERVISORS
Professor Nataša Škalko-Basnet
Doctor Gry Stensrud

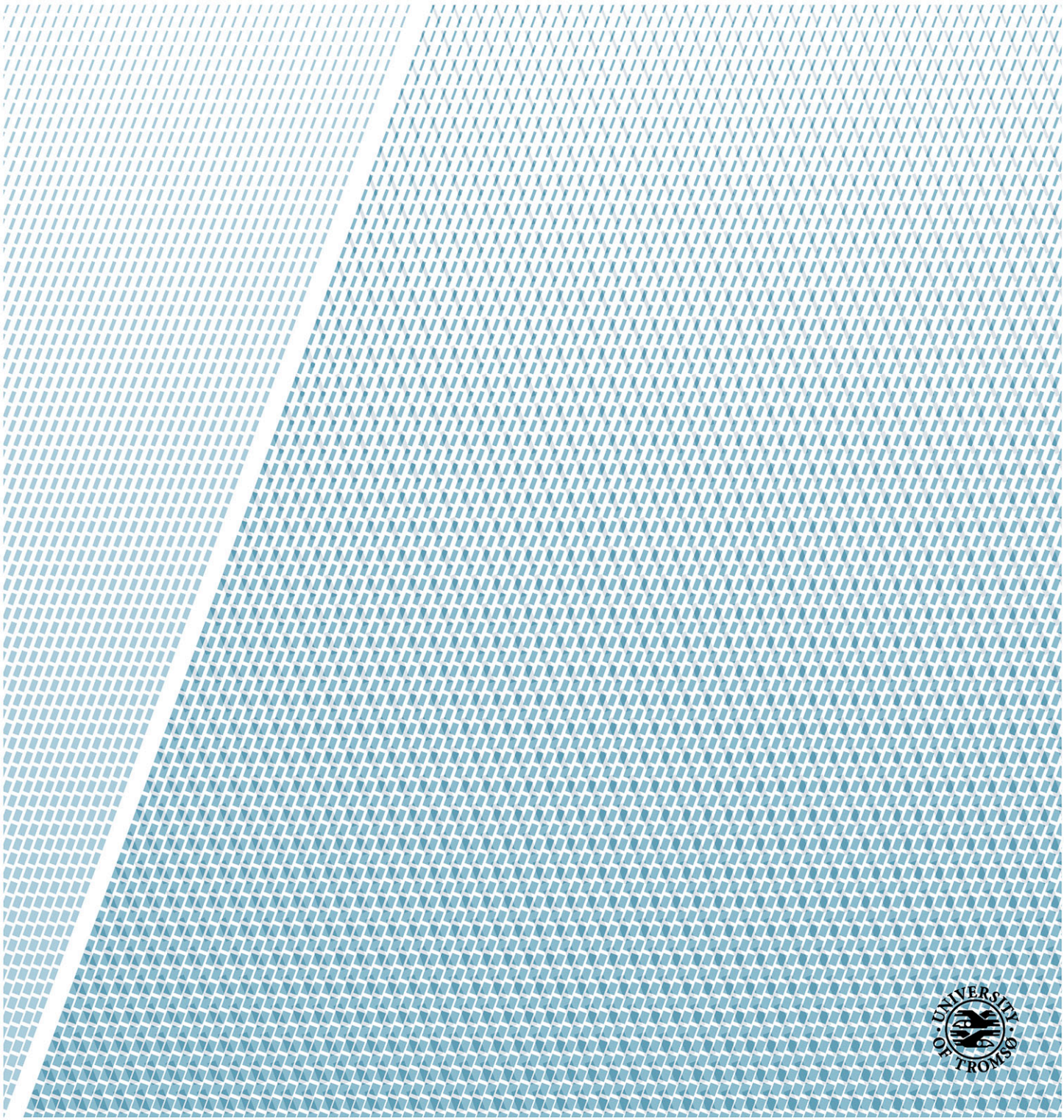

MATER THESIS FOR THE DEGREE MASTER OF PHARMACY

CHITOSAN LECITHIN NANOPARTICLES WITH NEW CHEMICAL ENTITY

ANTIMICROBIAL EVALUATION

BY

LISA MYRSETH HEMMINGSEN

MAY 2015

SUPERVISORS

Professor Nataša Škalko-Basnet

and

Gry Stensrud, Vice President Technical Development and Operations,
Photocure ASA

Drug Transport and Delivery Research Group

Department of Pharmacy

Faculty of Health Sciences

The University of Tromsø – The Arctic University of Norway

Acknowledgements

The work presented in this master thesis was carried out at Drug Transport and Delivery Research Group, Department of Pharmacy, The University of Tromsø, The Arctic University of Norway during the period form October 2014 to May 2015. During this period I have received help and encouragement from a lot of people.

First of all I would like to express my deep and sincere gratitude to my supervisor, Professor Nataša Škalko-Basnet, for the continuous and outstanding guidance and encouragement throughout the whole extent of the project. This support inspired me to strive for the best and opened my mind to a great and copious world of research and opportunities. Thanks to your sharing your endless knowledge, this have inspired me to hunger for even more knowledge and given me a strong desire to broaden my horizons.

I also want to thank my other supervisor, Doctor Gry Stensrud at Photocure ASA, for guidance and a great collaboration in this project. I would like to express my gratitude to both Gry and Photocure ASA for giving me the opportunity to work with this cutting-edge project with great challenges and a lot of possibilities.

I would like to thank the Drug Transport and Delivery Research Group for creating a great environment for this master project. Especially thanks to Associate Professor Ann Mari Holsæter and Ph.D. students Sveinung G. Ingebrigtsen, Elenaz Naderkhani and May Wenche Jøraholmen for sacrificing your valuable time to help me in the laboratory.

Many thanks to our great engineer Cristiane de Albuquerque Cavalcanti Jacobsen for all your technical help and the moral support you gave when there were struggles in the laboratory.

I would like to direct my appreciation to Associate Professor Pål J. Johnsen, Julia Kloos and the rest of the research group Microbial Pharmacology and Population Biology Research Group for your contribution to this project and for letting me work in your laboratory during this project.

Mohammed Al-Haroni, Associate Professor from the Department of Clinical Dentistry, I am grateful for your guidance and all the discussions during the microbial work in this project.

My appreciation further goes to Professor Morten Bøhmer Strøm, Professor Einar Jensen, Associate Professor Terkel Hansen, Ph.D. Elizaveta Igumnova and Senior Engineer Trude Anderssen in the research group Natural Products and Medicinal Chemistry for your guidance and advises.

Thanks to Elizabeth G Aarag Fredheim for providing the bacterial strains for this project and sharing your knowledge about these strains. This is highly appreciated.

Thanks to Chitinor AS for providing the chitosan for this project.

I would also like to thank my fellow master students in the Drug Transport and Delivery Research Group, Iren Wu, Kristina Rybak, Irja Kjærvik and Ayantu Chemeda, for your support and all the good talks during this master project. In addition, thanks to my fellow students at the Department of Pharmacy for all these unforgettable years. I will never forget my time here with you.

Finally, my deepest and sincerely gratitude goes to my family for the support your have given me during my time at the university. Thank you for believing in me and always being there for me.

- *Lisa Myrseth Hemmingsen, May 2015*

Table of contents

List of Figures

List of Tables

Abstract

Chronic wounds are often colonized with biofilm-producing bacteria, such as *Staphylococcus epidermidis*, and these wounds often have high degree of complexity and are often challenging to treat. There is a high resistance to the traditional antimicrobial treatments and that is why these infections sometimes are persistent. Photodynamic therapy (PDT) is proposed as a potential solution to the problems of biofilm wound infection. A New Chemical Entity (NCE) together with chitosan lecithin nanoparticles were investigated for potential biofilm elimination. The NCE was entrapped in particles (approximately 350-400 nm) and this resulted in approximately 12 % entrapment. The zeta potential of the NCE-containing nanoparticles was measured to be approximately 10 mV at a pH of just below 3. To evaluate the antimicrobial effect of the NCE in a free form and the NCE-containing nanoparticles the biofilm elimination studies were carried out in both planktonic bacteria and bacteria in biofilm. When investigating the activity of NCE in a free form the concentrations corresponding to the 1x MIC, 2x MIC and 3x MIC and the exposure to light were used in both planktonic bacteria and biofilm. The bacterial elimination was minimal, but in some of the strains, a tendency towards reduction of the biofilm was observed. Evaluation of the antimicrobial effects of the NCE-containing nanoparticles was carried out in the biofilm testing at NCE concentrations of 0.01, 0.1 and 1 mM and light exposure. The biofilm elimination was minimal here as well, but in one of the strains (RP62A) an indication of a potential effect was observed. In addition to evaluation of the NCE exposed to light, an assessment of the NCE without light exposure and empty nanoparticles was performed.

The NCE showed a potential as a photodynamic agent, but the biofilm testing conditions need to be optimized prior to further studies.

Keywords: photodynamic therapy; chronic wounds; biofilm; drug delivery system; nanoparticles

Sammendrag

Kroniske sår er ofte koloniserte med biofilm-produserende bakterier, som for eksempel *Staphylococcus epidermidis,* og disse sårene innehar ofte en høy grad av kompleksitet som gjør dem vanskelig å behandle. Den høye resistensen mot tradisjonell antibiotikabehandling er et kjent problem, noe som ofte er med på å gjøre disse infeksjonene langvarige. Fotodynamisk terapi er utpekt som en potensiell løsning på problematikken rundt biofilm-infiserte sår. Vi undersøkte det biofilm eliminerende potensialet til en ny kjemisk substans (NCE) i kitosan lecithin nanopartikler. NCE ble inkorporert i partiklene (ca. 350-400 nm), med en inkorporering på ca. 12 %. Zeta potensialet ble målt til rundt 10 mV ved pH rett under 3. For evalueringen av den antimikrobielle effekten av NCE i fri form og NCE i nanopartikler, ble det utført studier på biofilm-eliminering for både planktoniske bakterier og bakterier i biofilm. Effekten av NCE i fri form ble undersøkt i konsentrasjoner korresponderende til 1x MIC, 2 x MIC og 3 x MIC, og i kombinasjon med lys i planktoniske bakteriene og bakterier i biofilm. Graden av bakteriell eliminering var lav, men noen stammer viste en tendens til reduksjon av biofilmmassen. Antimikrobielle effekten av de NCE-holdige nanopartiklene ble utført med konsentrasjoner på 0,01, 0,1 og 1 mM NCE i kombinasjon med lys. Biofilm-elimineringen var lav også her, men i en stamme, RP62A, kunne man se en indikasjoner på NCSs biofilm-eliminerende potensialet. I tillegg til undersøkelse av NCE med lyseksponering, ble det også gjort en evaluering av NCE uten lyseksponering og av tomme nanopartikler.

NCE viser lovende effektivitet som en fotodynamisk substans, men testingen i biofilm må optimaliseres før dens potensialet kan undersøkes ytterligere.

Nøkkelord: fotodynamisk terapi; kroniske sår; biofilm; drug delivery systemer; nanopartikler

List of abbreviations

ALA = Aminolevulinic acid

aPDT = Antimicrobial photodynamic therapy

C/L = chitosan lecithin

EE = entrapment efficiency

ELISA = enzyme-linked immunosorbent assay

EUCAST = The European Committee on Antimicrobial Susceptibility Testing

FDA = US Food and Drug Administration

GRAS = Generally Recognized as Safe

HPLC = High-performance liquid chromatography

ica = intercellular adhesin

MIC = minimum inhibitory concentration

MRSA = methicillin-resistant *Staphylococcus aureus*

NCE = New Chemical Entity

NO= Nitric Oxide

NP = nanoparticle

OD = optical density

PCS = Photo correlation spectroscopy

PDT = Photodynamic therapy

PIA = polysaccharide intercellular adhesin

PLGA = poly(lactic-co-glycolide)

PpIX = Protoporphyrin IX

PS = Photosensitizer

PS/A = polysaccharide adhesin

QS = Quorum sensing

ROS = Reactive oxygen species

RR = relative recovery

TPGS = D-tocopheryl polyethylene glycol 100 succinate

TSB = tryptic soy broth

WHO = World Health Organization

1. General introduction

The skin is the largest organ of the body and holds a lot of important functions, such as protection from the environment (Sherwood, 2010). These protecting functions are essential to avoid diseases due to the environment around us, and the skin itself contains a large variety of microorganisms. This local environment of organisms is referred to as the skin microbiota and consists of bacteria, viruses, fungi and protozoa and exists on the skin due to the direct contact between the skin and the environment around. A fine balance between different bacteria is beneficial for the host and might prevent colonization by other microbes (Rosenthal *et al.*, 2011, Hannigan and Grice, 2013). When the skin barrier is disrupted, the skin loses its normal function and structure. Skin disruption initiates the wound healing process through four phases: haemostasis, inflammatory response, proliferation and remodelling (Enoch and Leaper, 2008). This process proceeds differently in different people and under diverse conditions. Wounds that heal within the expected amount of time, is referred to acute wounds. On the other hand, if the wound does not heal within a certain time frame due to an underlying problem, the wound is categorized as a chronic wound (Strodtbeck, 2001).

Chronic wounds are a major problem and difficulties in the treatment of these wounds are often experienced. In 2009, Sen *et al*. reported that 1-2 % of the population in developed countries will experience a chronic wound and that 2-4 % of the total health budget of Scandinavian countries is spent on the treatment of chronic wounds (Sen *et al.*, 2009). In addition to this, there is little consensus around the topic of antimicrobial treatment of infected, chronic wounds. It is often debated that the evidence of the effect is not strong enough (Høiby *et al.*, 2015). A reason for the problems regarding treatment of the infections is that some bacteria, like *Staphylococcus epidermidis*, form biofilms that often have reduced susceptibility towards our conventional antimicrobial substances. Biofilm is a confined environment constituted of extracellular polymeric substances, which is able to protect the bacteria against external factors and treatments (Percival *et al.*, 2012, Taraszkiewicz *et al.*, 2013). This problem has to be addressed, and a possible solution to the limitations of current antimicrobial therapy is the antimicrobial photodynamic therapy (aPDT).

aPDT is based on the action of a photosensitizer (PS) in combination with oxygen, when the PS is exposed to visible light that is corresponding to the absorption of the PS (Taraszkiewicz *et al.*, 2013, Cieplik *et al.*, 2014). This action will result in the formation of reactive oxygen species (ROS) that may cause damage to the microorganisms (Sharma *et al.*, 2012). The New Chemical Entity (NCE) of this project is a PS and a derivative of 5-aminolevulinic acid (5-ALA) that is naturally found in the body (Wachowska *et al.*, 2011).

There are some adverse effects associated with aPDT, such as pain and oedema, to mention a few (Morton *et al.*, 2008). This is often a reason to use a drug delivery system as carrier. In this project we used the chitosan lecithin nanoparticles (NPs) to overcome the issues related to possible adverse effect, but also to protect the NCE from degradation due to hydrolysis. These NPs, first described by Sonvico *et al*. (Sonvico *et al.*, 2006), are expected to have an antimicrobial effect on their own due to chitosan. This biodegradable and biocompatible polysaccharide is believed to exhibit the antimicrobial properties through different mechanisms (Blecher *et al.*, 2011, Liu *et al.*, 2011). In this project, the antimicrobial effect of both the NCE and the NPs was investigated and elucidated.

2. Introduction

2.1 The skin

The skin is the largest organ of the body, and it covers an area of approximately 1.95 m^2 in an average adult. There are many important functions of the skin, amongst these protection from the environment from e.g. pathogens, chemicals and physical trauma (Sherwood, 2010). Other functions include maintaining the fluid balance and body temperature, recognizing the environment and vitamin D metabolism (Irvine, 1991, Sherwood, 2010). The skin consists of two layers, the innermost is called dermis and the outermost is called epidermis as seen in **Figure 1**. On top of the epidermis is the *stratum corneum* that acts as a protective layer (Sherwood, 2010).

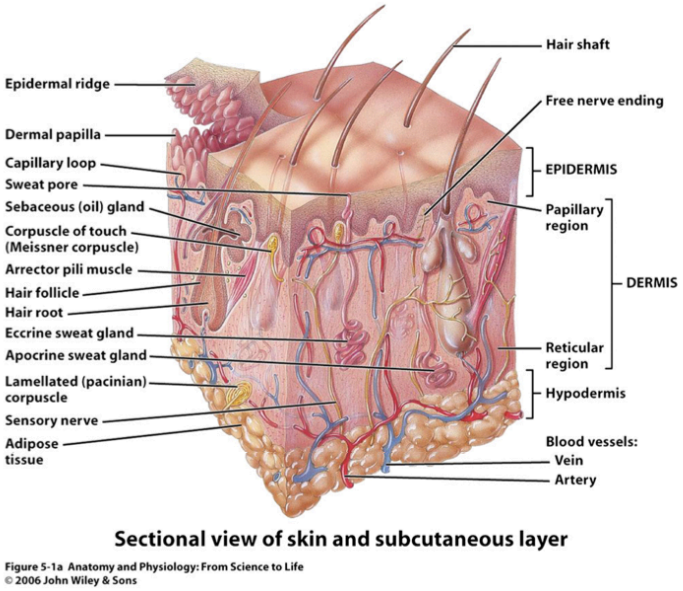

Figure 1. The structure of the skin. Shown here is the epidermis, dermis and hypodermis (with permission) (Jenkins *et al.*, 2006).

2.1.1 Epidermis

Epidermis is rapidly renewing and it is divided into three layers, the basal layer, the spinous layer and the granular layer, starting from dermis and moving upwards to the *stratum corneum*. This layering is illustrated in **Figure 2**. The epidermis has no blood supply directly connected to it, but it is supplied through diffusion of nutrients from the dermis that contains a

network of its own (Sherwood, 2010, Baroni *et al.*, 2012). Keratinocytes are the predominant cell type in the epidermis (Wickett and Visscher, 2006). They can be found in every layer of the epidermis, and when the keratinocytes die, they form the protective layer on the surface, the keratinized layer. These cells are connected by desmosomes which are interconnected intracellular keratin filaments (Sherwood, 2010). This is what makes the *stratum corneum* such an effective barrier of protection. In the *stratum corneum* the keratinocytes are transformed to corneocytes when the cell nucleus is digested, the cytoplasma of these cells is removed, lipids move to the intercellular space, microfiberils are created and a cell envelope replaces the original membrane. Cross-linked proteins with lipids constitutes this envelope (Wickett and Visscher, 2006).

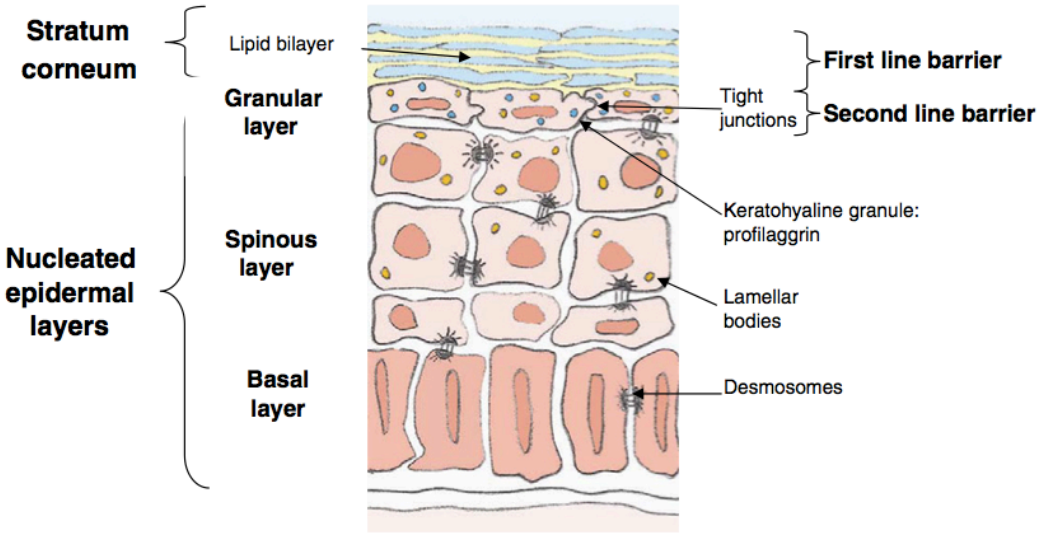

Figure 2. Structure of the epidermis. Shown are the *stratum corneum*, granular layer, spinous layer and the basal layer (Baroni *et al.*, 2012).

2.1.2 Brick and mortar model and skin penetration

The *stratum corneum* is often described as bricks and mortar model, where the corneocytes are the hydrophilic bricks and the lipid area around the corneocytes is the hydrophobic mortar (**Figure 3**). The mortar consists mainly of ceramides, cholesterol, cholesterol esters and long-chain fatty acids (Wickett and Visscher, 2006, El Maghraby *et al.*, 2008). This structure gives rise to the different routes of penetration through the skin. Two possibilities for skin penetration are often described. The first is the macro route, which involves the penetration through hair follicles, sebaceous glands, sweat glands or trans-epidermal. The second route is

the micro route, which build on the brick and mortar model. This route is divided in two different pathways, the intercellular pathway and the transcellular pathway. Penetration through the lipid layer is called the intercellular pathway, and penetration through the corneocytes and the lipid rich layer is called the transcellular pathway (Barry, 1991).

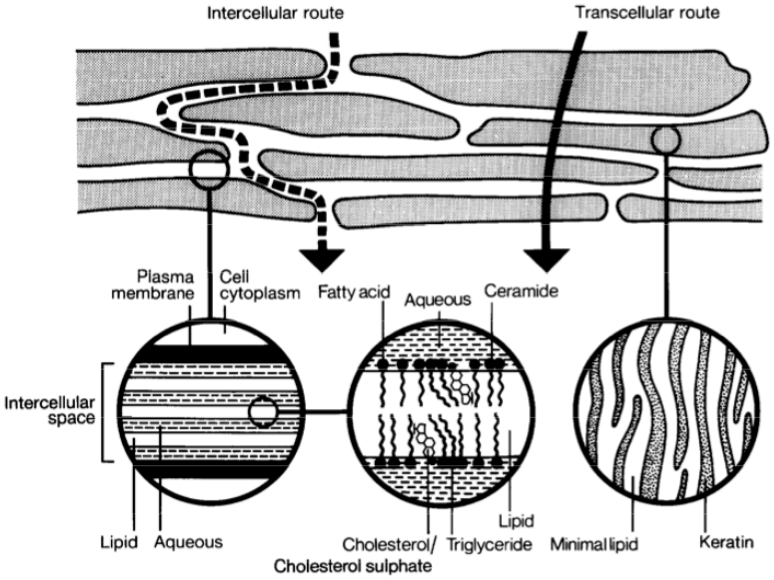

Figure 3. **Routes through the human skin with both the intercellular route and the transcellular route** (Barry, 1991).

2.1.3 Dermis

The dermis is the more vascular skin layer beneath the epidermis, and this is, as mentioned before, the layer that ensures a steady blood supply to the epidermis. This layer is also providing an anchor point for the epidermis. The main structural components of the dermis are elastin, which gives the skin the possibility to convert back to its original shape after stretching, and collagen, which provides strength to the skin. Every cell that is going to or leaving the epidermis has to cross the dermis, and this makes the dermis a guard for the epidermis (Spellberg, 2000). Dermis is also divided, but it is divided into two different layers. The outermost layer is the papillary layer, and this layer contains many blood vessels and nerve endings. Underneath the papillary layer lays the reticular layer of the dermis that is anchored to the subcutis (Lai-Cheong and McGrath, 2013).

2.2 Microbes

It is important that the skin provides a good protection from the environment, because the skin itself is the settlement of a lot of bacteria and other microorganisms. Even though these microorganisms might be the cause of chronic wound infections, some of them are important to maintain a stable condition on the skin where colonization of some bacteria is avoided.

2.2.1 Bacteria

Bacteria are often classified into two groups, as Gram-negative or Gram-positive bacteria. This classification is based on the work of Hans Christian Gram, who in 1884 discovered that there was a difference between some bacteria. Some of the bacteria would stain and exhibit a blue-violet colour when he added crystal violet complexed with iodine to the bacteria and then washed them with alcohol. These bacteria he called Gram-positive bacteria. Other bacteria would not stain, but were counterstained with safranin or carbolfuchsin to gain a pink colour. These bacteria he called Gram-negative bacteria (Yazdankhah *et al.*, 2001).

The difference between these bacteria is their cell wall and the arrangement of the wall (**Figure 4**).

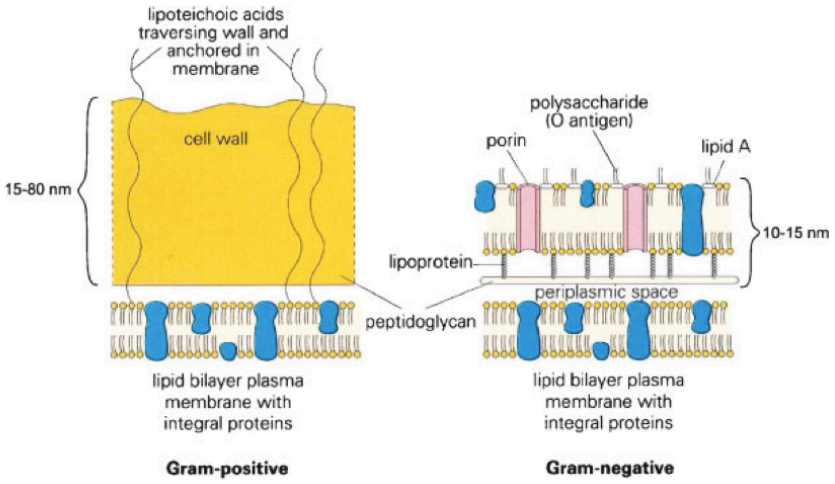

Figure 4. The structure of the cell wall of Gram-positive and Gram-negative bacteria (Jori *et al.*, 2006).

Gram-positive bacteria have a thick wall of peptidoglycan consisting of approximately 100 units. Peptidoglycan is composed of cross-linked N-acetylglucosamine and N-acetylmuramic acid in repeating units (Hanson and Neely, 2012). Another structure in the peptidoglycan

layer is teichoic acids, where wall teichoic acid is bounded to the peptidoglycan layer and stretches throughout the layer and the lipoteichoic acid that is embedded in the plasma membrane (Swoboda *et al.*, 2010). Underneath the peptidoglycan layer the bilayer lipid membrane is found (Hanson and Neely, 2012).

Gram-negative bacteria have a thinner peptidoglycan layer than the Gram-positive bacteria. In the envelope of the Gram-negative bacteria there are three main structures: the outer membrane, the peptidoglycan layer and the cytoplasmic membrane. The outer membrane mainly consists of phospholipids and lipopolysaccharide. The outer membrane serves as a protective layer for the bacteria and the porins in the membrane hinder the permeation of molecules above 700 Da (Silhavy *et al.*, 2010). In between the outer and inner membrane, the periplasmic space can be found. This is an aqueous compartment consisting of proteins (Jori *et al.*, 2006, Silhavy *et al.*, 2010).

2.2.2 Microbial spectrum of the skin under normal conditions

The skin has a diverse and complex composition of microorganisms, and the environment these organisms create is referred to as the microbiota (Hannigan and Grice, 2013). Bacteria, viruses, fungi and protozoa are the microorganisms that can be found on the human skin, as a result of the skin being in direct contact with the environment and its microorganisms (Rosenthal *et al.*, 2011). It is a fine balance between the host and the different bacteria on the skin, and a small interruption of this balance might cause infection. (Grice and Segre, 2011). The fine balance between the different bacteria also plays important role. The microbiota prevents the colonization of certain bacteria, so the chance of occupation and infection of pathogenic or opportunistic bacteria is less likely (Hannigan and Grice, 2013). Commonly we divide the microbiota into two different groups: the resident microbes and the transient microbes. The resident microbes are often viewed as commercial microbes that can be often find on the skin of humans. Then are recognized as not harmful and may give the host some advantages. They are also often able to re-establish after small changes in their environment. The transient microbes are not the established microbes on the skin, but can appear on the skin from the environment and stay there for hours or days. None of these types of microbes are pathogenic under normal conditions where the immune status functions normally, the status of hygiene is good and the skin is not damaged. If this is not the case, they might be able to colonize and cause infections. The bacteria used in this project are an example of a

bacteria normally considered to have a low pathogenic potential. *Staphylococcus epidermidis* is found on the human skin and may provide some benefits for the host, but is able to an infection if the host have some other complications like diabetes or has an impaired immune system (Kong and Segre, 2012).

The various parts of the body do not contain the same type of bacteria, neither the same amount of different bacteria. This is illustrated in **Figure 5**. The most abundant genera of bacteria found on the skin are *Staphylococcus*, *Propionibacterium* and *Corynebacterium* (Hannigan and Grice, 2013). Other publications describes the most abundant phyla on the human skin as *Actionobacteria*, *Firmicutes, Bacteroidetes* and *Proteobacteria* (Grice and Segre, 2011). Even though these are the most abundant genera, the variation is wide and the microbiota of a host is influenced by the age, gender, location, occupation, the use of antibiotics, hygiene and other factors. In moist areas *Staphylococcus spp.* and *Corynebacterium spp.* are abundant, while in drier areas the variability amongst the different phyla is larger (Grice and Segre, 2011).

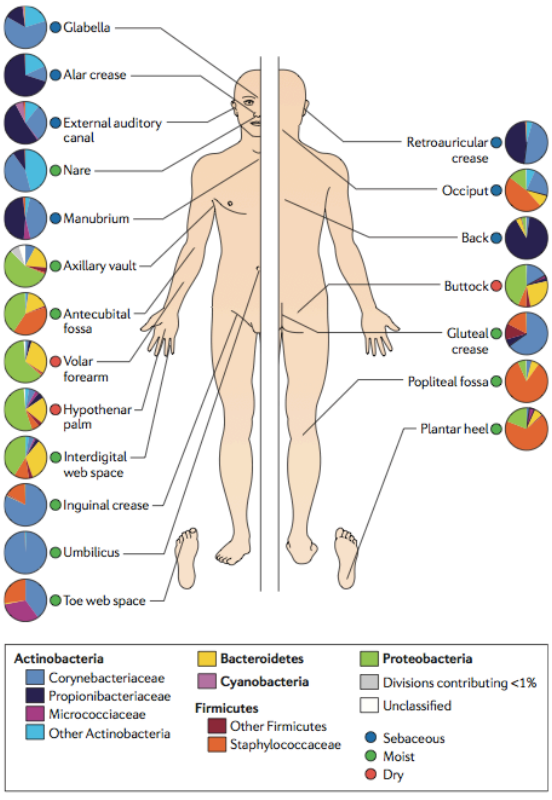

Figure 5. Representation of the distribution of skin bacteria according to Grice, E. A. *et al.* (Grice and Segre, 2011).

2.2.3 Microbial spectrum of wounded skin

When the skin barrier is broken the possibility for colonization of both pathogenic and non-pathogenic microorganisms is large. The three key sources of microorganisms are the environment around us, the skin in the area of the wound and endogenous sources involving mucous membranes. The danger of infection occurs when the number of microorganisms is sufficiently large (Bowler *et al.*, 2001). The development of a wound infection depends on different factors such the number of microorganisms, as mentioned, and the number of variants of microorganisms and, the pathogenicity the microorganisms present in the wound (Gardner and Frantz, 2008). Some bacteria affect the growth of other bacteria, either in a positive or negative way and this is why the variation of bacteria might be an actuating factor (Bowler *et al.*, 2001).

There is no agreement around what are the most common bacteria in wounds. Many of the findings vary, often due to the method of sampling or analysing. The bacteria often reported are *Staphylococcus aureus, Staphylococcus epidermidis*, *Streptococcus spp., Pseudomonas aeruginosa*, *Enterococcus spp.*, *Peptostreptococcus spp.* and *Bacteroides spp.* (Bowler *et al.*, 2001, Gardner and Frantz, 2008). Still some bacteria are often not detected in the analysis due to the fact that they are harder to grow or the growing is time consuming (Bowler *et al.*, 2001). Price *et al*. published a study on the microbiota of chronic wounds (Price *et al.*, 2011). They enrolled 12 patients with a total of 13 chronic wounds and collected the tissue with a curette. They used 16S rRNA-based pyrosequencing analysis. They were able to characterize 58 bacterial families, and the most common families in these samples were *Staphylociccaceae, Pseudomonadaceae, Stretococcaceae, Clostridiales Family XI* and *Enterobacteriaceae.*

2.2.4 Biofilm formation

Even though there are many different bacteria on the skin and there is not a full consensus about location and presence of certain bacteria on the skin, some of them generate infection from time to time. *Staphylococcus epidermidis* is one of the bacteria considered to have a low pathogenicity, but certain bacteria, like *Staphylococcus epidermidis*, are able to aggregate and form a biofilm. A biofilm is a confined environment constituted of extracellular polymeric substances, like proteins, lipids, polysaccharides and extracellular DNA (Percival *et al.*, 2012, Taraszkiewicz *et al.*, 2013). It is common that this encasement grows on medical implants,

but bacteria are also able to form biofilms on the skin and it is suggested that biofilm might be one of the large contributors to chronic wounds (Mah and O'Toole, 2001, Percival *et al.*, 2012). Biofilms are either composite by single specie or multiple species. The biofilms composited by multiple species are more often found naturally (Zhao *et al.*, 2013).

The formation of a biofilm is often divided into five steps, as seen in **Figure 6**. The first step in the process is the formation of a film on the surface where the biofilm is to attach. This film allows the bacteria to attach to the surface tight enough, which is the second step in a biofilm formation. After the bacterial attachment to the surface, the production of the material of the biofilm is initiated. This is the production of the extracellular polymeric substances. After this process is initiated, the maturation of the biofilm is initiated and the bacteria are embedded into the matrix as more species are recruited to the maturing biofilm. Another aspect of the progression of the biofilm is detachment of bacteria from the biofilm. This is a process that enhances the survival of the bacteria and allows the bacteria to disseminate (Zhao *et al.*, 2013, Vanysacker *et al.*, 2014).

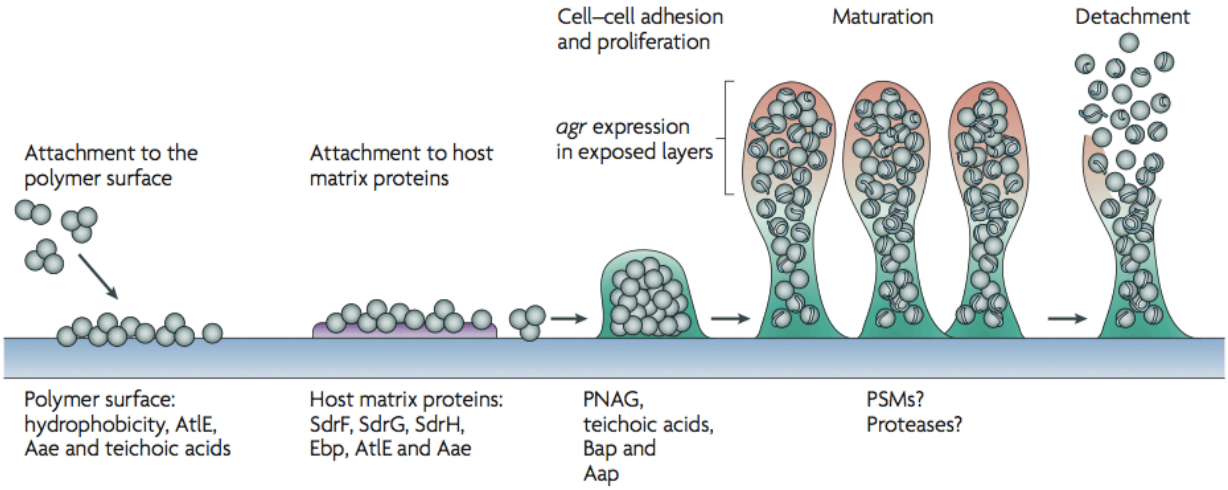

Figure 6. The formation of biofilm from the adhesion of the planktonic cells, through the proliferation, to the maturation of the film (Otto, 2009).

Formation of biofilm is regulated through multiple mechanisms, but the most investigated mechanism is quorum sensing (QS). QS is a communication mechanism with the release and recognition of chemical substances by the bacteria (Taraszkiewicz *et al.*, 2013).

The biofilm makes the bacteria more resistant to the more traditional treatment methods of bacterial infection, but the mechanisms behind this resistance are not fully understood. There are mainly three mechanisms that are used to explain this process. The first explanation is that the biofilm is acting as a blockage for the antimicrobial substances of both a physical and a chemical character. The substance is not able to penetrate the biofilm as efficiently. The second explanation is that the metabolic state of the bacteria is lowered and many of the antimicrobial substances aim for dividing bacteria or bacteria in an active metabolic state (Taraszkiewicz *et al.*, 2013, Zhao *et al.*, 2013). The last factor concerns the genetic diversity in the biofilm. This diversity might lead to a higher rate of mutation in the environment of the biofilm. Bacteria that are not limited by the antimicrobial substances or other normal limiting factors may exist in the biofilm, making the fight against infections difficult (Taraszkiewicz *et al.*, 2013).

When the biofilm has matured, the strategy of survival of the bacteria and maintenance of the infection is detachment of a cluster from the biofilm. This detachment gives a spreading of the bacteria and enhances the possibility of a persisting infection (Zhao *et al.*, 2013). This is another reason why the biofilm-producing bacteria are difficult to fight off.

2.2.5 Staphylococcus epidermidis

Staphylococcus epidermidis is Gram-positive cocci common amongst other, on the human skin able to create biofilms. It is also coagulase-negative staphylococci meaning that it does not produce the enzyme coagulase. This enzyme converts fibrinogen to fibrin. It is not considered very virulent, but due to its ability to produce a biofilm, it is able to cause infections and induce to the host great skin complications (Huebner and Goldmann, 1999, Otto, 2009).

Even though *Staphylococcus epidermidis* has a low virulence, it has been reported that rather than inducing an acute infection it leads to a chronic infection, which can be hard to treat (Otto, 2009).

2.2.6 Biofilms formed by Staphylococcus epidermidis

Staphylococcus epidermidis is often found in biofilms in the wounds, but also in biofilms on the medical devices like catheters, pacemakers and implants. It is not only *Staphylococcus epidermidis* that produces biofilms; *Staphylococcus aureus* and *Pseudomonas aeruginosa* also form biofilms (Darouiche, 2001, Cramton and Götz, 2004). The steps of the biofilm formation of *Staphylococcus epidermidis* are as the steps described above. *Staphylococcus epidermidis* adhere to the surface by adhesins, such as capsular polysaccharide adhesin (PS/A) and autolysin. Another important adhesin is the polysaccharide intercellular adhesin (PIA) responsible for the cell-to-cell adhesion inside the biofilm. PIA is produced by intercellular adhesin (ica) A, B, C and D in different steps. icaR regulates this process (Darouiche, 2001, Cramton and Götz, 2004, Cooper *et al.*, 2014). Other factors affect the biofilm production of *Staphylococcus epidermidis*, but the ones mentioned above are amongst the most widely studied.

2.2.7 Biofilm models

There are many research reports on the biofilm-infections and a lot of work has been done to simulate the natural biofilm and to test new anti-biofilm strategies. The complexity of a natural biofilm is often high and hard to mimic. *In vitro* biofilm models are sometimes divided into two groups, so called closed and open systems according to the nutritional availability. Closed systems refer to the batch cultures and the open describes the continuous cultures. The main focus in our work was on the closed systems. The agar plate methods are amongst the simplest of the models used in the formation of biofilm (McBain, 2009). The Congo red agar method is amongst the most studied of the agar plate methods. Freeman *et al*. first described this method in 1989 and the method was able to show positive results by a colour change (Freeman *et al.*, 1989). The medium of choice was brain heart infusion broth with Congo red strain. The brain heart infusion broth was supplemented with 5 % sucrose. The detected colour variation is due to the ability of Cargo red to change colour when in contact with lipoproteins or other macromolecules (Cangelosi *et al.*, 1999). Even though this method was reported as a sensitive method when first published, other scientists later stated that this method lacked sensitivity (Mathur *et al.*, 2006).

Other closed methods described are the microtiter plate methods (McBain, 2009); such as the tissue culture plate method (Christensen *et al.*, 1985) and the Zürich model (Guggenheim *et al.*, 2001) In this project, the method described by Christensen *et al*. in 1985 was used in the biofilm preparation. Here the bacteria is diluted 1:100 in tryptic soy broth (TSB) and incubated on polystyrene microtiter plates. The plates are stained with crystal violet after incubation and the optical density (OD) is measured using enzyme-linked immunosorbent assay (ELISA) reader (Christensen *et al.*, 1985). The Zürich biofilm model also involves the use of a polystyrene microtiter plate. Hydroxyapatite discs are placed in the microtiter plate incubated with saliva. The saliva is replaced with a mixture of saliva, modified fluid universal medium and glucose. For example, oral bacteria were added to the wells and incubated anaerobically (Guggenheim *et al.*, 2001).

Christensen *et al*. also developed a method for biofilm formation in tubes (Christensen *et al.*, 1982). In this method, they also used TSB supplemented with glucose as medium. The bacteria were incubated for 24 hours at 37 °C and strained. A film lining the inner surface of the tube indicated positive results for biofilm formation. The bacteria were studied using electron microscopy (Christensen *et al.*, 1982). This method is quite easy, but still highly sensitive and specific is reported (Oliveira and Cunha M. de, 2010).

Even though the main focus of this project was on the closed methods, some of the open models need to be mention such as the flow cell model, the modified Robbins device and the constant depth film fermenter. The flow cell model is based on the flow of a culture fluid sent form a reservoir to a flow cell. This model allows real-time observation of the biofilm. The modified Robbins device is also based on the flow of a fluid through a chamber, but there the biofilm is grown on the end of pegs or coupons (McBain, 2009, Pratten and Ready, 2010). In the constant depth film fermenter, the biofilm is grown on pegs in sampling pans placed on a rotatable table. The feeding of the biofilm is in a drip-wise fashion and waste is let out in an outlet in the bottom (Norwood and Gilmour, 2000, McBain, 2009).

2.2.8 Vancomycin

In the testing in the biofilm models, controls are needed to investigate if a new chemical substance has the desired effect. It is often difficult to choose the right type of antimicrobial

substance due to the difficulties related to treating a biofilm. For this project, three antibiotics were chosen as the controls, namely vancomycin, chloramphenicol and ciprofloxacin.

Vancomycin was originally isolated from *Amycolatopsis orientalis* and is classified as a glycopeptide antibiotic. The weight of vancomycin is around 1500 Daltons. As an antibiotic, it inhibits the cell wall synthesis of bacterial cells. It inhibits the synthesis of peptidoglycan by making complex with D-alanyl-D-alanine part of the peptide precursor and derby preventing the polymerization of peptidoglycan (Wilhelm and Estes, 1999, Arthur, 2010). Vancomycin is mostly effective against Gram-positive bacteria and has limited effect against Gram-negative bacteria due to the size of the molecule. The size prevents its crossing the membrane of Gram-negative bacteria (Diekema *et al.*, 1999, Wilhelm and Estes, 1999). This size might also be a problem when treating biofilm infections. Even though vancomycin is effective against a lot of the Gram-positive bacteria, resistance against this antibiotic has been reported. Resistance in *Staphylococcus haemolyticus* and *Staphylococcus aureus* has been showed, in addition to the appearance of decreased susceptibility towards vancomycin amongst *Staphylococcus epidermidis*. Intermediate resistance of *Staphylococcus* was shown as early as 1987 (Schwalbe *et al.*, 1987, Hiramatsu *et al.*, 1997, Hiramatsu, 1998, Garrett *et al.*, 1999). *Enterococcus spp*. has also shown resistance towards vancomycin and a high resistance pattern was shown early (Leclercq *et al.*, 1988). New options to treat infections are needed due to the increased resistance shown in several bacteria. Herewith the photodynamic treatment might be a good alternative to prevent that normal infections and biofilm infections.

2.2.9 Chloramphenicol

Chloramphenicol was first named chloromycetin and came from *Streptomyces* (Ehrlich *et al.*, 1947), and have a molecular weight of 323.1 g/mol (Cho *et al.*, 2015). The mechanism of action of the antibiotic is through the inhibition of the protein synthesis. More specifically, it will bind the large subunit of the peptidyl transferase centre A site in bacteria. This inhibits the binding of tRNA. The activity of chloramphenicol is broad, and it is effective against a variety of both Gram-positive and Gram-negative bacteria (Anderson *et al.*, 2012a).

2.2.10 Ciprofloxacin

Ciprofloxacin is a fluoroquinolone antibiotic with a molecular weight of 331.1 g/mol and it is effective against different Gram-positive and Gram-negative bacteria (Shah, 1991,

Bouyarmane *et al.*, 2015). The mode of action of ciprofloxacin is inhibition of the DNA synthesis. Quinolones bind to topoisomerase IV or DNA gyrase and interfere with the relaxing of the chain in the started synthesis (Anderson *et al.*, 2012b).

2.3 Wounds and wound healing

2.3.1 Wounds

Wounding of the skin is defined as the condition when the integrity of the skin is damaged and the skin barrier is disrupted. The functionality of the skin is changed and the original structure of the skin is altered (Enoch and Leaper, 2008). Wounds are often classified as acute or chronic. Acute wounds are wounds that heal within an expected amount of time. Chronic wounds are the wounds that do not heal properly because of an underlying complication and the healing process exceeds the expected period. The underlying are regarded as factors that enhance the complexity of the wound (Strodtbeck, 2001). In addition, the biofilm also affects the wound healing making it even more complex.

Several lines of research suggest that these definitions (acute and chronic wounds) do not cover the complexity of the different wound types and that both acute and chronic wounds might be difficult to treat. Ferreira *et al*. (Ferreira *et al.*, 2006) describes that some wounds can be complex wounds and these wounds can be either chronic or acute wounds. There is no single definition suitable, but they formulated some conditions that were necessary for categorization. Others have also discussed the factors concerning the complexity of wounds. These conditions to be considered are for example when a considerable amount of the skin is lost, the wound is infected, destruction of the skin to the level where the blood supplies might be altered or some form of pathology (Ferreira *et al.*, 2006, Boateng *et al.*, 2008).

2.3.2 Wound healing and skin repair

Wound healing is often divided into four phases: haemostasis, inflammatory response, proliferation and remodelling or scar maturation (Enoch and Leaper, 2008).

Haemostasis is the process when the skin is injured and the body tries to minimize blood loss. The mechanism to prevent this is initiation of vascular constriction. Platelets are recruited to the area of the wound, and they adhere to the injured vessel and collagen. In addition, there is

a release of cytokines, growth factors and several pro-inflammatory substances (Beldon, 2010). Fibrin clots form and plugs the blood vessel in addition to act as a temporary matrix that growth factors binds to and cells crawl on to (Shaw and Martin, 2009). The growth factors released in this step introduce chemotaxis of neutrophils, macrophages, smooth muscle cells and fibroblasts (Beldon, 2010).

In the inflammation response (**Figure 7**), cytokines, such as prostaglandins and histamine from the mast cells, are released to create a defence in the wounded area. This gives a local dilatation of the vessels and increased permeability. The monocytes are able to go into the wounded are due to this increased permeability. As another defence against infections, neutrophils are recruited to the wounded area. Their work is to ingest the bacteria to minimize the risk of infection. When the neutrophils have devoured the bacteria, they are removed. The line of defence is not completed with the neutrophils, because the macrophages continue the defence against the bacteria. The macrophages remove the remaining neutrophils, dead cells and other components not belonging in the wound bed. In addition, they recruit fibroblasts and smooth muscle cells (Beldon, 2010). The inflammatory cells generate nitric oxide (NO) and ROS. These compounds are also a part of the defence mechanisms of the skin (Shaw and Martin, 2009). Angiogenesis is a process that also takes place in wound healing. This process ensures the supply of blood to the wounded area by creating new vessels from the other accessible network around. Endothelial cells migrate to the area by following an angiogenic stimulus that is released from amongst other the macrophages already mentioned. The number of cells increases and then they are able to create these vessels (Auerbach *et al.*, 2003).

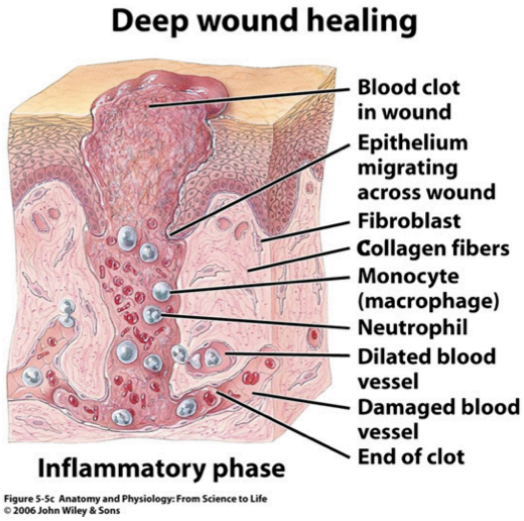

Figure 7. The inflammatory phase in wound healing (with permission) (Jenkins *et al.*, 2006)

The next step in the process is the proliferation of cells and granulation. The phases of inflammation and proliferation and granulation overlaps (Beldon, 2010). Fibroblasts, recruited by the macrophages, are the predominant cells in these phases (Enoch and Leaper, 2008). The extracellular matrix is partially produced by the fibroblasts, in context that they are responsible for the production of collagen and other components of the extracellular matrix. Collagen gives the wounded area strength (Strodtbeck, 2001). Extracellular matrix and collagen are components of the granulation tissue. The newly formed blood vessels, from the angiogenesis, stretch through the granulation tissue and create a network to provide nutrients (Enoch and Leaper, 2008).

Endothelial cells migrate on the edge of the wound in a leapfrog fashion (Enoch and Leaper, 2008). When cells climb over each other to be able to reach all the way into the wounded area to close the wound is referred to as leapfrogging (**Figure 8**). This continues until the cells reach the cells migrating from the other side and assure the close up of the area (Strodtbeck, 2001).

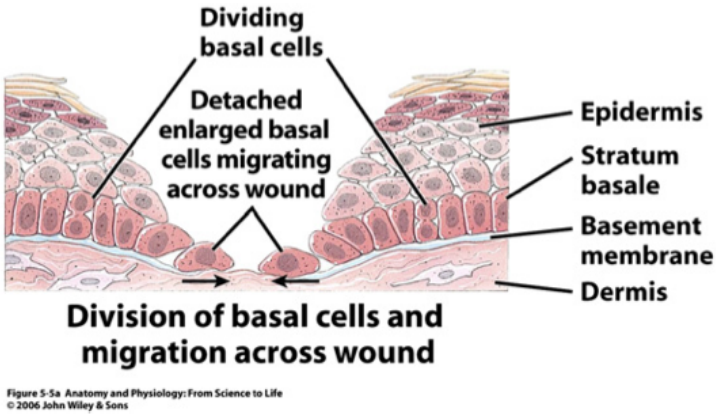

Figure 8. The reepithelialization of the wound bed showing the leapfrogging process (with permission) (Jenkins *et al.*, 2006).

Remodelling is the last phase in the process of wound healing (Enoch and Leaper, 2008). In this phase the wound is remodelled and matured (**Figure 9**) to establish a construction on the skin that is close to normal (Shaw and Martin, 2009). In this process, collagen is continuously broken down and rebuilt. Metalloproteinases break down the collagen under tight regulations (Enoch and Leaper, 2008). The inflammatory response also decreases as the wound heals. Via phagocytosis by the macrophages or apoptosis, the neutrophils are removed from the wounded area. Both the vascular system and the lymphatic system receives some macrophages, together with some neutrophils after the remodelling phase (Shaw and Martin, 2009).

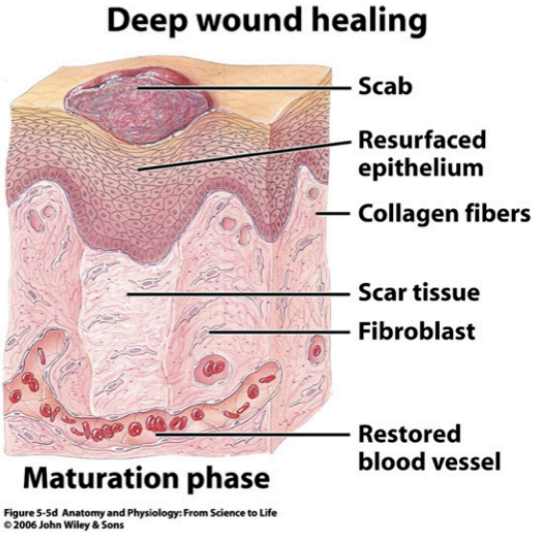

Figure 9. Maturation phase or remodelling of the wound bed (with permission) (Jenkins *et al.*, 2006).

2.3.3 Contaminated and infected wounds

Microorganisms exist all around and the contamination occurs in all wounds regardless of the condition of the wound. The human skin is the habitat of a variety of microorganisms where they exist in large amount abundantly. This makes it impossible to avoid contamination of the wounds and a may lead to a possible impaired healing. To minimize the bioburden it is important to keep the wound clean (Wysocki, 2002, Frank *et al.*, 2005). The degree of microbial growth and the extent of the microbial colonization are divided into four categories: contamination, colonization, critical colonization and infection (Frank *et al.*, 2005, Singh *et al.*, 2013).

Contamination of wounds is almost inevitable, but is not going to affect the wound healing process (Frank *et al.*, 2005, Singh *et al.*, 2013). Colonization of a wound does not initiate a reaction from the immune system, but presence of bacteria is higher. These bacteria replicate in the wound area (Singh *et al.*, 2013). Critical colonization occurs when the quantity of microorganisms in the wound further increases. This increase may affect the process of wound healing and could damage the tissue around the wound (Frank *et al.*, 2005, Singh *et al.*, 2013). Infection is described as the phase where the immune system responds to the microorganisms, but the microorganisms still manage to replicate to a sufficient quantity. Multiple factors influence the risk of infection, among these the condition of the host in addition to nutritional status (Frank *et al.*, 2005).

2.4 Photodynamic therapy

The demand for new ways to treat complex wounds and other skin infections are increasing with the increasing resistance in the microorganism in our environment. Photodynamic therapy (PDT) might be a solution to this escalating problem. PDT is a treatment method continuously studied to battle different diseases, but it is currently mostly used for the treatment of cancer and infections. This type of therapy has been tested on e.g. *Streptococcus mutans, Enterococcus faecalis, Candida albians, Staphylococcus aureus, Pseudomonas aeruginoa* and other. In addition, it is also tested for many types of cancer and there has been made photosensitizers for e.g. lung cancer, biliary duct carcinoma, colon cancer, skin cancer, prostate cancer and more (Agostinis *et al.*, 2011, Sharma *et al.*, 2012, Cieplik *et al.*, 2014).

To initiate this kind of therapy, three components are required: a photosensitizer (PS), light and oxygen (Taraszkiewicz *et al.*, 2013). The light used is visible light of a wavelength corresponding to the absorption of the PS (Cieplik *et al.*, 2014). The PS becomes excited by the absorption of light and as an end result two types of cellular damage are seen: damage to the DNA and oxidative modifications of biomolecules (Maisch *et al.*, 2011, Taraszkiewicz *et al.*, 2013).

2.4.1 The photosensitizer (PS)

In the beginning of aPDT the same PS as applied in the treatment of cancer was used. The PS for cancer treatment, such as hematoporphyrin derivate, is clinically approved as Photofrin®. The metabolic product of aminolevulinic acid (ALA), protoporphyrin IX (PpIX), is also used as a PS for the treatment of skin cancer. Tetrapyrroles have been tested against cancer. These are the compounds as benzoporphyrin derivate and *m*-tetra(hydroxyphenyl)chlorin (Sharma *et al.*, 2012). Later these structures were modified to be more effective against bacteria. These modifications often involved changing the cationic charge and the hydrophilic properties of the structure to optimize it. Phenothiazine dyes like methylene blue and toluidine blue (**Figure 10**) in addition to modified porphyrins are also used in aPDT (Sharma *et al.*, 2012).

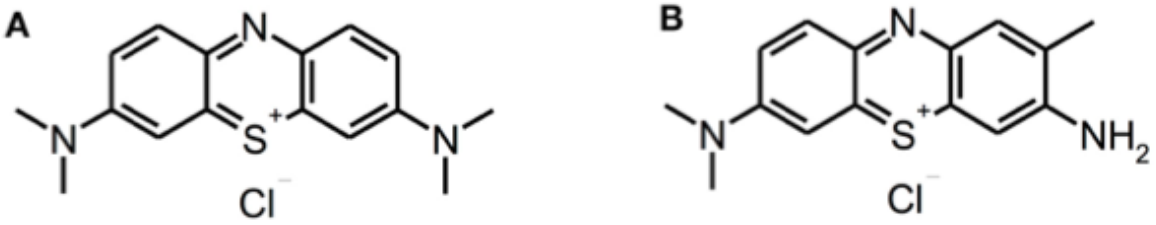

Figure 10. Two of the phenothiazine dyes. A is methylene blue and B is toluidine blue (with permission) (Cieplik *et al.*, 2014)

2.4.2 Two reaction types

When absorbing the right amount of energy from the light, the PS is excited and the photodynamic reaction is initiated (Taraszkiewicz *et al.*, 2013). The ground state of the PS is a singlet state, but when excited the PS forms a triplet-excited state or an excited singlet state. The singlet state PS is short-lived while the triplet-state PS is long-lived. It is often the case that the long-lived state is more effective, because the time allows the PS to react directly

with oxygen or transfer energy to biomolecules (Sharma *et al.*, 2012, Taraszkiewicz *et al.*, 2013). Through which route the PS gets back to a ground state depends on the mechanism. There are two mechanisms of reaction: type I and type II (Cieplik *et al.*, 2014). This is illustrated in **Figure 11**.

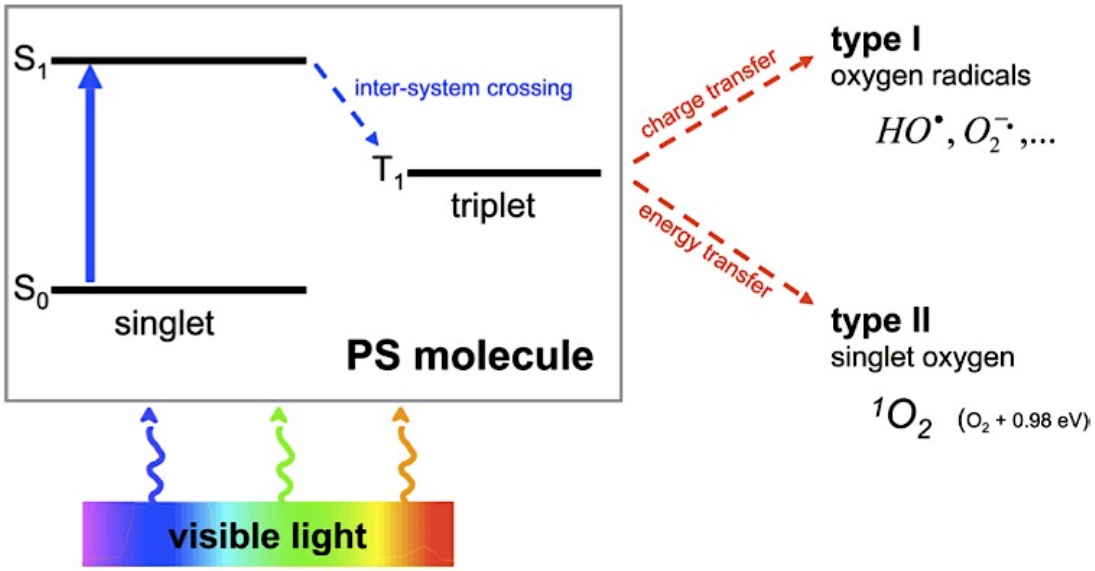

Figure 11. The process of photodynamic therapy with illustration of both reaction type I and type II (with permission) (Cieplik *et al.*, 2014).

In reaction type I, radicals are produced due to a transfer of electrons (Taraszkiewicz *et al.*, 2013). In this reaction, ROS are generated. Superoxide anion ($O_2C^{\bullet-}$) is created and this might go further to hydrogen peroxide (H_2O_2) and hydroxyl radical ($^{\bullet}OH$) (Sharma *et al.*, 2012, Cieplik *et al.*, 2014). The cellular damage and lipid peroxidation are mainly originating from the activity of H_2O_2 (Taraszkiewicz *et al.*, 2013).

Type II-reactions involve the energy transfer to the ground state oxygen (O_2) from the excited triple state PS. This energy transfer generates a singlet oxygen ($^1O_2$) that is highly reactive. Because of the reactivity of $^1O_2$ it will react with macromolecules and oxidize them. This causes the damage to the cell and cell death (Sharma *et al.*, 2012, Taraszkiewicz *et al.*, 2013).

2.4.3 Oxidative stress

The reduction of oxygen is an ongoing activity and an important process in biology. These natural processes are a reason for the formation of ROS. O_2 in itself is stable due to the two unpaired, spin-aligned electrons in the p-orbital, but it is able to accept electrons and this might form superoxide. Electron transfer to superoxide is easier than an electron transfer to O_2 (Ziegelhoffer and Donohue, 2009). The total reduction of oxygen in the cellular respiration generates water, but when oxygen is partially reduced, ROS are generated.

Even though bacteria are exposed to ROS all the time due to the cellular respiration and metabolic processes, they have the defence mechanisms to avoid the damage these species can create. The defence against ROS involves amongst other superoxide dismutase, glutathione peroxidase and catalase. Superoxide dismutase removes superoxide through catalytic processes; glutathione peroxidase and catalase removes hydrogen peroxide (Vatansever *et al.*, 2013). This defence is important for the bacteria due to the possible damage. Superoxide and hydrogen peroxide mainly damage the proteins and hydroxyl radicals can damage DNA (Ziegelhoffer and Donohue, 2009).

The processes described above are normal processes in the bacteria, but when ROS generation is increased due to the increase in the metabolic processes or the introduction of external sources or when the capacity of the defence is decreased, the situation of oxidative stress occurs (Vatansever *et al.*, 2013). This overwhelming failure of the defence against oxidative stress is the aim of the aPDT.

2.5 A derivative of 5-aminolevulinic acid

The new chemical entity (NCE) is a derivative of 5-aminolevulinc acid (**Figure 12**). 5-aminolevulinc acid and its derivatives are used as a treatment for many different diseases. Among these diseases actinic keratosis, the most common premalignant tumours and basal cell carcinomas, are especially interesting. The drug used here is a methylated 5-aminolevulinate and is approved as Metvix® in most European countries (Szeimiesa *et al.*, 2002, Morton, 2003). A derivate of 5-aminolevulinc acid is also used as a diagnostics

marketed as Hexvix®. It is used to detect bladder cancer and the substance is hexylaminolevulinate (Fotinos *et al.*, 2006).

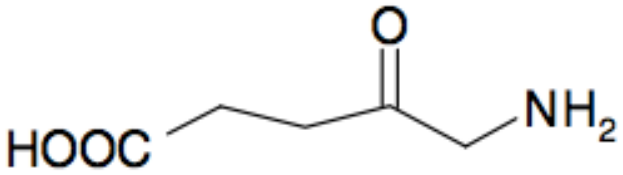

Figure 12. The chemical structure of 5-ALA (Donnelly *et al.*, 2006).

2.5.1 The heme biosynthetic pathway

The derivative of 5-ALA is a prodrug that is converted into PpIX though the heme biosynthetic pathway (**Figure 13**). 5-ALA is naturally occurring in the body as a product of succinyl coenzyme A from the citric acid cycle and glycine. This reaction is catalysed by the enzyme aminolevulinc acid synthase and the cofactor pyridoxal-5-phosphate. This is also a rate-limiting step in this pathway and takes place in the mitochondria. The step is regulated by a feedback inhibition from heme. ALA is transported from the mitochondria to the cytosol where two molecules of ALA react and produce porphobilinogen with aminolevulinate dehydratase as a catalyst. The next step is catalysed by porphobilinogen deaminase and produces hydroxymethylbilane from four molecules of porphobilinogen. Hydroxymethylbilane is either turned into uroporphyrinogen III in a reaction catalysed uroporphyrinogen III synthase or it is converted to urophyrinogen I. Uroporphyrinogen III is converted to coproporphyrinogen III by the enzyme uroporphyrinogen decarboxylase and coproporphyrinogen III is converted to protoporphyrinogen IX by coproporphyrinogen oxidase. Coproporphyrinogen oxidase is in the intermembrane space of the mitochondria. PpIX is synthesized in the mitochondria from protoporphyrinogen IX via the enzyme protoprophyrinogen oxidase. This is the step that is the target of photodynamic therapy. PpIX is converted into heme by ferrochelatase in another rate-limiting step (Peng *et al.*, 1997, Ajioka *et al.*, 2006, Wachowska *et al.*, 2011).

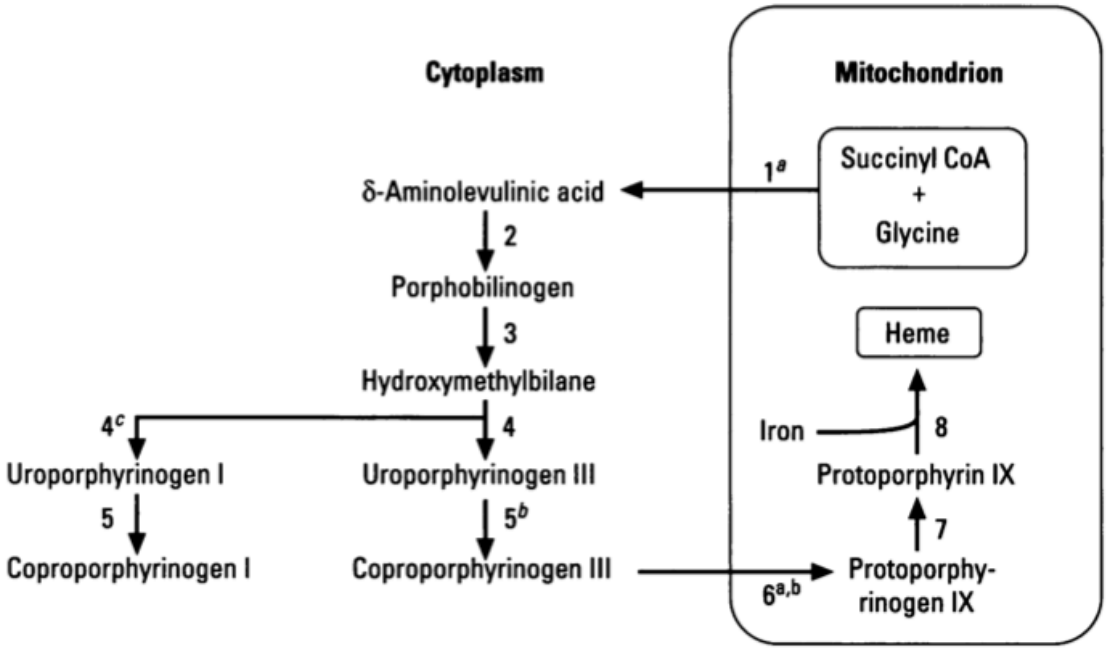

Figure 13. The heme biosynthetic pathway (Daniell *et al.*, 1997).

2.5.2 Protoporphyrin IX

As mentioned above, the synthesis of PpIX is tightly regulated through the heme biosynthetic pathway, mainly through the feedback regulation of aminolevulinic acid synthase. The levels of PpIX are maintained in the body due to regulated synthesis and clearance. This regulation is possible to avoid when introducing ALA from an external source, because in that case the rate-limiting step is avoided. This will provide an accumulation of PpIX and is important the PDT efficiency (Juzeniene *et al.*, 2013). The structure of PpIX is shown in **Figure 14**.

As described earlier the clearance of PpIX is dependent on the activity of ferrochelatase and the amount of iron available. The iron is inserted into the PpIX and therefore an iron chelator is often introduced to reduce this incretion of iron. In addition of being regulated by the presence of iron, the clearance is also regulated by the concentration of ALA, temperature and pH (Juzeniene *et al.*, 2013).

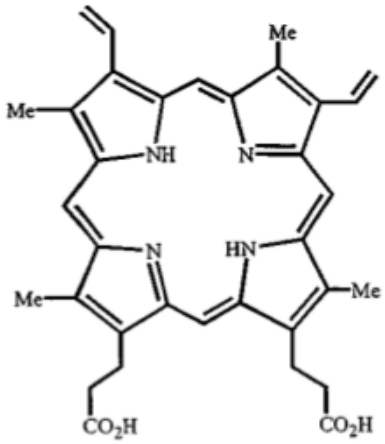

Figure 14. The structure of protoporphyrin IX (with permission) (Lim *et al.*, 2000)

2.6 Previous work on the topic

As mentioned, PDT is an emerging topic within treatment of different diseases and in the recent years, numerous articles have been published on the subject. It has been known for a long time that light might have a positive effect on a variety of diseases, but the link between a PS and the light is more recent. The earliest publication on the relationship between light and a PS is an article from Raab in 1900. Raab combined the acridine red and light and saw that this eliminated infusoria (Dougherty, 1996, Ackroyd *et al.*, 2001). Hausmann was, to my knowledge, the first one to conduct a study on the biological effect of hematoporphyrin in 1911. The effect was tested on the blood cells and paramecium and he also explained the effect on the mice skin. The first described use of porphyrins in human was performed by Meyer-Betz in 1913 (Ackroyd *et al.*, 2001). In the aftermath of these studies, more research on the effect of PSs and the effect on different types of cells followed.

2.6.1 Antimicrobial PDT

Many different strategies have been proposed for to use aPDT in wound healing with a variety of different active substances. One of the often used is curcumin. Curcumin is proposed to have properties such as anti-inflammatory and anti-cancer. In one study, the freeze-dried curcumin was tested against *Enterococcus faecalis* and *Escherichia coli in vitro*. The authors found that a supersaturated solution of the freeze-dried curcumin had an antibacterial effect on both bacteria (Wikene *et al.*, 2014).

Alvarenga LH, *et al*. discovered that methylene blue-mediated photodynamic therapy had a toxic effect on *Aggregatibacter actinomycetemcomitans* in a concentration of 100 μM at an irradiation for 5 minutes. None of the previous studies have shown as good efficiency of this substance, which might indicate the importance of dose and irradiation. The treatment showed a 99.85% cell death including a structural change in the biofilm with a radiation of 75 J/cm^2 (Alvarenga *et al.*, 2015).

Both *in situ* and *in vitro* effects were tested by Teixeira A.H. *et al*. using toluidine blue on *Streptococcus mutans*. They found that the treatment was toxic to the bacteria in biofilm *in vitro*, but when they tested the *in situ* conditions, they found no statistically significance between the people that received the treatment compared to the control groups (Teixeira *et al.*, 2012).

5-ALA and its derivative 5-ALA methyl ester were tested against two vancomycin resistant *Enterococcus faecalis* strains *in vitro*. The bacteria were exposed to 10 mM 5-ALA or 5-ALA methyl ester radiated by a 633 ± 10 nm LED for 60 minutes. The observed reduction was 5.02 and 4.91 $\log_{10}$ for the bacteria (Liu *et al.*, 2014).

Muller *et al*. showed a very low reduction of several of species of bacteria using methylene blue as the PS with a radiation at 665 nm for 60 seconds. This *in vitro* study might have some room for improvement. The radiation might have been too short and the samples for PDT could be prepared differently (Muller *et al.*, 2007).

In an *in vivo* study of a new PS, phthalocyanine derivative (RLP068 / Cl), carried out by Simonetti O. *et al*. in 2011 the PS in gel form with teicoplanin, a placebo gel or no treatment were compared. The test subjects were mice bearing wounds infected with MRSA. The authors found that the group receiving PS had a significant improvement compared with placebo and no treatment. The short treatment with PDT was also better compared with the antibiotic. The treatment length was shorter and provided avoidance of the intraperitoneal injection (Simonetti *et al.*, 2011).

Topaloglu and colleagues tried to use indocyanine green with an 809-diode laser against *Staphylococcus aureus* and *Pseudomonas aeruginosa* in an *in vitro* study. They compared indocyanine green to a control group that did not receive any treatment; a group that received only laser treatment and a group that only received indocyanine green. They found that the bacteria treated with indocyanine green and laser had a significant reduction in viable bacteria (Topaloglu *et al.*, 2013). The studies are summarized in **Table 1**.

Table 1. Overview of relevant aPDT studies

Active substance	Findings		Reference
Curcumin	Toxic towards *Enterococcus faecalis* and *Escherichia coli in vitro*.	*In vitro*	(Wikene *et al.*, 2014)
Methylene blue	Toxic towards *Aggregatibacter actinomycetemcomitans.*	*In vitro*	(Alvareng a *et al.*, 2015)
Toluidine blue ortho	Toxic towards *Streptococcus mutans in vitro*, but no significant findings *in situ*.	*In vitro* *In situ*	(Teixeira *et al.*, 2012)
5-ALA and 5-ALA methyl ester	Found a reduction of surviving of two vancomycin resistant *Enterococcus faecalis* strains when treated with both 5-ALA and 5-ALA methyl ester	*In vitro*	(Liu *et al.*, 2014)
Methylene blue	Showed almost no reduction in viability of several species. E.g., *Actinomyces naeslundii, Veillonella dispar, Streptococcus sobrinus, Streptococcus. oralis* etc.	*In vitro*	(Muller *et al.*, 2007)
Phthalocyanine derivative (RLP068／Cl),	Toxic towards MRSA in *in vivo* study on mice.	*In vivo*	(Simonetti *et al.*, 2011)
Indocyanine green	Toxic towards *Staphylococcus aureus* and *Pseudomonas aeruginosa* in *in vitro* study.	*In vitro*	(Topalogl u *et al.*, 2013)

2.7 The carrier

Even though the NCE in this project was destined to eliminate bacteria, it does not totally discriminate human cell and it might cause some adverse skin reactions. In addition, the NCE is prone to degradation due to hydrolysis. In this project, NPs were applied as a carrier for the

NCE to reduce its degradation and hopefully decrease the adverse effects. The chosen NPs were made of chitosan and lecithin. The NPs were self-organized due to the ionic interaction between chitosan and lecithin (Sonvico *et al.*, 2006). Lecithin is often used in the preparing NPs and is regarded as safe and biocompatible. Chitosan is often used because it has shown desirable properties, like biocompatibility, biodegradability, bioadhesion, increased penetration and antimicrobial activity (Tan *et al.*, 2011).

2.7.1 Nanoparticles

NPs can be defined as particulate dispersions or solid particles with a size in the range of 10-1000 nm. When drug is included in the particles it is dissolved, entrapped, encapsulated or attached to a nanoparticle matrix (Mohanraj and Chen, 2006). Although the exact size range defining nanoparticles or microparticles is not agreed upon, the most important properties of these structures in the nano-range are related to their small size (George, 2003, Mahapatro and Singh, 2011, Wilczewska *et al.*, 2012). The attention around NPs as a delivery system has increased in the last years. The particles have properties that are desirable in drug delivery and both the particle size and surface properties is controllable depending on the preparation. The aim in a production of NPs is to control the two mentioned factors (size and surface properties) in addition to the to control of the release profile of the substance embedded in the NP and consequent local or an targeted action in a specific location in the body (Mohanraj and Chen, 2006, Mahapatro and Singh, 2011). In addition to the advantages such as protection of the substance and targeting, depending on the formulation choice, different routes of administration may be (Mohanraj and Chen, 2006). The particle size, if very small, might be a limiting factor for the NPs, since it might lead to limited drug loading (Amritkar *et al.*, 2011).

2.7.2 Nanoparticles as drug delivery systems

Nanoparticles are often applied as a drug delivery system and are gaining greater importance for future drug therapy. It is important to assure that the aimed action of the drug takes place in the intended location in the body, both to maximize the desired effects and to decrease the undesirable adverse effects. In many cases, the drug itself exhibits limitations and challenges, such as in our case. Often a drug delivery system is used to protect the drug from degradation or a large and rapid clearance. In addition to contributing to a positive effects the delivery

systems has to be biocompatible and not exhibit any level of toxicity (Wilczewska *et al.*, 2012).

The loading of a substance to a NPs can be done in different ways. The substance might be embedded or encapsulated inside the NPs and/or particle surface. Many different substances have been loaded to the NPs (Mahapatro and Singh, 2011). In the delivery system used in this project, we decided to use chitosan, however there are numerous other polymers which could have been applied such as poly-ε-caprolactone, polyacrylamide, polyarylate, albumin and gelatine (Wilczewska *et al.*, 2012).

There are many different reasons why NPs are widely studied as a promising drug delivery system. As mentioned above, nanocarriers are often used to protect the drug from either degradation or clearance, and due to this, the carrier might be able to increase the bioavailability of the substance. As with the NCE, one aims for new substances to display good stability. The body and the skin are a harsh environment for many substances and the nanocarriers can help to increase the stability of these drugs (Mohanraj and Chen, 2006). NPs can also be used for both passive and active targeting (Danhier *et al.*, 2010).

When making use of a drug delivery system, the common adverse effects might be avoided. Nevertheless, it is important to test the adverse effect profile of the drug delivery systems with the drug, as other adverse effects may appear. These effects are often due to the reactions of the immune system to the delivery system (Zolnik *et al.*, 2010). This is something it is important to be aware of when developing and testing new formulations.

Another advantage of NPs as drug delivery system is that you NPs can assure an extended release of the drug (Parveen *et al.*, 2012). They are also suitable for various administration routes such as pulmonary, oral, dermal and intravenous routes (Desai, 2012).

There are also some drawbacks with the use of NPs in drug formulations. The problems often emerge when the complexity behind the formulation increases In addition, it might be costly and time consuming to develop these systems. The optimization process is often challenging in several ways. It is not always achievable to obtain the desired degree of optimization and the formulations are often compromises between cost and effectiveness (Wagner *et al.*, 2006, Bernkop-Schnurch, 2013).

2.7.3 Nanoparticles and drug delivery to the skin

As mentioned earlier, the skin is the largest organ of the body and is exposed to the environment at all times, and due to this, it is necessary that the skin have good protecting properties. The skin also has a pH gradient as an important feature and it is suggested that maintenance of a pH gradient increases the antimicrobial protection. In addition to this, the integrity of the *stratum corneum* is necessary the shedding processes in the skin (Baroli, 2010). These factors need to be considered when designing NPs. The desired penetration of NPs varies according to what type of the treatment is necessary. In this project, the NPs were designed for a localized therapy. Drug delivery to the epidermis or the dermis often fails or it is not optimal (Prow *et al.*, 2011). When localized therapy is the aim, one has to assure that the systemic exposure is fully avoided or minimized. The optimal size of the carriers used in skin therapy is often debated. The prefix, nano-, used to describe the nanoscaled structures used, is regarded to cover structures around 100 nm (Prow *et al.*, 2011). The carriers used on the skin are often larger than this, and a clearly defined size for topical administration is still not agreed upon but it has been indicated that a size between 200 and 300 nm is preferable (Hurler *et al.*, 2012).

In the routes of penetration through the skin, the interesting sites for small NPs targeting are the hair follicles, whereas the larger NPs might target the furrows of the skin and the *stratum corneum* itself (Baroli, 2010, Prow *et al.*, 2011). The thickness of the *stratum corneum* varies throughout the body. When treating the wounded skin, the barrier is intact and the possible drug/nanoparticle penetration might be significantly different in comparison to intact skin. As the penetration through the damaged skin may be increased, the drug might be able to reach deeper into the skin (Baroli, 2010) which might rise toxicity issues, especially in chronic therapy. The temperature of the skin also plays an important role in the skin delivery. Wounded areas often have a higher temperature than the intact skin and this might contribute to the increased penetration into the wounded skin. The different locations of the skin on the body also differ in the temperature (Baroli, 2010, Beldon, 2010, Grice and Segre, 2011).

The factors affecting the NPs penetration into the skin are directly related to the location on the skin and condition of the skin. The location of the skin is a quite known factor, but the information about the penetration through the impaired skin (such as inflamed or wounded

skin) is lacking. In addition to these, the penetration depends on the properties of the carrier itself and the molecule entrapped in the carrier (Baroli, 2010). NPs containing polymers may be modified to express the desired properties, such as, for example, the surface charge and the size according to the method of preparation, as mentioned earlier. Both the size and the shape have great effect on the skin penetration of the nanocarriers, (Baroli, 2010).

2.7.4 Drugs delivered by chitosan and lecithin nanoparticles

These NPs, made of chitosan and lecithin, were proposed as a delivery system for different drugs and active substances. Amongst several published studies, the one considering amphotericin-B entrapped in chitosan lecithin (C/L) NPs indicated a prolonged release of amphotericin-B (Chhonker *et al.*, 2015), which can be of relevance in wound dressings. Other studies describe these types of NPs loaded with tamoxifen citrate (Barbieri *et al.*, 2013), artesunate (Chadha *et al.*, 2012) and melatonin (Hafner *et al.*, 2009).

The chitosan lecithin-based NPs developed in this project, were of similar composition as those investigated for the possible penetration through the healthy skin. Şenyiğit *et al*. investigated the accumulation of clobetasol loaded C/L NPs in pig skin (Senyiğit *et al.*, 2010). The NPs made here had a diameter of 258.25 ± 15.13 nm and a zeta potential of 34.10±1.80 mV. They also tested the stability over 3 months and confirmed the stability of the particles. The skin accumulation was tested using an *in vitro* model with a Franz-type diffusion cell across pig ear skin over a period of 6 hours. They compared the NP dispersion with clobetasol to a cream containing clobetasol and to chitosan gel containing clobetasol, all with a concentration of 0.05 %. The NP dispersion showed a significantly higher accumulation in both the epidermis and the dermis compared with the tested dosage forms, indicating that this might be a potential carrier system for dermal or epidermal delivery of chemical entities. Although more testing is still needed, but these results are encouraging.

Tan *et al*. did the evaluation of C/L NPs loaded with quercetin for topical delivery (Tan *et al.*, 2011). The NPs made in this study had a diameter of 168 nm with a zeta potential 10.85 ± 0.05 mV. These NPs also contained D-tocopheryl polyethylene glycol 1000 succinate (TPGS) since it is known that TPGS-containing NPs had better entrapment efficiency than NPs without TPGS. This accumulation was also investigated in an *in vitro* study using a Franz diffusion cell with mouse skin and analysed on HPLC-column. In addition, in an *in vivo* study

the tested solutions were evaluated in mice *post mortem*. The *in vitro* tests showed that the NPs enhanced the accumulation in both epidermis and in dermis compared with the quercetin in propylene glycol solution. This increase was 1.45 times in epidermis and 1.32 times in dermis, respectively. In the *in vivo* study, the increase was 2.3 times in epidermis and 1.2 times in dermis, respectively for NPs compared with the control solution. They also documented microscopically that the skin treated with NPs appeared swollen and the junctions between the cells looked loosen and the intercellular space had also increased.

Özcan *et al*. compared poly(lactic-co-glycolide) (PLGA)-NPs with C/L NPs to investigate the permeation in an *ex-vivo* study (Özcan *et al.*, 2013). The particles were loaded with betamethasone valerate. The size of the PLGA NPs containing betamethasone were 280.9 ± 1.7 nm with a zeta potential of -5.62 ± 0.28 mV. The betamethasone-containing C/L NPs had a size of 274.6 ± 14 nm and a zeta potential of 40.8 ± 2.80 mV. The accumulation was tested with a Franz diffusion cell with the use of rat skin. The formulations tested were NPs dispersion, gel and commercial cream. The C/L NPs had a significantly higher accumulation in epidermis while the PLGA NPs had a significantly higher accumulation in dermis. Both had higher accumulation in both skin layers than the commercial cream. They also tested the anti-inflammatory effects *in vivo* where they treated carrageenan (a gelling agent)-induced acute oedema in rat paws. They measured the swelling of the paws to check for effect. The PLGA NPs exhibited no statistically significant difference from the commercial cream, but the C/L NPs showed a significant improvement compared to both the commercial cream and the control group.

2.7.5 Drug delivery strategies in antimicrobial PDT

In the recent years, the focus on photodynamic therapy and especially aPDT has increased in parallel to the increased focus around nanotechnology and drug delivery systems. For this project C/L NPs were chosen as a suitable carrier, but a lot of different carrier systems have been applied in the aPDT, such as liposomes, NPs and cyclodextrins to mention a few (Bombelli *et al.*, 2008, Ferro *et al.*, 2009, Planas *et al.*, 2015).

Methylene blue (**Figure 10 A**) has been loaded into amino- and mannose-targeted mesoporous silica nanoparticles (NPs) to test its activity against *Escherichia coli* and *Pseudomonas aeruginosa* in bacterial suspensions (Planas *et al.*, 2015). The size of the NPs

was 200 and 180 nm and the zeta potential was -25 and -20 mV for the amino- and mannose-targeted mesoporous silica NPs, respectively. The loading of the particles was 73 and 94 %, respectively. The authors found that the NPs reduced the dark toxicity of methylene blue in *Escherichia coli* bacteria. The mannose-NPs were better for targeting of *Pseudomonas aeruginosa*.

Dias Ribeiro *et al*. tested chloro-aluminum phthalocyanine in nanoemulsions against methicillin-susceptible and methicillin-resistant *Staphylococcus aureus* (MRSA), both in bacterial suspensions and as biofilm (Dias Ribeiro *et al.*, 2015). Nanoemulsions were both prepared as cationic and anionic emulsions to evaluate the effect of the charge. In planktonic suspensions, the susceptible bacteria both the free chloro-aluminum phthalocyanine and the cationic emulsion with a light dose of 25 J/cm^2 induced elimination of the bacteria. In the MRSA, the required light dose to induce the same effect was 50 J/cm^2. The cationic nanoemulsion showed the best activity against both types of biofilm.

Different compositions of delivery systems affect the efficiency of the carrier and this has also been tested for liposomes. Bombelli *et al*. prepared cationic liposomes with 1,2-dimyristoyl-sn-glycero-3-phosphatidylcoline and different surfactants (Bombelli *et al.*, 2008). They loaded the different liposomes with m-tetrahydroxyphenylchlorin and tested the antimicrobial effect against MRSA and compared it with the free form of m-tetrahydroxyphenylchlorin. They suggested that zeta potential; the melted liquid crystalline state of the lipid double layer and entrapment ability were the important parameters are crucial when investigating biological activity.

Ferro *et al*. used a formulation of cyclodextrins together with 5-[-4-(1-dodecanoylpyridinium)]-10,15,20-triphenyl-porphine, a porphyrin, and tested it against MRSA and *Escherichia coli* (Ferro *et al.*, 2009). Fullerenes are indicated to have a photodynamic activity. Grinholc *et al.* tested the activity of a monosubstituted cationic C60 fullerene derivative both *in vitro* and *in vivo* (Grinholc *et al.*, 2015). They saw an effect *in vitro*, but reported a regrowth *in vivo*.

2.7.6 Chitosan

Chitin is the most abundant polymer found in nature second to cellulose and when N-deacetylated it is converted into chitosan (Filipovic-Grcic *et al.*, 2001, Jayakumar *et al.*, 2010). Rouget was the first to discover chitosan, a cationic polysaccharide, in 1859. His observation was that chitin became soluble in the organic acids when boiled in concentrated potassium hydroxide solution and he identified the structure shown in **Figure 15**. The component did not receive its name before Hoppe-Seyler focused on its structure back in 1894. He called it chitosan (Muzzarelli, 1977). Chitin is found in the shell of crustaceans, in insects and in fungi (Jayakumar *et al.*, 2010). In this project, the chitosan was retrieved from shrimps. The structures chitin and chitosan are presented in **Figure 15**.

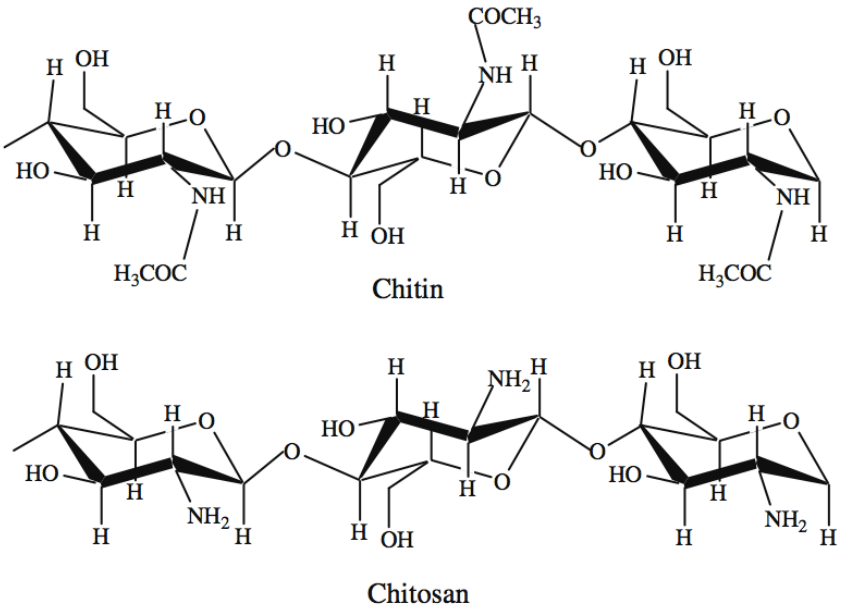

Figure 15. Structure of chitin and chitosan (Jayakumar *et al.*, 2010).

As mentioned earlier chitosan is biodegradable, biocompatible, regarded as safe and exhibits antimicrobial effects on its own (Jayakumar *et al.*, 2010, Liu *et al.*, 2011). As seen in **Figure 15** the composition of chitosan is made up of repeating units of β (1→4)-linked D-glucosamine residues with a changing number of N-acetyl-glucosamine groups (Liu *et al.*, 2011). Chitosan has been tested for different medical applications. Amongst these applications are the wound healing, tissue repair and regeneration, stimulation of the immune system, anticoagulation, artificial membrane, antitumor properties and anticolesteremic properties (Muzzarelli, 1977, Jayakumar *et al.*, 2010, Liu *et al.*, 2011).

Chitosan is often used due to its low toxicity and is accepted as a component that is generally recognized as safe (GRAS) by the US Food and Drug Administration (FDA) (Li Q., 1992, Filipovic-Grcic *et al.*, 2001, Baldrick, 2010). In addition, it is used as a food additive in Japan, Italy and Finland (Baldrick, 2010). Some studies have tested the safety of chitosan or its derivatives in animal models. In 2009, Takahashi *et al*. tested the chronic toxicity and carcinogenicity of N-acetyl-glucosamine in both female and male rats. They gave the rats 0%, 1.25%, 2.5% or 5% of N-acetyl-glucosamine in a pelleted diet for 52 weeks to test for chronic toxicity. Another group of rats got 0%, 2.5% or 5% of N-acetyl-glucosamine in a pelleted diet for 104 weeks to test for carcinogenicity. Two deaths were observed in the first group. In the second group, 18 rats from the control group died or nearly died, 14 rats from the 2.5% group died or were near death and 11 rats from the 5% group died or were near death (Takahashi *et al.*, 2009). In another study, they gave 15 males 4.5 g chitosan every day for 12 days, but no side effects were reported. This study was designed to investigate the effect of chitosan on fat absorption rather than the safety of chitosan (Gades and Stern, 2003).

Degradation of chitosan in the body occurs through depolymerisation and a chitosan with a larger degree of deacetylation is prone to a less rapid degradation. Chitosan oligosaccharides with different lengths are the product of this degradation and are excreted through the urine and do not seem to retain in the body (Baldrick, 2010, Raftery *et al.*, 2013).

The bioadhesive properties of chitosan might be important in the development of new drug delivery systems, e.g. mucoadhesive dosage forms (Filipovic-Grcic *et al.*, 2001, Baldrick, 2010). In a study published by Hurler and Škalko-Basnet, chitosan in hydrogel formulation exhibited good bioadhesion on pig skin (Hurler and Škalko-Basnet, 2012). He *et al*. also tested the mucoadhesive properties of chitosan. They suggested that this adhesiveness occurred because of electrostatic interactions between the positively charged chitosan and the negatively charged mucous glycoprotein (He *et al.*, 1998).

Chitosan is not soluble under the natural or basic conditions, but dissolves in organic acids when the pH is less than 6 (Li Q., 1992, Liu *et al.*, 2011). A number of research groups have tried to improve the properties of chitosan by its chemical modifications, particularly its solubility. The methylation of chitosan is amongst the strategies to enhance its solubility (Liu *et al.*, 2011).

In this project, the antimicrobial properties of chitosan were of interest. The mechanisms of the antimicrobial activity of chitosan are not fully elucidated, but two different mechanisms are often described. Chitosan is positively charged (**Figure 15**) and the bacterial cell membrane has negatively charged groups. This creates a possibility for an interaction between chitosan and the bacterial cell membrane. It is expected that this interaction might cause disturbances in the bacterial cell wall, further leading to cell leakage (Fei Liu *et al.*, 2001, Rabea *et al.*, 2003, Blecher *et al.*, 2011). Chitosan may also interfere with the microbial DNA and this could further lead to inhibition of the synthesis of mRNA and proteins (Blecher *et al.*, 2011).

Chitosan is suggested to improve wound healing through a number of different actions such as the haemostatic action, macrophage activation, fibroblast activation, elevated synthesis of extracellular matrix, foster formation of granulation tissue, enhanced functions of polymorphonuclear leukocytes and enhanced expression of cytokines and growth factors (Ueno *et al.*, 2001, Muzzarelli, 2009, Baldrick, 2010).

2.7.7 Lecithin

The lipid used in this project was soybean lecithin. Lecithin is a term that many use to describe a mixture of phospholipids that also contains amongst other triglycerides and free fatty acids found in egg yolk or soybeans (Szuhaj, 1983, Qingyi Xu, 2011). The main phospholipids in these mixtures are phosphatidylcholine (**Figure 16**) and phosphatidylethanolamine (Hafner *et al.*, 2011, Qingyi Xu, 2011).

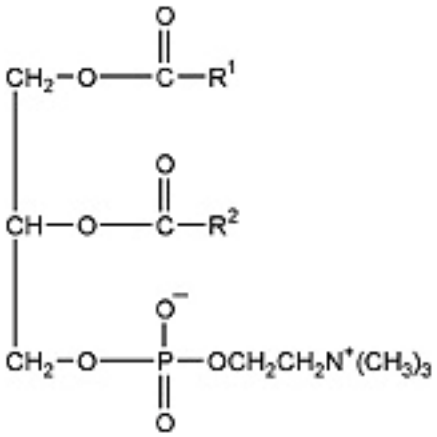

Figure 16. Phosphatidylcholine (Shah and Singh, 2014)

Lecithin is regarded as biocompatible and safe. The safety of lecithin is verified both by the FDA and World Health Organization (WHO). It is GRAS by the FDA and was considered as safe in a toxicological evaluation released by WHO (WHO, 1974, Hafner *et al.*, 2011, Qingyi Xu, 2011).

2.8 The New Chemical Entity

Photocure ASA provided information about the NCE to last year's master students (Thoresen, 2014).

As mentioned earlier, the NCE is a derivative of 5-ALA. 5-ALA is in itself a prodrug of PpIX, which is the PS of this treatment. PpIX is a photoactive substance and will be excited when exposed to light of the right wavelength. The excitation wavelengths of PpIX are 546, 630 and 646 nm, and the excitation gives a yield of approximately 56 % of a singlet oxygen (Redmond and Gamlin, 1999, Fotinos *et al.*, 2006). This gives rise to the PDT. Both 5-ALA and PpIX are naturally occurring in the body, but when more PpIX is administrated exogenously the photosensitization of PpIX will follow (Fotinos *et al.*, 2006). One of the reasons for making a derivative of 5-ALA is to avoid some of the limitations of this substance. 5-ALA is only able to penetrate approximately 2-3 mm into the skin; this is seen in nodular skin tumours (Peng *et al.*, 1997).

The compound is soluble in water (3.6 g/g water) and has a pKa of approximately 8.3. It has a low stability in water and is hydrolysed.

3. Aim

The aim of the study was to evaluate the antimicrobial potential of NCE-containing nanoparticles against biofilm formation by *Staphylococcus epidermidis* in photodynamic therapy.

- The initial effort evolved around preparation of chitosan lecithin nanoparticles to optimize their size, surface properties and NCE entrapment.
- The optimization process was also focused around improving the stability of the NCE and increasing the antimicrobial effect by targeting for a synergic effect between the NCE and the chitosan of the nanoparticles.
- To evaluate the antimicrobial potential of NCE-containing NPs we aimed to optimize the *Staphylococcus epidermidis* biofilm formation. As a first step we evaluate the antimicrobial effect of the NCE in planktonic bacteria. The NCE and NCE-containing NPs were tested in the biofilm. We also aimed to confirm the anti-biofilm potential of empty NPs, which was expected to be a consequence of chitosan present in the NPs.

4. Materials and methods

4.1 Materials

4.1.1 Materials

Acetic acid (≥99.8 %), Sigma-Aldrich, St. Louis, USA

Acetonitrile CHROMASOLV® gradient for HPLC (≥99.9 %), Sigma-Aldrich, St. Louis, USA

Ammonium acetate (98.0%), AnalaR NORMAPUR, VWR, Leuven, Belgium

Blood agar plates, University Hospital of North Norway, Tromsø, Norway

Chitopharm™ S, Mw 50000 – 1000000 Da, approx. 85-90 % deacetylation, Chitinor AS, Haugesund, Norway

Chloramphenicol (≥98 %, TLC), Sigma-Aldrich, Steinheim, Germany

Cirpofloxacin (≥98 %, HPLC), BioChemika, Fluka, Sigma-Aldrich Chemie GmbH, Steinheim, Germany

Crystal violet (Gram´s crystal violet solution), Fluka Analytics, Sigma-Aldrich Chemie GmbH, Steinheim, Germany

D(+)glucose anhydrous, Merck KGaA, Darmstadt, Germany

Distilled water

Ethanol (96 %, v/v), Sigma-Aldrich, St. Louis, USA

Hydrochloric acid, puriss. p.a., ACS reagent, reag. ISO, reag. Ph. Eur., fuming (≥37 %, APHA: ≤10), Sigma-Aldrich, St. Louis, USA

Lipoid S45 (45 % (w/w) phosphatidylcholine), Lipoid GMBH, Ludwigshafen, Germany

Methanol, CHROMASOLV® for HPLC, Sigma-Aldrich, St. Louis, USA

MILLI-Q filtered water

New Chemical Entity, Photocure ASA, Oslo, Norway

Potassium chloride, Merck KGaA, Darmstadt, Germany

Potassium phosphate monobasic, for analysis EMSURE® ISO, Merck, Darmstadt, Germany

Sodium chloride, puriss. p.a. (≥99.5 %), Sigma-Aldrich, St. Louis, USA

Sodium phosphate dibasic, (≥98.5 %), for molecular biology, Sigma-Aldrich, St. Louis, USA

Tryptic soy broth, Sigma-Aldrich, Steinheim, Germany

Vancomycin hydrochloride from *Streptomyces orientalis*, Sigma-Aldrich, St. Louis, USA

4.1.2 Instruments

Aktilite® CL128, lamp for photodynamic therapy, Photocure ASA, Oslo, Norway

Beckman L8-70M Ultracentrifuge, Beckman Coulter Inc., Palo Alto, USA

Beckman SW 60 Ti rotor for ultracentrifuge, 60 000 rpm, serial O5U 2693, Beckman Coulter Inc., Palo Alto, USA

Biocap RNA/RNA, LAF bench, nr 189 2000, BP 403 27104, 230 V, 50 Hz, 73 W, Erlab, Val De Reuil Codex, France

Branson 5510, Bransonic Ultrasonic cleaner, Branson Ultrasonics Corporation, Danbury, USA

Ceroclav autoclave, Multicontrol 12L/18L, Ceroclave sterilizer GmbH, Traun, Austria

GENESYS™ 20 Visible Spectrophotometer, model 4001/4, Thermo Fisher Scientific Inc., Waltham, USA

Getinge autoclave, US-3 V90, Getinge Skärhamn AB, Skärhamn, Sweden

IKA MS2 Minishaker, IKA® Works Inc., Wilmington, USA

IKA-Vibrax-VXR, electronic shaker, IKA®-Werke GmbH & Co. KG, Staufen, Germany

Metrohm, 744 pH meter, type: 1.744.0010, Ion analysis, Metrohm, Herisau, Switzerland

MILLI-Q BIOCELL, 0.22 µm, Millipak® 40, Bergman AS, Trondheim, Norway

NICOMP Submicron particle sizer (PCS), model 370, NICOMP particle sizing system, Santa Barbara, USA

RTC Basic B, Stirrer and hotplate, Ika Labortechnik, GMBH & Co, Staufen, Germany

Sartorius BP211D, scale, Sartorius AG, Göttingen, Germany

Sartorius LP620S, scale, Sartorius AG, Göttingen, Germany

Sartorius TE601 battery powered scale, Sartorius AG, Göttingen, Germany

VersaMax, tunable microplate reader, Molecular Devices, Sunnyvale, USA

Waters e2795, HPLC separation module, Alliance HT, Waters Corporation, Milford, USA

Waters 2489, UV/visible detector for HPLC, Waters Corporation, Milford, USA

Zetasizer nanoseries, model Zen 2600, Malvern Instrumentals Ltd, Malvern, UK

4.1.3 Software and programs

ELISA: SoftMax® Pro Software, version 5.4.1, Molecular Devices, 2010, Sunnyvale, USA

HPLC: Empower Pro, Empower 3 software, 2010, Waters Corporation, Milford, USA

PCS: CW388 Application version 1.68, NICOMP particle sizing system, Santa Barbara, USA

Zetasizer software 7.03, 2002-2013, Malvern Instrumental Ltd, Malvern, UK

4.1.4 Utensils

Accu-jet® pro Pipette Controller Brand, BrandTech Scientific, Wertheim, Germany

Acrodisc® 25 mm Syringe Filter with 0.2 µm Supor® Membrane, Sterile, Non-pyrogenic, Pall International, Fribourg, Switzerland

ART® 1000 E Barrier tip, Rached, Sterile, 1000 µL pipette tips, Thermo Scientific, Roskilde, Danmark

BD Plastipak™, 1 mL luer, Becton, Dickinson and Company, Franklin Lakes, USA

BD Plastipak™, 2 mL luer, Becton, Dickinson and Company, Franklin Lakes, USA

BD Plastipak™, 5 mL luer, Becton, Dickinson and Company, Franklin Lakes, USA

BD Plastipak™, 10 mL luer, Becton, Dickinson and Company, Franklin Lakes, USA

Centrifuge tubes, polycarbonate, 11 x 60 mm, 3 mL, Beckman Coulter Inc., Palo Alto, USA

Cotton tipped applicatior, Selefa, OneMed Oy, Helsinki, Finland

Dialysis membrane, Visking, Size 1, Inf. Dia. 8/32", 6.3 mm: 30 M (approx.), Medicell Membranes Ltd., London, UK

Disposable cuvettes, standard, Brand®, Wertheim, Germany

Disposable culture tubes, Biosilicate glass, 6x50 mm, Kimble Chase, Vineland, USA

Falcon® Serological pipette, sterile-R, non-pyrogenic, 5 mL, Corning incorporation, Life sciences, One bection circle, Durham, USA

Falcon® Serological pipette, sterile-R, non-pyrogenic, 10 mL, Corning incorporation, Life sciences, One bection circle, Durham, USA

Falcon® Serological pipette, sterile-R, non-pyrogenic, 25 mL, Corning incorporation, Life sciences, One bection circle, Durham, USA

Finnpipette®, 200-1000 µL, Thermo labsystems, Helsinki, Finland

Finnpipette® F2, 20-200 µL, Thermo scientific, Vantaa, Finland

Finnpipette® F2, 0.5-5 mL, Thermo scientific, Vantaa, Finland

Low-temperature freezer vials, self-standing, 2 mL, Lip seal design, VWR International, Leuven, Belgium

Nunc™ inoculation loop, blue, 10 micro L SI, Thermo Scientific, Roskilde, Denmark

Nunc™ MicroWell™ 96-well microplates w/lid Nuclon D Si, Nuclon™ Delta surface, polystyrene plates, 167008, Thermo Scientific, Roskilde, Danmark

PALL, Sciences, Bulk Acrodisc® 25 mm syringe filter w/0.2 µm Supor® membrane, Pall Life Sciences, Port Washington, USA

Ultra-High Performance Centrifuge Tubes, 15 mL, VWR International, Leuven, Belgium

Ultra-High Performance Centrifuge Tubes, 50 mL, VWR International, Leuven, Belgium

Waters Atlantis T_3 4.6 x 150 mm HPLC-column, Milford, USA

Waters Atlantis T_3 5 µm, 4.6 x 20 mm guard cartridge, Milford, USA

4.1.5 Bacterial strains

Staphylococcus epidermidis ATCC 35984 (RP62A), CCUG: Culture Collection, The University of Göteborg, Sweden

Staphylococcus epidermidis ATCC 35984 (RP62A), CCUG: Culture Collection, The University of Göteborg, Sweden

Staphylococcus epidermidis RH 6-61, (clinical isolate), Rikshospitalet, The University Hospital, Oslo, Norway

Staphylococcus epidermidis RH 6-65, (clinical isolate), Rikshospitalet, The University Hospital, Oslo, Norway

Staphylococcus epidermidis RH 6-47, (clinical isolate), Rikshospitalet, The University Hospital, Oslo, Norway

Staphylococcus epidermidis RH 6-42, (clinical isolate), Rikshospitalet, The University Hospital, Oslo, Norway

Staphylococcus haemolyticus RH 51-03 (clinical isolate, negative control), Rikshospitalet, The University Hospital, Oslo, Norway

All other chemicals used were of analytical grade.

4.2 Preparation and characterization of NPs

4.2.1 Preparation of empty nanoparticles

The preparation of the empty chitosan/lecithin nanoparticles was based on the method of Sonvico *et al.* (Sonvico *et al.*, 2006). The nanoparticles were prepared by adding 0.5 mL of a chitosan solution in acetic acid (0.5 %, w/v) to 44 mL distilled water. Four mL of the ethanolic lecithin solution (2.5 %, w/v) was injected to the chitosan solution in distilled water through a syringe (2 mL/min) under mechanical stirring. The ratio of chitosan and lecithin was 1:20 (w/w). The suspension was stirred for approximately 1 hour and left in the refrigerator overnight before further investigation.

4.2.2 Preparation of NCE-containing nanoparticles

The preparation of the NCE-containing chitosan/lecithin nanoparticles is based on a method of Sonvico *et al.* (Sonvico *et al.*, 2006). The nanoparticles were prepared by adding 0.5 mL of a chitosan solution in acetic acid (0.5 %, w/v) to 44 mL distilled water. NCE (30 or 50 mg) was dissolved in 4 mL of ethanolic lecithin solution (2.5 %, w/v) and injected into the chitosan solution in distilled water through a syringe (2 mL/min) under mechanical stirring. The ratio of chitosan and lecithin was 1:20 (w/w). The suspension was stirred for approximately 1 hour and left in the refrigerator overnight before further investigation

4.2.3 Analysis of the particle size

The size of the nanoparticles was determined by photo correlation spectroscopy (PCS) on the NICOMP Submicron particle sizer, model 370, with an angle of 90 degrees. The PCS or dynamic light scattering is based on the Brownian motions of particles in a medium were the viscosity of the given medium is known due to the temperature of the medium. The temperature of the measurements was 24°C ± 1°C. The samples of particle suspensions were prepared in a laminar airflow bench to avoid contamination with dust particles. For that purpose, the measuring tubes were sonicated in an ultrasonic bath for 10-15 minutes and washed with filtered water before the measurements. The samples were diluted with filtered water to attain an intensity of 250-350 KHz throughout of the measurements (Hupfeld *et al.*, 2006). The size distribution of the NPs in suspension measured in three cycles of 10 minutes. Other parameters used in the analysis are included in **Table 2**.

Table 2. Parameters used in the PCS analysis

Parameter	
Distribution fit	NICOMP (the chi-square exceeded 3.0)
Sensitivity	Auto set
Viscosity	23 °C: 0.9325 cP
	24 °C: 0.9111 cP
	25 °C: 0.8904 cP
Liquid refractive index	1.333
Channel width	Auto set
Intensity set point	300 KHz
Cell	Drop-in cell
Weighting	Intensity-weighted
Toggle solid/vesicle particle	Solid particle
Laser	Helium neon laser
	Wavelength: 632.8 nm (Hupfeld *et al.*, 2006)

4.2.4 Determination of zeta potential

The zeta potential was determined by using Zetasizer Nano Z 2600. The test cells were washed with ethanol and filtered water before the measurements. The samples were prepared by diluting the suspensions with an appropriate amount of water to a total volume of 1 mL. The samples were measured in three runs at a temperature of 25°C.

4.2.5 HPLC analysis

The preparation of the mobile phases and dilution solvent was based on a method developed by Photocure ASA. Two mobile phases, namely mobile phase A and B, were prepared by dissolving 1.5 g ammonium acetate in acetonitrile and water (volume ratio of 100:900 mL; A and 900:200 mL;B (v/v)). To prepare a calibration curve, eight standard solutions (2, 1.75, 1.5, 1.25, 1, 0.75, 0.5 and 0.25 mg/mL) were prepared from a stock solution (10 mg/mL) by diluting with a dilution solvent. The dilution solvent was prepared by mixing 40 mL of the mobile phase A with 160 mL of mobile phase B. The HPLC analysis was carried out by using an Atlantis T3 4.6 x 150 mm column and an Atlantis T3 5 μm 4.6 x 20 mm guard cartridge.

The conditions for the HPLC analysis are described in **Table 3**. The conditions for the shutdown method are described in **Table 4**.

Table 3. Conditions of the HPLC analysis

Conditions for the HPLC analysis	
Flow	0.4 mL/min
Column temperature	25 ± 5 °C
Sample temperature	25 ± 5 °C
Wavelength of the detector	270 nm
Solvents	Solvent A: Mobile phase A Solvent B: Mobile phase B
Run time	11 minutes
Equilibration time	5 minutes
Gradient	0 % mobile phase A to 19.8 % mobile phase A.

Table 4. The conditions for the shutdown method

The conditions for the shutdown method	
Flow	1 mL/min
Column temperature	25 ± 5 °C
Sample temperature	25 ± 5 °C
Solvent	Solvent C: Acetonitrile

4.2.6 Preparations of samples for HPLC analysis and determination of NCE entrapment

The determination of the entrapment efficiency was done by dialysis followed by the HPLC analysis. The NCE-containing NPs were separated from unentrapped NCE by dialysis in dialysing tubing. Five mL of the samples were dialysed against 500 mL distilled water for 6 hours. An aliquot (100 µL) of the NCE-containing NPs free from unentrapped NCE was dissolved in 900 µL methanol to destroy the NPs. This solution was analysed using the same HPLC method as described above. The amount of free (unentrapped) NCE in dialysis medium was also determined by HPLC analysis. To determine the recovery, a sample (100 µL) of the original NCE-containing NPs suspension (containing both free and entrapped

NCE) was dissolved in 900 µL methanol to destroy the NPs and analysed using HPLC. Three vials were prepared for each sample and three injections were measured for each vial.

4.2.7 Determination of pH

The measurement of the pH of the samples was done with Metrohm, 744 pH meter at room temperature (24±2°C) for all the NPs suspensions.

4.3 Preparation of solutions for microbial testing

4.3.1 Preparation of 0.9 % (w/v) NaCl solution

This solution was prepared by dissolving 9 g NaCl in 1000 mL distilled water followed by autoclaving.

4.3.2 Preparation of tryptic soy broth (TSB)

TSB (30 g) was dissolved in 1000 mL Milli-Q water and autoclaved, according to Sambrook and Russell (Sambrook and Russell, 2001).

4.3.3 Preparation of glucose solution

Glucose (12.5 g) was dissolved in 50 mL distilled water and then filtered through a 0.22 µm filter. The solution was transferred to an autoclaved glass flask according to Sambrook and Russell (Sambrook and Russell, 2001).

4.3.4 Preparation of vancomycin stock solution

The stock solution (20 mg/mL) was prepared by dissolving 40 mg vancomycin in 2 mL Milli-Q water. The solution was then filtered through a 0.22 µm pore size filter.

4.3.5 Preparation of chloramphenicol stock solution

The stock solution (20 mg/mL) was prepared by dissolving 40 mg chloramphenicol in 2 mL ethanol. The solution was then filtered through a 0.22 µm pore size filter.

4.3.6 Preparation of ciprofloxacin stock solution

The stock solution (20 mg/mL) was prepared by dissolving 40 mg ciprofloxacin in 2 mL 0.1 M hydrochloric acid solution.

4.3.7 Preparation of the NCE stock solution

The stock solution (200 mg/mL) was prepared by dissolving 200 mg NCE in 1 mL Milli-Q water. The solution was filtered through a 0.22 μm pore size filter. The solution was freshly prepared before every test to avoid possible degradation due to hydrolysis and stored in the refrigerator for a maximum 15-20 minutes before each test.

4.3.8 Preparation of the NCE-containing NPs for antibacterial test

The procedure was based on the method originally developed by Thoresen (Thoresen, 2014). NCE-containing NPs suspension (2.4 mL) was centrifuged for 2 hours at 165000 *g* at 10 °C. The pellets were resuspended in an aliquot of TSB with 0.5 % glucose after the centrifugation. The new suspension was further diluted with TSB with 0.5 % glucose to attain a NCE concentration of 0.01, 0.1 and 1 mM, respectively.

4.3.9 Preparation of empty NPs for antibacterial test

The procedure was also based on the work of Thoresen (Thoresen, 2014). NPs suspension (2.4 mL) was centrifuged for 2 hours at 165000 *g* at 10 °C. The pellets were resuspended in an aliquot of TSB with 0.5 % glucose after the centrifugation. The new suspension was further diluted with TSB with 0.5 % glucose to attain the amount of 17.5 and 35 mg/ml of the lipid/chitosan content, respectively.

4.4 Testing of the minimum inhibitory concentration (MIC) of planktonic bacteria

The bacteria were diluted in TSB with 0.5 % glucose to a suspension close to 0.5 McFarland standard (Garcia and Isenberg, 2010). The optical density of the suspensions was approximately 0.063 at a wavelength of 600 nm. The stock solutions of the antibacterial substances were added to the prepared dilutions at different concentrations starting with 2 mg/mL and continuing in a logarithmic manner to determine the MIC. Bacterial suspensions (200 μL) were transferred to microtiter plates and incubated at 37 °C overnight. The plates

with the NCE were exposed to light from the Aktilite® lamp at 37 J/cm^2 at a distance of 5 cm for 8 minutes and 49 seconds.

4.5 Preparation of biofilm and biofilm elimination

The preparation of the biofilm was according to a modified method by Christensen *et al*. (Christensen *et al.*, 1985).

4.5.1 Preparation of bacterial biofilm

All the bacterial strains were cultured on blood agar plates at 37 °C overnight (16-18 hours) and the plates were stored at 4 °C prior to further use. A single colony of each strain was inoculated in 5 mL TSB and grown overnight at 37 °C in a shaker at approximately 200 rpm. This bacterial suspension was then diluted 1:100 in TSB with 0.5 % (v/v) glucose. This new suspension (150 µL) was added to 96-well microtiter plates and incubated under continuous shaking (approximately 75 rpm) at 37 °C for 20 hours. The content of the wells was poured out on tissues and the plate was washed with Milli-Q water three times. The plate was incubated for another hour at 55 °C. The 0.4 % crystal violet (200 µL) was added to each well and the plate left for 5 minutes. The plate was then washed with Milli-Q water two times before adding 200 µL 70 % (v/v) EtOH to each well. The OD was measured to investigate the possible formation of a biofilm. The ELISA reader was set to 490 nm.

4.5.2 Testing of antibacterial effect on bacterial biofilm

A single colony of each bacterial strain was inoculated in 5 mL TSB and grown overnight (16-18 hours) at 37 °C in a shaker (approximately 200 rpm). This bacterial suspension was then diluted 1:100 in TSB with 0.5 % (v/v) glucose. This new suspension (150 µL) was added to 96-well microtiter plates and incubated under continuous shaking (approximately 75 rpm) at 37 °C for 14 hours. The plate was emptied using a micropipette and the volume was replaced with the solutions with different antibacterial substances diluted in TBS with 0.5 % glucose according to the 1x MIC, 2x MIC and 3x MIC as described for the MIC test in Section 4.4. Each plate contained controls comprising only TSB with 0.5 % glucose. The plates containing the NCE were exposed to light from the Aktilite® lamp at 37 J/cm^2 with a wavelength of approximately 630 nm at a distance of 5 cm for 8 minutes and 49 seconds. Four plates were prepared for each test and incubated at 37 °C for 1, 3, 6 and 24 hours,

respectively. The content of the wells was poured out on tissues and the plate washed with Milli-Q water three times. The plate was incubated for another hour at 55 °C. The 0.4 % crystal violet (200 µL) was added to each well and the plate was left for 5 minutes at room temperature. The plate was then washed with Milli-Q water two times before adding 200 µL 70 % (v/v) EtOH to each well. The OD was measured to investigate the possible formation of a biofilm. The ELISA reader was set to 490 nm. Three parallels of three biological parallels were tested for each strain for each antimicrobial substance.

4.5.3 Testing of antibacterial effect of NPs on bacterial biofilm

The testing of both the empty and the NCE-containing NPs was done in the same manner as the testing of the NCE solutions (4.5.2). Instead of the incubation for 1, 3, 6 and 24 hours, two plates were prepared and incubated for 6 and 24 hours, respectively. The concentrations used were as described in 4.3.8 and 4.3.9.

4.5.4 Testing of the antibacterial effect of the NCE without light exposure

The procedure used in this test was as described in 4.5.2, except that the substance was not exposed to light. In addition, instead of incubation for 1, 3, 6 and 24 hours, two plates were prepared and incubated for 6 and 24 hours, respectively.

4.5.5 Testing of the possible interaction between the NCE and the microtiter plate

We detected a small, but significant difference in colouration of the plate for the negative control between the NCE and the other antibacterial substances. To assure that the difference was not due to an interaction between the NCE and the microtiter plate we performed an experiment in which only the NCE in TSB was applied onto the microtiter plate. The NCE stock solution was diluted in TBS with 0.5 % glucose according to the 1x MIC, 2x MIC and 3x MIC as described for the MIC testing in 4.4. The solution (150 µL) was added to 96-well microtiter plates and the plates were exposed to light from the Aktilite® lamp at 37 J/cm^2 with a wavelength of approximately 630 nm at a distance of 5 cm for 8 minutes and 49 seconds. Each plate contained controls comprising of only TSB with 0.5 % glucose. The plate was placed in the incubator at 37 °C for 6 hours. The content of the wells was poured out on tissues and the plate was washed with Milli-Q water three times. The plate was incubated for another hour at 55 °C. The 0.4 % crystal violet (200 µL) was added to each well and the plate

was left for 5 minutes at room temperature. The plate was then washed with Milli-Q water two times before adding 200 µL 70 % (v/v) EtOH to each well. The OD was measured to investigate for colouration and a possible interaction between the microtiter plate and the NCE. The ELISA reader was set to 490 nm.

4.6 Statistical evaluation

The determination of the level of significance was calculated by Student's *t*-test. The confidence level used in the calculations was 95 % for all the measurements.

5. Results and discussion

5.1 Characterization of NPs

5.1.1. Characterization of empty NPs

The size and polydispersity index (PI) of empty NPs were determined according to the method described earlier (4.2.3) and are presented in **Table 5**. The first preparations were made with a chitosan and lipid ratio of 1:5 (w/w) as presented in the Table. The NPs were large; the PI was quite high, therefore we adjusted the chitosan lipid ratio to 1:10 and 1:20 (w/w), respectively. The increase in lipid content resulted in smaller size and PI. The chitosan lipid ratio of 1:20 (w/w) gave the particles closest to the desired size for topical administration onto the skin. The size we aimed for was between 200 and 300 nm (Hurler *et al.*, 2012). Our results correspond to the findings of Hafner *et al.* (Hafner *et al.*, 2009, Hafner *et al.*, 2011). The groups of Sonvico and Taner also prepared chitosan NPs using the same ratio (Sonvico *et al.*, 2006, Taner *et al.*, 2014). We have also employed the different stirring speed, the injection methods and rates, however the preparation method described in 4.2.1 was found to be optimal in respect to the particle size. The difference in the average size due to the different chitosan lipid ratio is presented in **Figure 17**.

In addition to resulting in smaller NPs, the chitosan lipid ratio of 1:20 (w/w) exhibited a lower residual, chi-square and baseline adjustment. These parameters indicate the accuracy of the measurement and polydispersity. A lower chi-square indicates that the measured values deviate less from the expected frequency within that spesific sample. The baseline adjustment indicates the adjustment that is needed to obtain the lowest possible chi-square. A value < 0.03 indicates that the grade of adjustment is low. The residual represents the presence of aggregates that is not worth considering in the sample. The optimal value is a value as close as possible to zero (Frantzen *et al.*, 2003). The values of chi-square and baseline adjustment are included in the **Appendix Table 1**. To ensure a precise and reproducible measurement the intensity of suspensions used in the measurements was adjusted to be between 250 and 350 kHz, according to earlier work by Hupfeld *et al.* (Hupfeld *et al.*, 2006). However, due to relatively high polydispersity, we opted to present the size distributions as the cumulative percentage of the Gaussian distribution (number of particles smaller than, in our case 75 % of particles smaller than). The NICOMP distribution is presented in **Appendix Table 2.** The cumulative percentage in the Gaussian distribution was not too far from an applicable value whereas some of the values represented as the NICOMP distributions are seemingly far from

the true values of the samples and is not a good representation of the true frequency of the intractable samples.

Table 5. Cumulative size distributions in percentage (< 75 %) of empty NPs. The cumulative percentage and the zeta potential are presented as a mean (n = 3).

Chitosan lipid ratio (w/w)	Cumulative percentage (75 % of particles smaller) (nm)	PI (mean)	Zeta potential (mV)
1:5	1089.1 ± 18.1	0.518 ± 0.043	16.9 ± 0.35
1:5	1031.9 ± 69.9	0.438 ± 0.042	18.4 ± 0.21
1:5	779.0 ± 195.7	0.663 ± 0.235	15.9 ± 0.46
1:5	1134.6 ± 91.1	0.653 ± 0.056	17.5 ± 0.26
1:5	1113.3 ± 36.6	0.561 ± 0.029	16.3 ± 0.32
1:5	1061.3 ± 34.2	0.437 ± 0.029	16.5 ± 0.06
1:5	770.3 ± 9.4	0.471 ± 0.016	15.7 ± 0.26
1:5	837.4 ± 1.0	0.480 ± 0.006	15.3 ± 0.20
1:5	1186.9 ± 71.1	0.459 ± 0.069	20.1 ± 0.42
1:5	1107.7 ± 35.6	0.437 ± 0.020	20.6 ± 0.58
1:5	1184.2 ± 230.6	0.468 ± 0.209	18.9 ± 0.10
1:5	971.9 ± 9.0	0.407 ± 0.016	19.1 ± 0.21
1:10	693.1 ±35.2	0.507 ± 0.045	11.5 ± 0.36
1:10	756.0 ± 35.2	0.416 ± 0.020	9.9 ± 0.27
1:20	318.6 ± 27.0	0.158 ± 0.103	2.6 ± 0.18
1:10	579.2 ± 80.2	0.381 ± 0.104	9.3 ± 0.20
1:20	366.9 ± 28.0	0.498 ± 0.090	4.6 ± 0.32
1:20	383.7 ± 16.4	0.454 ± 0.062	5.8 ± 0.41

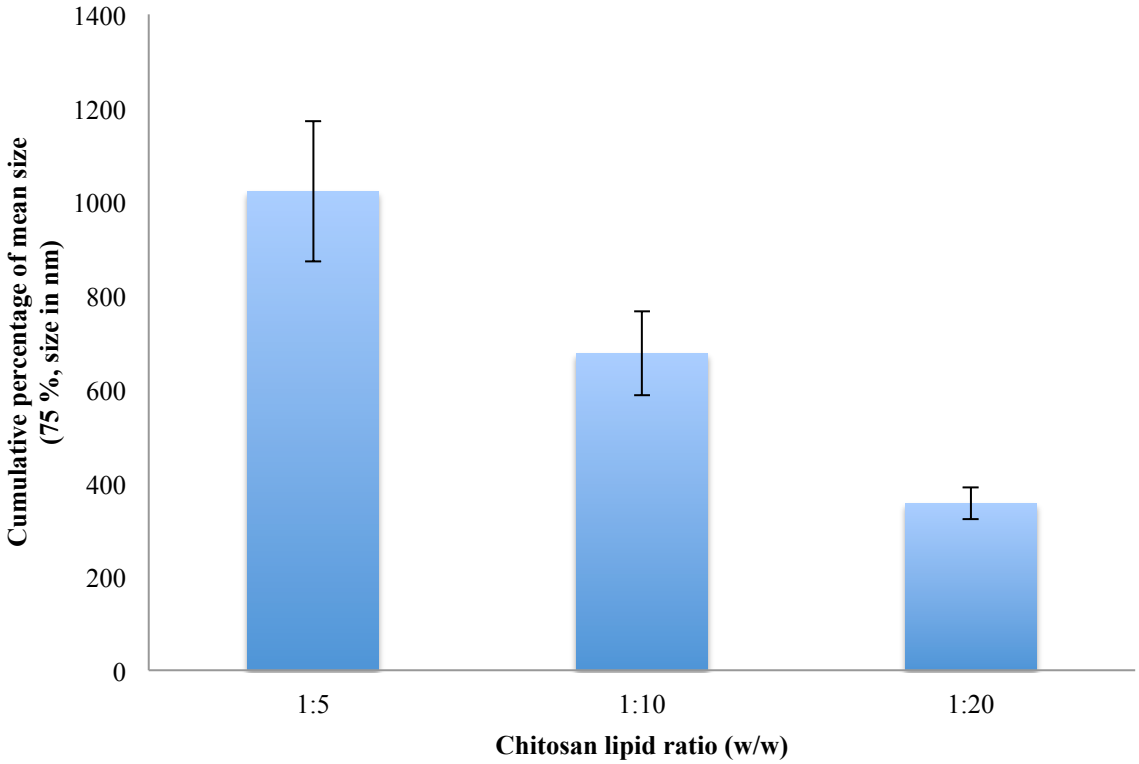

Figure 17. The effect of chitosan lipid ratio on the mean particle size (cumulative percentage below 75 %). The size is presented as the mean (nm) of Gaussian distribution.

The zeta potential of the empty NPs was also measured as shown in **Table 5**. The positive charge of the NPs indicates that chitosan is present on the surface of particles and lipid rather exists in the core of the particles. The zeta potential is usually used to describe the surface charge of the NPs, but more specifically the value describes the interfacial potential between the particle and the liquid. The theory describes an existing double electrical field on the surface of the particle consisting of the Stern layer and the diffusion layer. In between these two layers one can find the shear plane, where hydrodynamic motion is possible. In addition to the composition of the particle and the type of liquid used, the zeta potential also depends on the pH, temperature and concentration of the counter ions (Kirby and Hasselbrink, 2004). The zeta potential is also important for the stability of particle suspensions, and it is suggested that a zeta potential of above 30 mV or below -30 mV assures a stable suspension (Heurtault *et al.*, 2003, Mohanraj and Chen, 2006). The zeta potential was found to change according to the change of the chitosan lipid ratio, with corresponding changes in the size. This is illustrated in **Figure 18**. This decrease could be a consequence of the reduced amount of surface-available chitosan, resulting in less positive NPs.

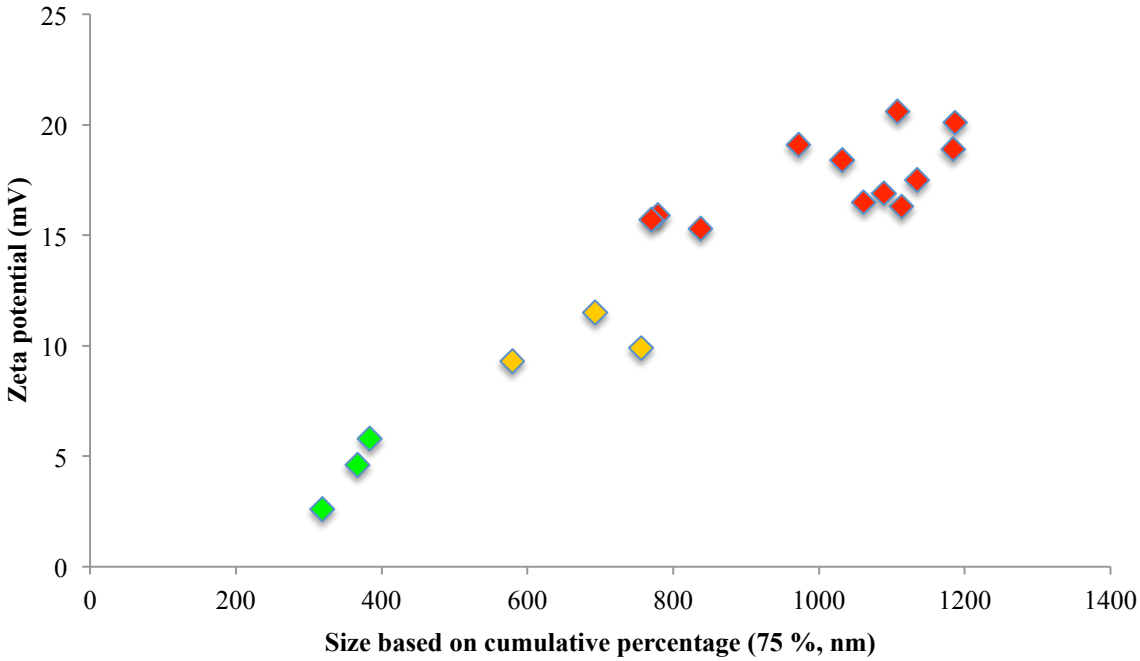

Figure 18. Zeta potential of empty NPs. The green colour refers to NPs with chitosan lipid ratio of 1:20 (w/w), the yellow to chitosan lipid ratio of 1:10 (w/w) and the red to chitosan lipid ratio of 1:5 (w/w).

The amino groups of chitosan molecule at low pH of the acetic acid medium used to dissolve chitosan become protonated. This will ensure a positive surface charge of the particle as seen in **Table 5**. By increasing the lipid content in the NPs (change in the chitosan lipid ratio) the outer surface contains less chitosan, which results in lower positive charge as expected.

5.1.2. Characterization of NCE-containing NPs

Hence, the chitosan lipid ratio of 1:20 (w/w) was chosen as the suitable ratio for the preparation of the NCE-containing NPs. The 1:5 ratio (w/w) was also tested, but as seen in **Table 6** this batch displayed a large size and a slightly higher polydispersity than the NCE-containing NPs with a 1:20 (C/L, w/w) ratio as seen in **Figure 19**. The **Table 6** indicates that the size of the particles increases, as they are loaded with the NCE. We experienced the same limitations of the size determination methods as observed for empty NPs. Moreover, to be able to directly compare the sizes of empty and NCE-containing NPs, we applied Gaussian distribution as a cumulative percentage of particles smaller than certain mean diameter. The NICOMP fit is also presented in **Appendix II**. The values for NCE-containing NPs were

found to be more similar to the Gaussian fit than the empty NPs. The residual and the polydispersity were decreased as well.

Table 6. Cumulative size distributions in percentage (< 75 %) of NCE-containing NPs. The cumulative percentage and the zeta potential are presented as a mean (n = 3).

Preparation	Chitosan lipid ratio (w/w)	Amount of the NCE (mg)	pH	Cumulative percentage (75 %, nm)	PI (mean)	Zeta potential (mean, mV)
1	1:5	30	3.38	906.5 ± 19.1	0.343 ± 0.030	28.5 ± 0.49
2	1:20	30	2.96	378.6 ± 4.3	0.237 ± 0.008	11.5 ± 0.29
3	1:20	30	2.97	338.5 ± 4.5	0.245 ± 0.016	9.2 ± 0.15
4	1:20	30	2.98	433.7 ± 8.5	0.187 ± 0.015	15.2 ± 0.26
5	1:20	30	2.94	402.7 ±2.8	0.219 ± 0.017	11.9 ± 0.20
6	1:20	50	2.73	412.3 ± 5.1	0.229 ± 0.016	16.7 ±0.46
7	1:20	30	2.93	370.4 ± 3.2	0.238 ± 0.013	11.3 ± 0.35
8	1:20	30	2.94	382.8 ± 3.2	0.221 ± 0.007	8.3 ± 0.15
9	1:20	30	2.95	414.5 ± 7.4	0.198 ± 0.018	7.1 ± 0.10

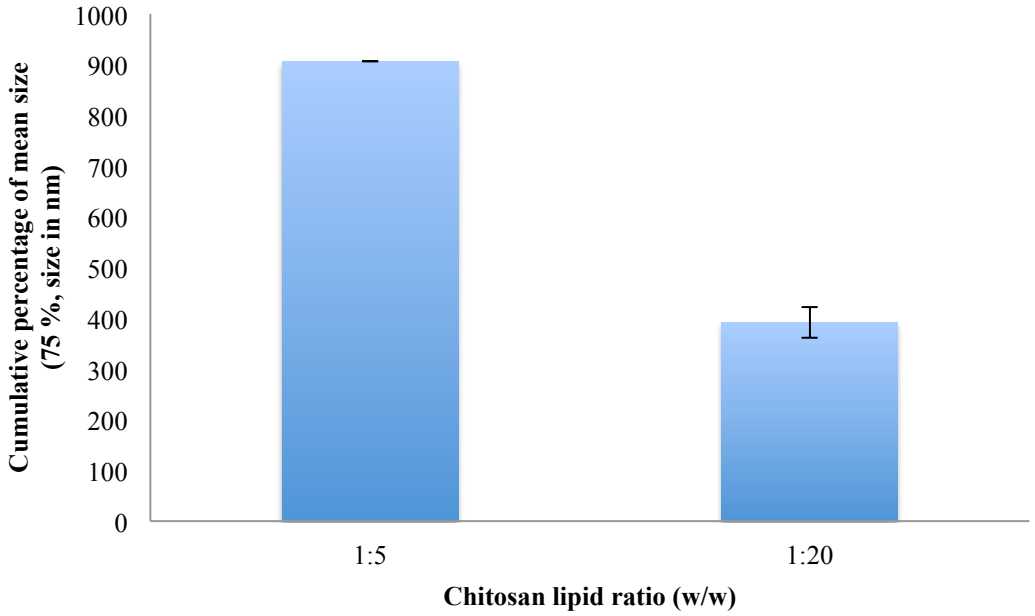

Figure 19. The effect of chitosan lipid ratio on the mean particle size (cumulative percentage below 75 %). The size is presented as the mean (nm) of Gaussian distribution. The chitosan lipid ratio 1:5 (w/w) is only represented with one NPs suspension.

The zeta potential of the NPs increased when the NCE was introduced, as can be seen in the sample 6 (50 mg of the NCE used in the preparation) in **Table 6** and **Figure 20**; a higher amount of NCE used in the preparation appears to increase the zeta potential even more. Considering the low pH of the suspensions, the lowered zeta potential may be an effect of both chitosan as discussed earlier but also the protonation of the NCE. As seen in **Figure 12**, the structure of 5-ALA, that the NCE is a derivative of, contains an amino group in addition to a carboxyl group. The trend of the changed zeta potential according to change in chitosan lipid ratio has been observed for the NCE-containing NPs as well.

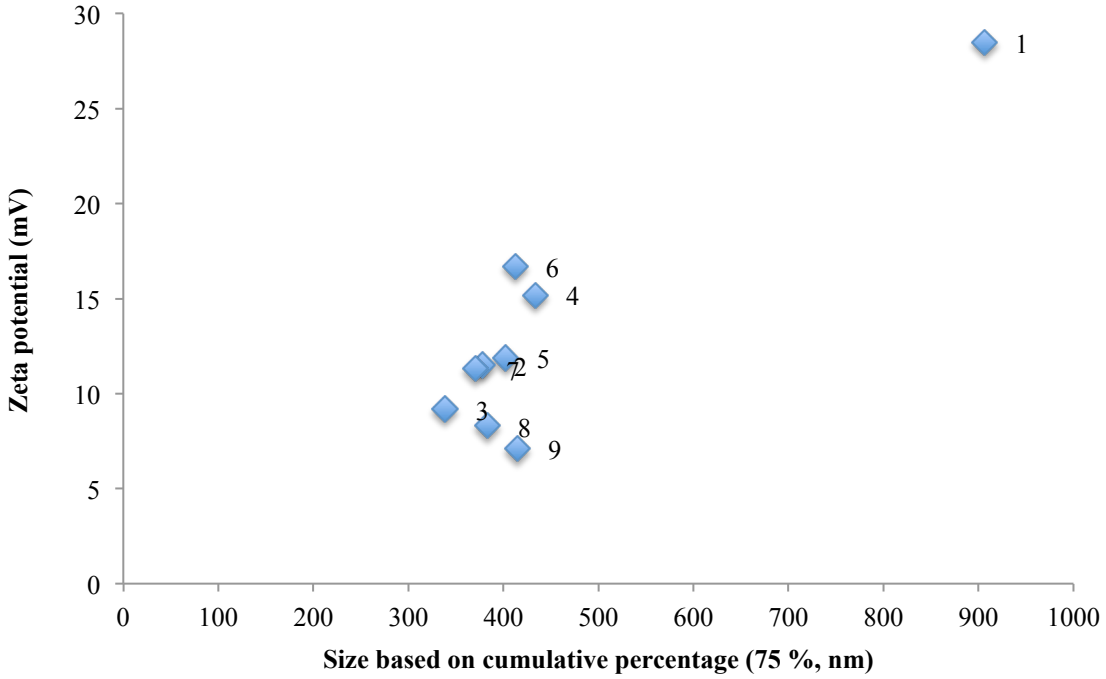

Figure 20. Zeta potential of NCE-containing NPs. The marks are correlated to the numbers according to the designation in **Table 6**.

5.1.3. HPLC analysis and NCE entrapment

The entrapment was determined using dialysis as separation method and the HPLC analysis partially developed by Photocure ASA. Due to the problems with the column, the original method (Hadafow, 2014) was modified. Originally, the column used was a HILIC column, but it was replaced by a silica-based, reversed-phase C_{18} column. The column was selected based on the published literature (Sithisarankul *et al.*, 1999, Gilmore *et al.*, 2006, Shen *et al.*, 2006). The mobile phases used in the project were the same as the ones used in the method described by Photocure ASA and Hadafow (Hadafow, 2014). The mobile phases we used are in agreement with the literature (Mitchell *et al.*, 2009, Ripolles *et al.*, 2011, Boonchiangma *et al.*, 2012). The rest of the conditions used in the HPLC analysis were based on a run through the column with only one concentration (5 mg/mL) and a slow gradient change of the mobile phases. From this we calculated the ratio between the two mobile phases where the peak of NCE showed on the chromatogram. Different flow rates were also tested in the same manner. After the method was validated, a standard curve for the NCE was prepared (**Figure 21**).

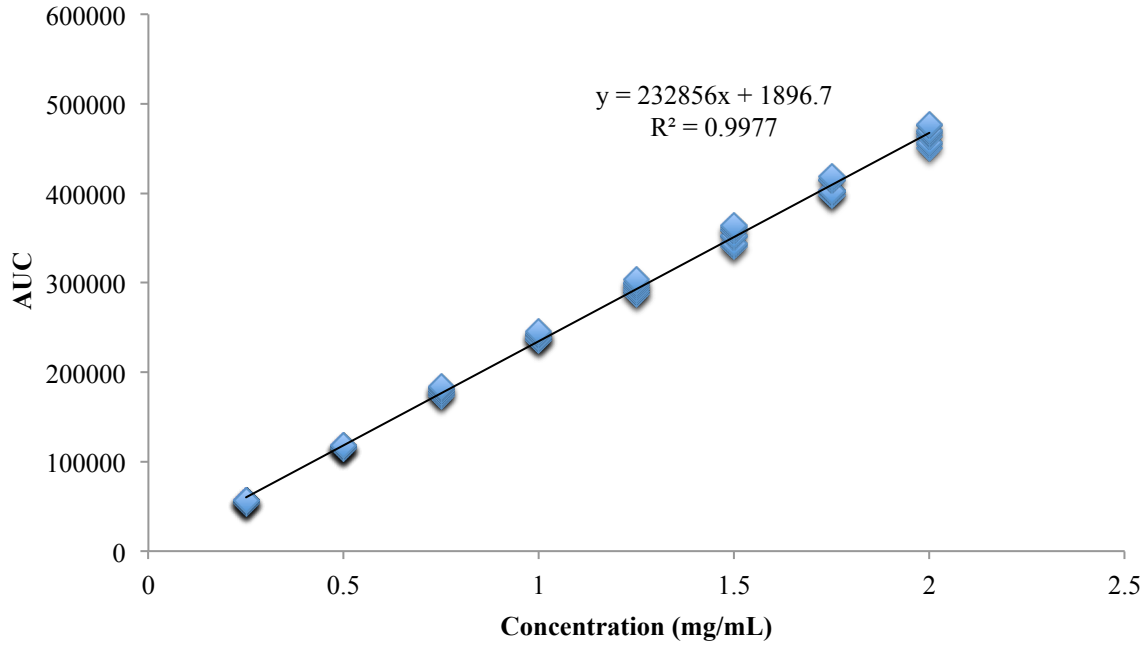

Figure 21. Standard curve for the NCE.

The separation of the NCE and the degradation product is clearly indicated in **Figure 22**. Even though the separation was good there are still possible improvements that may be included in this analysis. The readings might be better if a standard for the degradation product was available. Due to the rapid degradation in aqueous medium, the deviations for the higher concentrations are larger. However, this is an additional reason to include NCE in the delivery system, which can protect it from the hydrolysis.

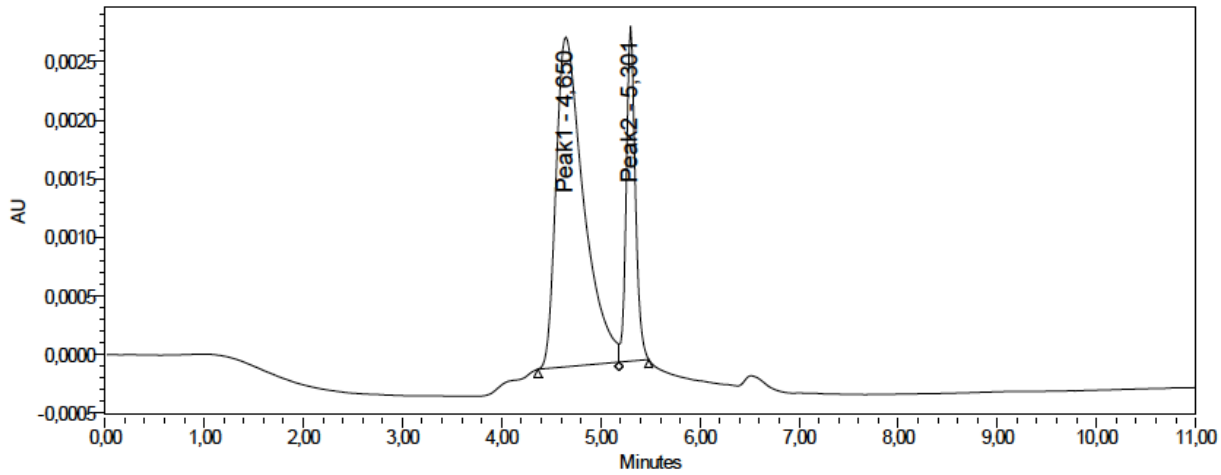

Figure 22. The HPLC chromatogram for 0.25 mg/mL NCE in the analysis. The NCE is presented here as peak 1 and the degradation product is presented as peak 2.

Table 7. The entrapment efficiency (EE) and the relative recovery (RR) of the NCE determined by the HPLC analysis. The values are presented as a mean of the samples prepared with 30 mg of the NCE and chitosan lipid ratio of 1:20 (w/w).

EE %	RR %
11.60 ± 2.13	74.85 ±17.35

The entrapment efficiency was found to be rather low. The optimization of the chitosan and lipid ratio should be performed by preferably multifactorial design.

When considering the structure of the NCE there might be ways to increase the entrapment of the substance, e.g. it might be possible to increase the entrapment if we used active loading of the NPs. In the articles described earlier, most of the substances entrapped in this type of NPs have a hydrophobic character (Section 2.7.4). The entrapment varies between the different articles, but often the entrapment efficiency is much higher that in our case.

5.2 Antimicrobial testing

The NCE is a new substance and except for the work of Thoresen (Thoresen, 2014), the knowledge of the concentration dependency in biological effects of the NCE is minimal. Thoresen used 5-ALA as a reference to determine the concentration needed to achieve the necessary effect of the NCE. We decided to test the MIC of the NCE to determine the concentration needed. The concentration of other antimicrobial substances needed to eliminate a biofilm is often much higher that required for planktonic bacteria, but in this case we benefit from the use of a drug delivery system expected to enhance its biological activity. Therefore, prior to determining the anti-biofilm effect of the NCE, we tested the MIC of the NCE and compared it with known antibiotics.

5.2.1. Determination of MIC

The MIC was determined by adding different concentrations of the NCE and the control antibiotics to planktonic bacteria. The MIC of the different antimicrobial substances and NCE are presented in **Table 8**. The clinical breakpoint for interpretation of determined MIC is also included in this Table to differentiate the susceptible and the resistant strains. The clinical breakpoints are collected from The European Committee on Antimicrobial Susceptibility Testing (EUCAST) (2015).

Table 8. Overview of the MIC S (susceptible) and R (resistant) needed to achieve the clinical breakpoint according to EUCAST (2015).

	Vancomycin (µg/mL)	Chloramphenicol (µg/mL)	Ciprofloxacin (µg/mL)	NCE (µg/mL)
Staphylococcus epidermidis RH 6-65	4^S	8^S	32^R	8192
Staphylococcus epidermidis RH 6-47	4^S	128^R	32^R	8192
Staphylococcus epidermidis RP62A (42-77) 1	4^S	16^R	64^R	8192
Staphylococcus epidermidis RP62A (42-77) 2	8^R	16^R	16^R	8192
Staphylococcus epidermidis RH 6-61	4^S	8^S	32^R	8192
Staphylococcus epidermidis RH 6-42	4^S	8^S	32^R	8192
Staphylococcus haemolyticus RH 51-03	8^R	8^S	64^R	8192

Considering the breakpoints defined by EUCAST it seems that there are a lot of resistance in the strains of the chosen antibiotics. This would have been even more of a problem if the tests were done *in vivo*, but this is also important when considering that the society needs new antimicrobial substances to fight of infections. The results indicate that new solutions for this problem are needed and it is important to move in new directions to be able to cope with the problem of resistance in our normal bacterial strains. Photodynamic therapy, especially applied in the novel delivery systems, is expected to lead to improved antimicrobial therapy.

During our experiments we realized that the MIC testing was performed overnight (16-18 hours) and it might have been better to test the MIC for e.g. 24 hours to directly correlate it to the biofilm testing described in the following chapters. The incubation of the bacteria was approximately 16-18 hours and to optimize the testing we suggest to incubate for preferably 24 hours.

5.2.2. Biofilm growth

After the MIC of the different antimicrobial substances was established, we started the biofilm growth experiment. Christensen *et al.* described the method chosen for the biofilm formation relatively early (Christensen *et al.*, 1985); the current method includes several modifications of the original method. In the testing of biofilm formation two different supplements for the TSB were tried out, namely glucose in addition to NaCl. We also tested the difference between biofilm formation with and without shaking during the incubation. The formation of biofilm was tested for all the strains included in this project. The rest of the method was the same for all the strains and as described above. The resulting biofilm formation is presented in **Table 9**.

Table 9. Biofilm formation The readings are given in optical density (OD).

	Glucose	NaCl	Glucose + shaking (approx. 75 rpm)	NaCl + shaking (approx. 75 rpm)
Staphylococcus epidermidis RH 6-65	0.260	0.320	0.380	0.180
Staphylococcus epidermidis RH 6-47	0.075	0.049	0.041	0.034
Staphylococcus epidermidis RP62A (42-77 (1))	0.220	0.240	0.190	0.110
Staphylococcus epidermidis RP62A (42-77 (2))	0.140	0.190	0.140	0.100
Staphylococcus epidermidis RH 6-61	0.130	0.110	0.070	0.044
Staphylococcus epidermidis RH 6-42	0.170	0.110	0.110	0.069
Staphylococcus haemolyticus RH 51-03	0.076	0.020	0.019	0.011

After evaluation of the results included in **Table 9,** the selection of the method of biofilm growth as well as the selection of strains to be included were done. The method of choice was the use of glucose with shaking and the strains chosen were *Staphylococcus epidermidis* RH 6-65, RP62A (1) and *Staphylococcus haemolyticus* RH 51-03. The reason that these strains

were chosen was that RP62A is a control strain and it is fully characterized, *S. haemolyticus* RH 51-03 is the negative control and RH 6-65 gave a good biofilm as compared to the other strains. Glucose as a supplement to TSB with shaking was chosen due to the good formation of biofilm by RH 6-65 as compared to NaCl and no shaking. The negative control had a rather low OD value in respect to these criteria.

The formation of biofilm in RH 6-65 was better comparing to the other strains; however the growth of biofilm was rather low in comparison to the published work (Christensen *et al.*, 1985, He *et al.*, 2014). For example, He and colleagues reported the growth of biofilm exceeding an OD of 3 (He *et al.*, 2014), but other strains were used in their experiments. This is almost 8 times higher than the highest OD value obtained in our tests. The method has to be optimized to achieve a good formation of biofilm for these strains. Even in the method modified earlier for this project, the OD values were higher than the values we achieved here. Most of other methods or modifications of the original method by Christensen and colleagues (Christensen *et al.*, 1985) apply an incubation time of 24 hours (Wojtyczka *et al.*, 2014, Mishra *et al.*, 2015). This is an additional reason why in the future the method should involved 24 hours incubation.

Even though the OD values were rather low, we decided to proceed with these three strains and the method conditions described above. Although lower growth, we could still see a difference between the strains and that was considered to be the main focus.

5.2.3. Biofilm elimination

When testing the biofilm elimination we decided to continue with all the three selected antibiotics as the positive control for the NCE. The reason why this was done was that there is a little agreement around regarding the treatment of chronic wounds or diabetic foot ulcers with antibiotics. Some scientists still believe that treatment with antibiotics is the right way to go when handling wounds infected with biofilm-forming bacteria and it has been indicated that some antibiotics indeed eliminate biofilms (Wojtyczka *et al.*, 2014). Other researchers argue that the data to support the use of antibiotics are not convincing enough to recommend this treatment in the clinical practice (Høiby *et al.*, 2015). There is a little consensus in the literature available on this topic and this made the choice of antibiotic rather difficult. Vancomycin is often used as a last line treatment and in more complicate infections and

Thoresen also tested this antibiotic last year (Thoresen, 2014). Ciprofloxacin and chloramphenicol were chosen due to the fact that they are often prescribed by the doctors to treat skin treat infections and are included in the Norwegian guidelines for the treatment of diabetic foot ulcers (Akselsen, 2012) in addition to some other antibiotics (Singh *et al.*, 2010, Wojtyczka *et al.*, 2014). In addition, these three antibiotics have three different points of action. Vancomycin impacts the cell wall synthesis, chloramphenicol inhibits protein synthesis and ciprofloxacin inhibits the DNA synthesis. After the MIC test we decided to test the antimicrobial substances in a concentration of 1x MIC, 2x MIC and 3x MIC to ensure that the results are comparable.

We started by testing each of the antimicrobial substance against each strain chosen for this study. The first strain tested was RH 6-65 and the results for this strain at the different concentrations of antimicrobials are presented in **Figure 23**, **Figure 24** and **Figure 25**, respectively. As seen in these figures, the differences in the effect of antimicrobial substances and concentrations are not significant. It seems that vancomycin may have slightly stronger effect than the other antimicrobial substances after 24 hours and that ciprofloxacin might exhibit weaker effect on the biofilm, however the standard deviations are wide. Surprisingly, the control where none of the antimicrobial substances was added also exhibited certain antimicrobial effect. This remains to be further elaborated and more experiments are needed.

When preforming a *t*-test with a 95 % confidence level on these results, surprisingly no treatment (control) appeared to give a significantly reduced growth compared with e.g. ciprofloxacin at 1x MIC after 24 hours (**Figure 23**) and at 2x and 3x MIC after and 24 hours (**Figure 24** and **Figure 25**). The NCE eliminated more biofilm than ciprofloxacin at 2x MIC after 24 hours (**Figure 24**). In addition, more biofilm was eliminated in the groups that received the NCE than both the control group and the ciprofloxacin group at 3x MIC after 6 hours of incubation (**Figure 25**). Unexposed bacteria often exhibit a reduced biofilm-growth compared with the bacteria exposed to the different antimicrobial substances. A reason for this might be that bacteria exposed to a treat forms more biofilm to protect themselves, in contrast to unexposed bacteria that does not have the need for protection. Another point that has to be further investigated is the nutritional status of the bacterial suspensions in the wells. Bacteria with good excess to nutrients often form more biofilm than bacteria with a lower nutritional status. Seemingly, the model has to be evaluated for nutrient availability over the

whole time extent of the incubation and preparation. It would be preferable to know that nutrients were available during the whole process and in an appropriate amount.

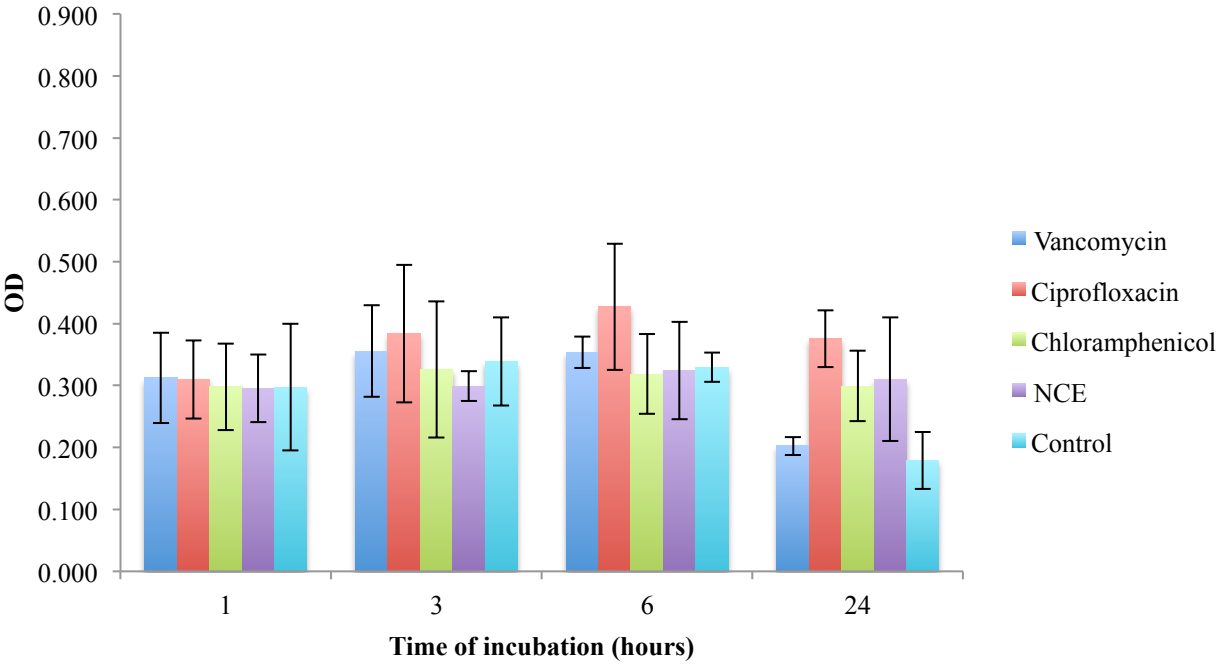

Figure 23. The biofilm elimination of the strain RH 6-65 at 1x MIC of various antimicrobial substances. The NCE samples were exposed to light as described above. The values represent three replicates of three biological parallels.

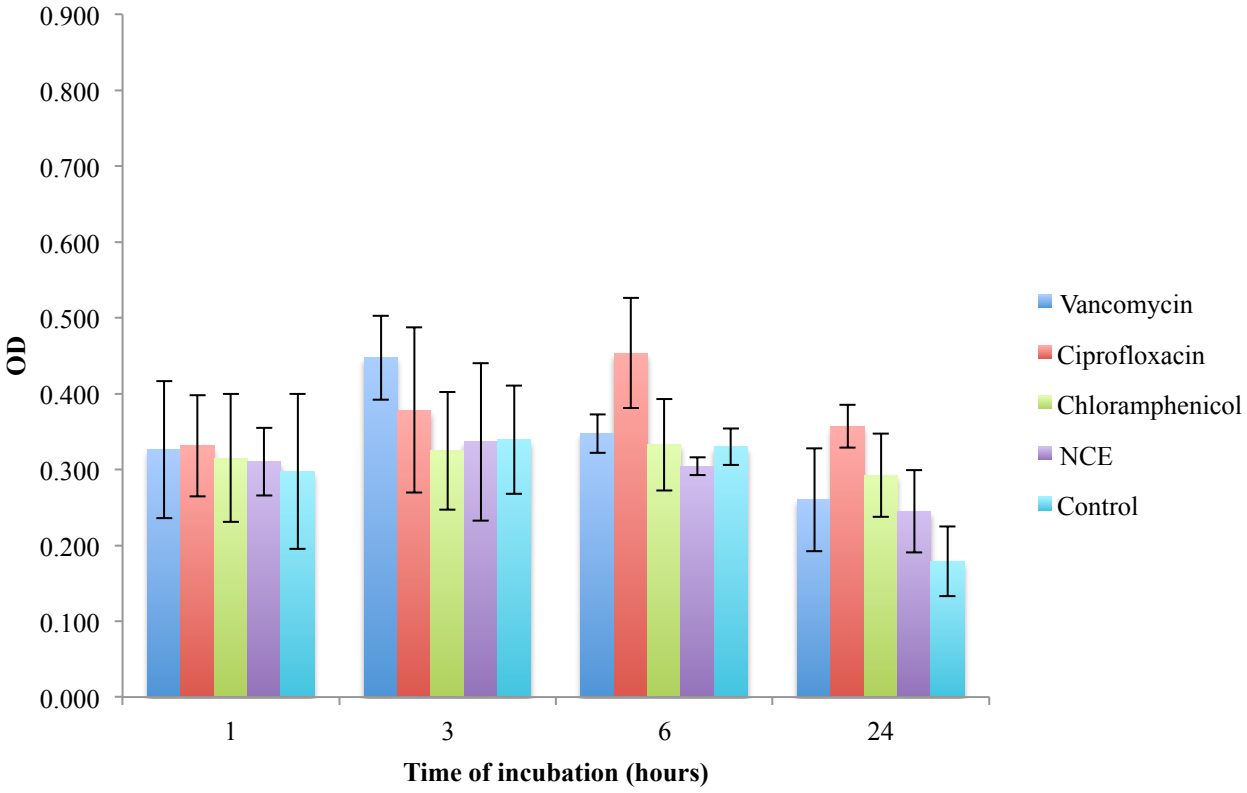

Figure 24. The biofilm elimination of the strain RH 6-65 at 2x MIC of various antimicrobial substances. The NCE samples were exposed to light as described above. The values represent three replicates of three biological parallels.

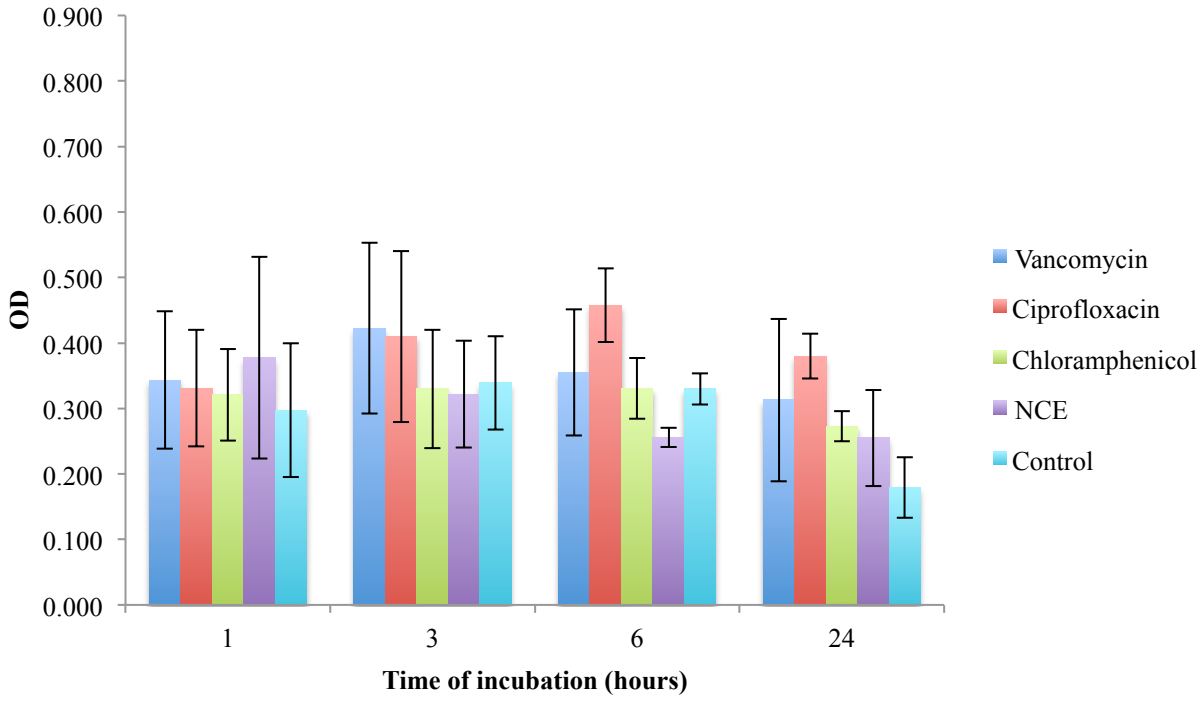

Figure 25. The biofilm elimination of the strain RH 6-65 at 3x MIC of various antimicrobial substances. The NCE samples were exposed to light as described above. The values represent three replicates of three biological parallels.

The next strain we tested was the RP62A (2) under the same conditions as for RH 6-65. The results are presented in **Figure 26**, **Figure 27** and **Figure 28**. As seen in these figures, none of the results were statistically different. The standard deviations of the samples are wide and this was due to the fact that one of the replicates had always a much higher OD value than the other. A *t*-test was preformed for these measurements too, but no statistical difference was detected. One of the possible explanations why one replicate stood out from the rest could be due to limited mixing and possible precipitates in the crystal violet solution.

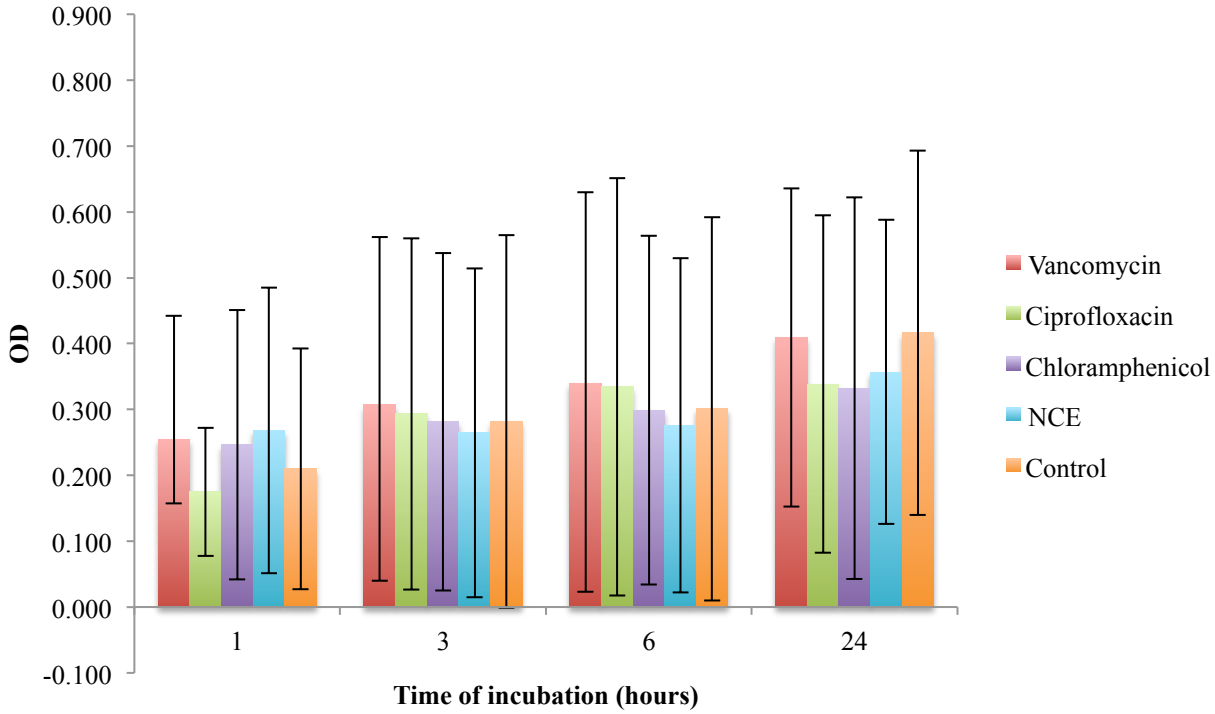

Figure 26. The biofilm elimination of the strain RP62A (2) at 1x MIC of various antimicrobial substances. The NCE samples were exposed to light as described above. The values represent three replicates of three biological parallels.

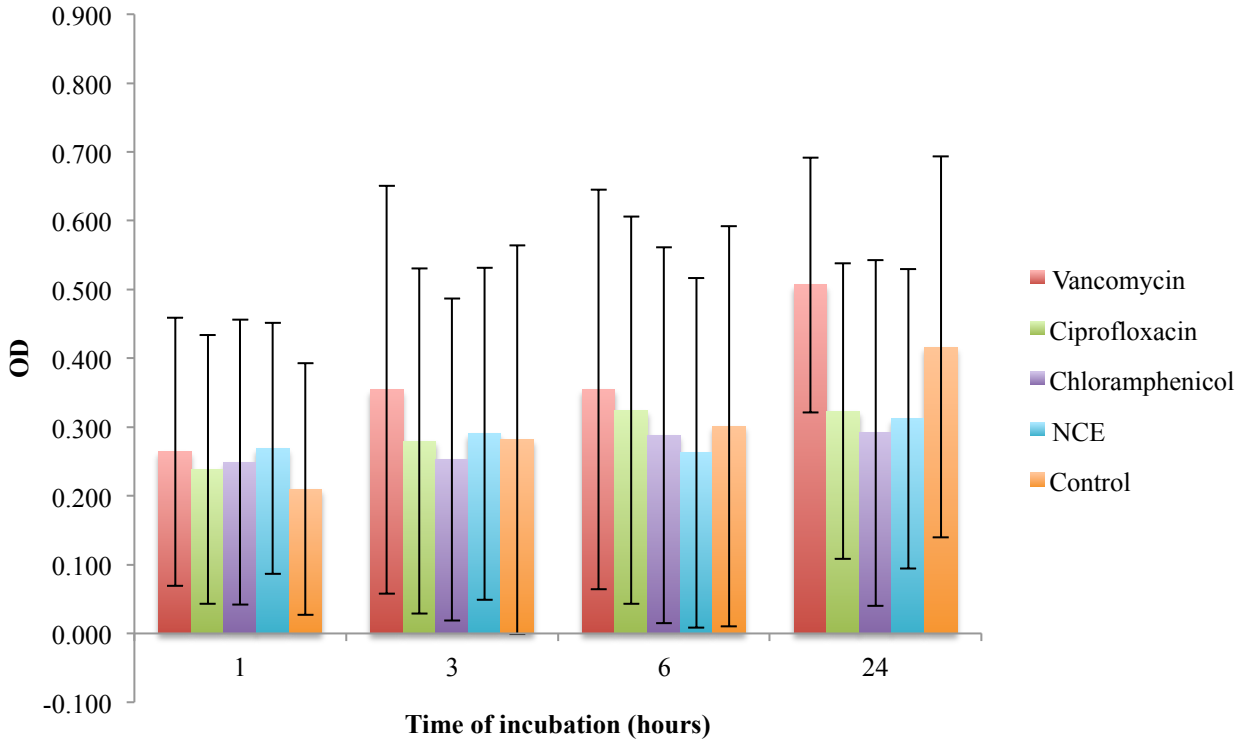

Figure 27. The biofilm elimination of the strain RP62A (2) at 2x MIC of various antimicrobial substances. The NCE samples were exposed to light as described above. The values represent three replicates of three biological parallels.

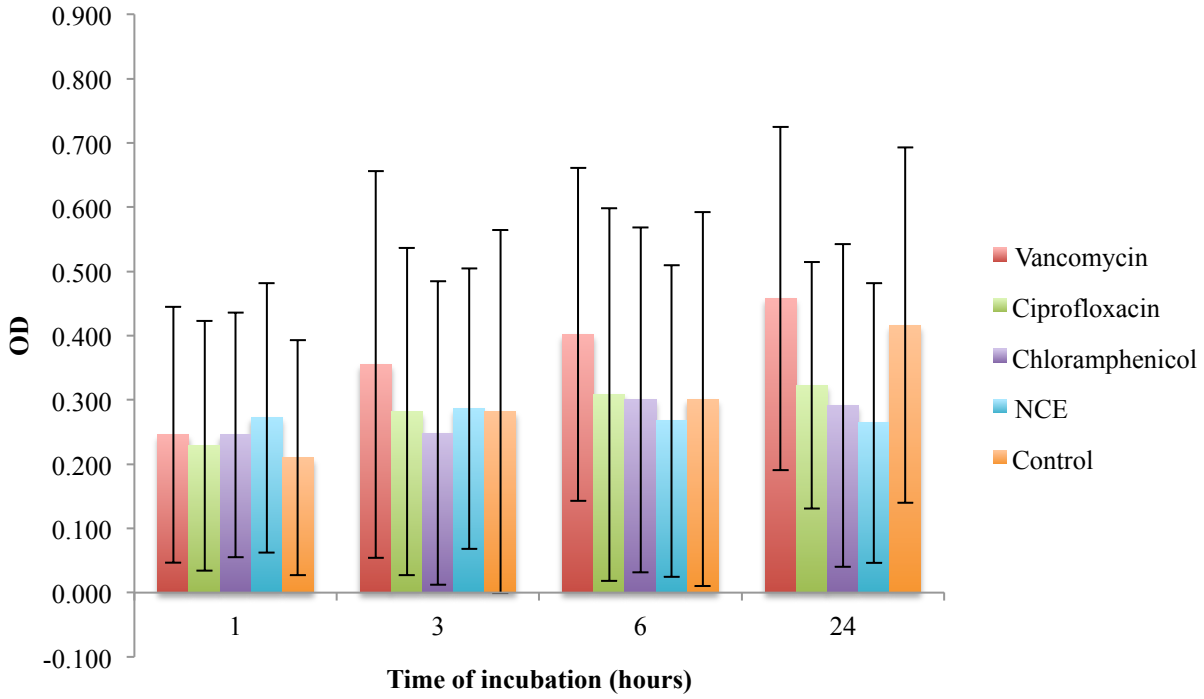

Figure 28. The biofilm elimination of the strain RP62A (2) at 3x MIC of various antimicrobial substances. The NCE samples were exposed to light as described above. The values represent three replicates of three biological parallels.

The negative control, *Staphylococcus haemolyticus* RH 51-03, was also tested in the same manner and the results are presented here. Investigating the results (**Figure 29**, **Figure 30** and **Figure 31**) one can see that the OD values are much lower than for the other strains, indicating a very low bacterial load. When carefully evaluating the OD values for the NCE at e.g. the concentration of 2x MIC (**Figure 30**), it seems that the OD values of NCE are higher than for the other antimicrobial substances at the same concentration. Higher OD values would normally indicate a stronger biofilm formation, but in this case this is not likely scenario. This strain (RH 51-03) is not supposed to form a biofilm, thereof we tried to elucidate this.

In **Figure 32,** the scaling of the diagram is changed; in this experiment the NCE exhibited a higher OD value than other antimicrobial substances. The bacterial load is still rather low, but one can see a clear difference between the NCE and the other antimicrobials. A *t*-test with a 95 % confidence level was preformed and the NCE gave significantly higher OD values than all the other antimicrobial substances including the control at a concentration of 2x MIC after 1 and 3 hours and, in addition, a higher OD value than the antibiotics after 6 hours (**Figure**

32). These results need to be further investigated to explain the reasons behind the effects. One can postulate that there might be some dead planktonic bacteria stuck to the bottom of the wells due to the presence of NCE. In order to eliminate that the NCE interacted with the plate, we tested the interaction between the NCE and the plate free of biofilm. These results are presented in **Figure 33** and indicate that the interaction between the NCE and plate was not the reason for findings in **Figure 32**.

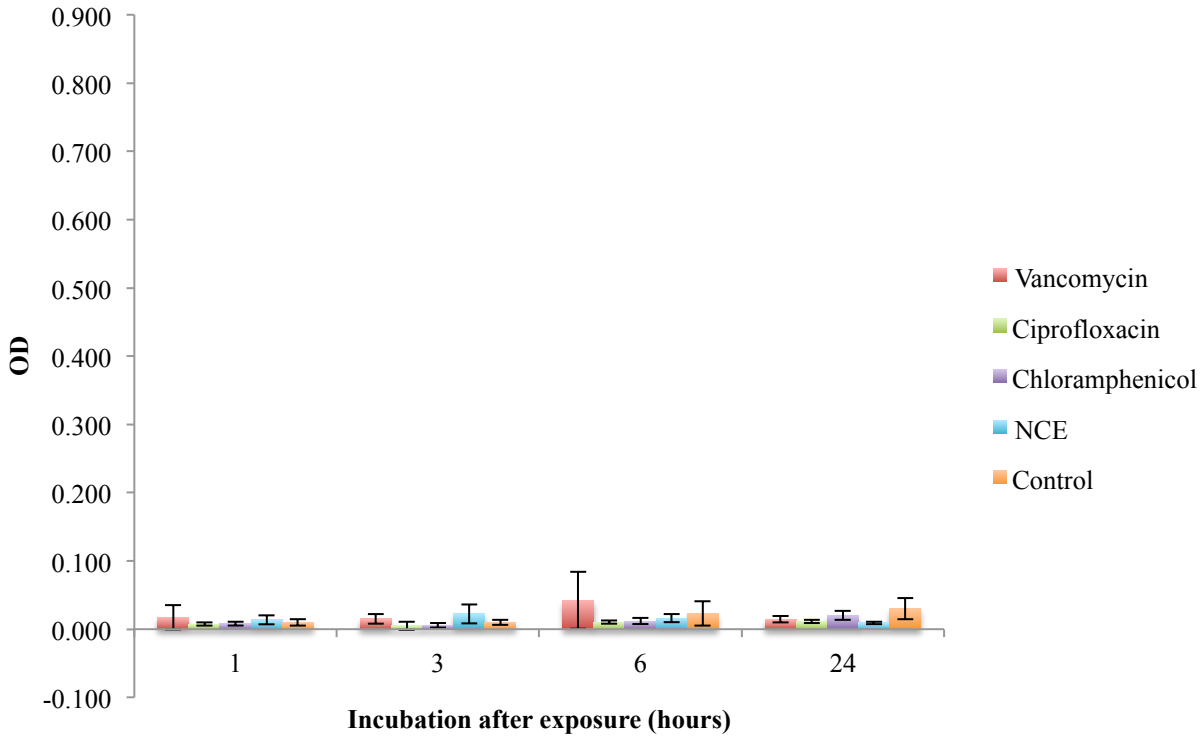

Figure 29. The biofilm elimination of the negative control strain at 1x MIC of various antimicrobial substances. The NCE samples were exposed to light as described above. The values represent three replicates of three biological parallels.

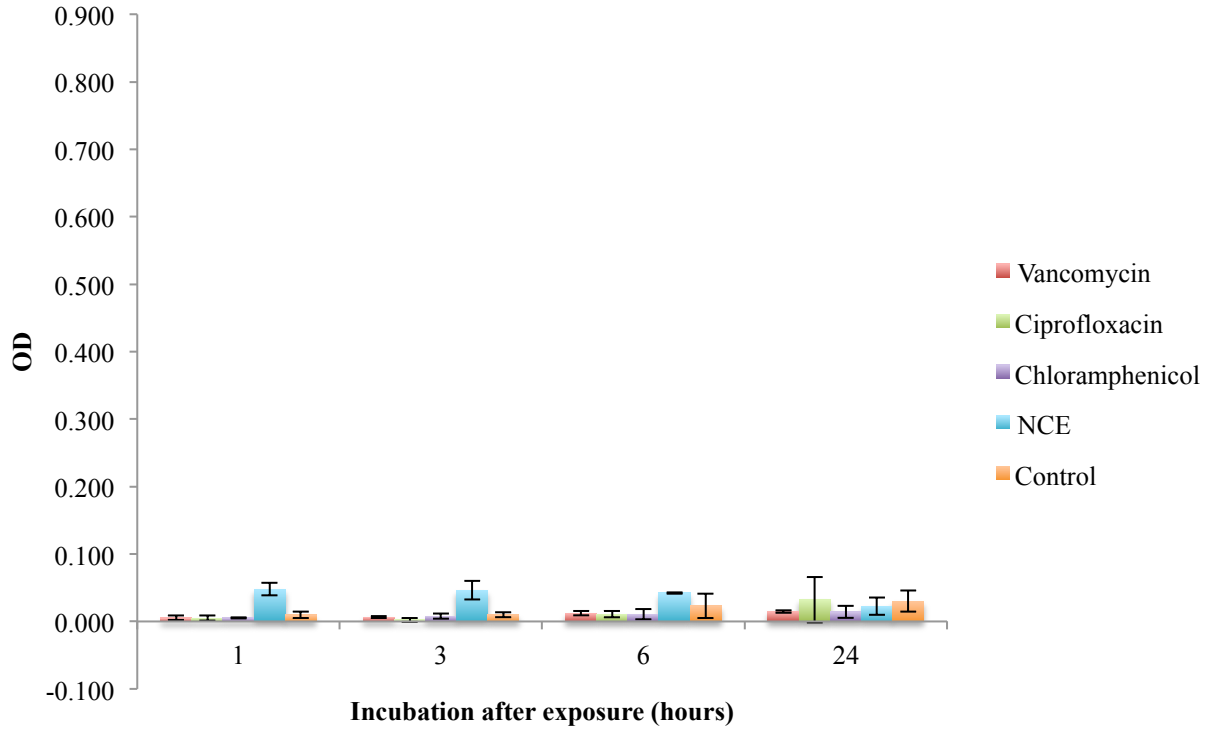

Figure 30. The biofilm elimination of the negative control strain at 2x MIC of various antimicrobial substances. The NCE samples were exposed to light as described above. The values represent three replicates of three biological parallels.

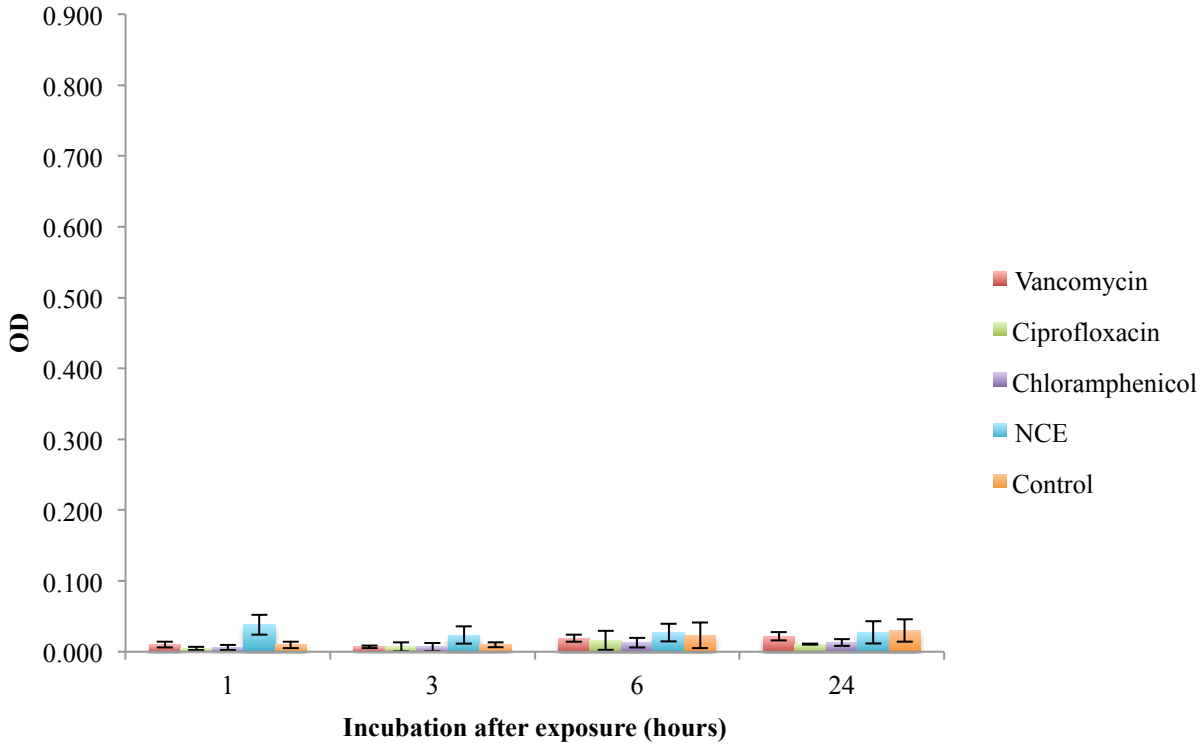

Figure 31. The biofilm elimination of the negative control strain at 3x MIC for each antimicrobial substance. The NCE samples were exposed to light as described above. The values represent three replicates of three biological parallels.

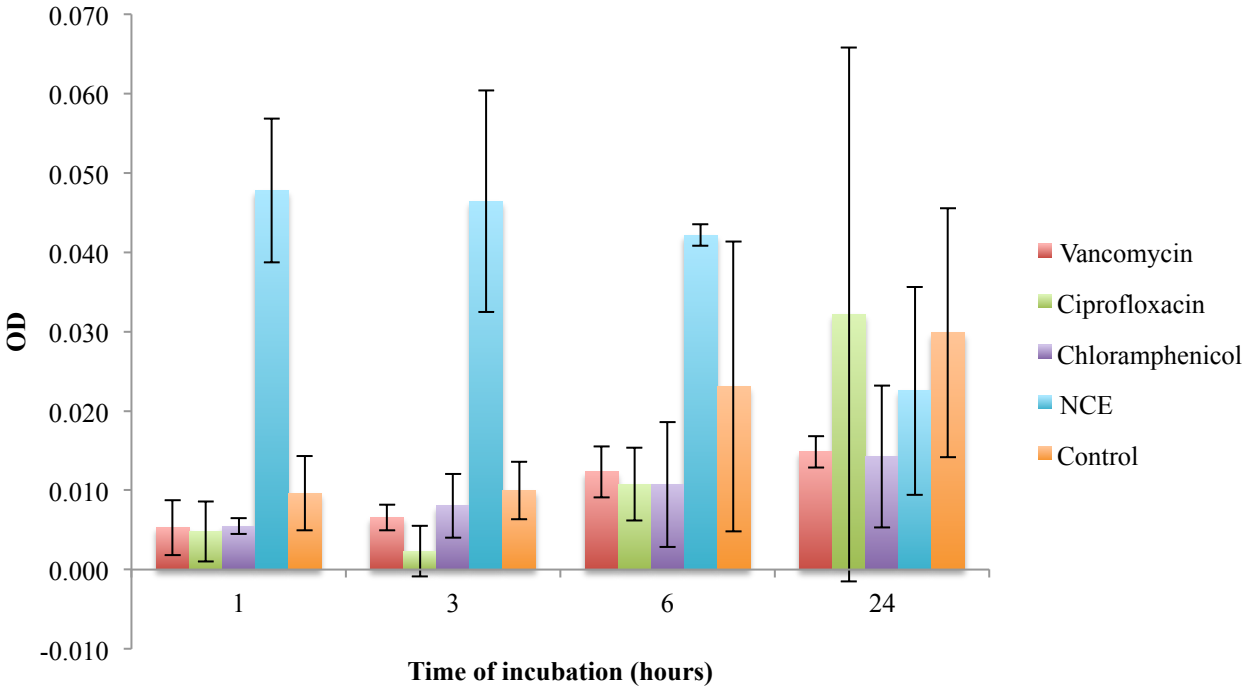

Figure 32. The elimination test of the negative control strain at 2x MIC of various antimicrobial substances. The NCE samples were exposed to light as described above. The values represent three replicates of three biological parallels.

*Here the results are presented in another scale than in **Figure 29 - Figure 31**.

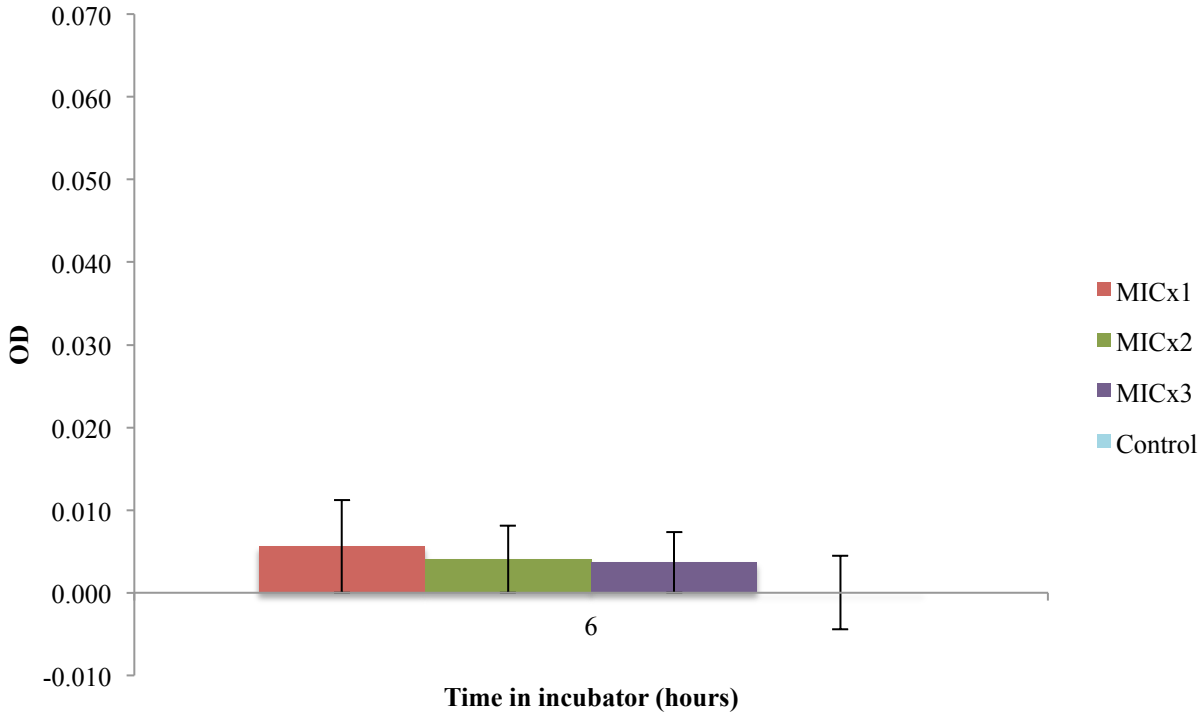

Figure 33. The interaction between the NCE and the bacteria-free plate.

*The same scaling as in **Figure 32** is used.

We decided to include the other type of the strain, namely RP62A, in this set of experiments due to the observed differences between RP62A (1) and RP62A (2) in the MIC test and the biofilm formation without exposure to antimicrobial substances. The measurements for RP62A (1) are presented in **Figure 34**, **Figure 35** and **Figure 36**. The standard deviations were rather high always due to one of the measurements; the other two were quite similar. This made it difficult to confirm the significance in the statistical test. At the concentration of the MIC after one hour both chloramphenicol and ciprofloxacin showed stronger biofilm elimination than both the NCE and the control (**Figure 34**). This result was quite surprising, however similar pattern was observed in the experiment with 2x MIC (**Figure 35**). At a concentration of 3x MIC the NCE gave more biofilm reduction than vancomycin after 3 hours of incubation (**Figure 36**). It seems as the NCE eliminates more biofilm than these antibiotics, but due to wide deviations this needs to be further confirmed.

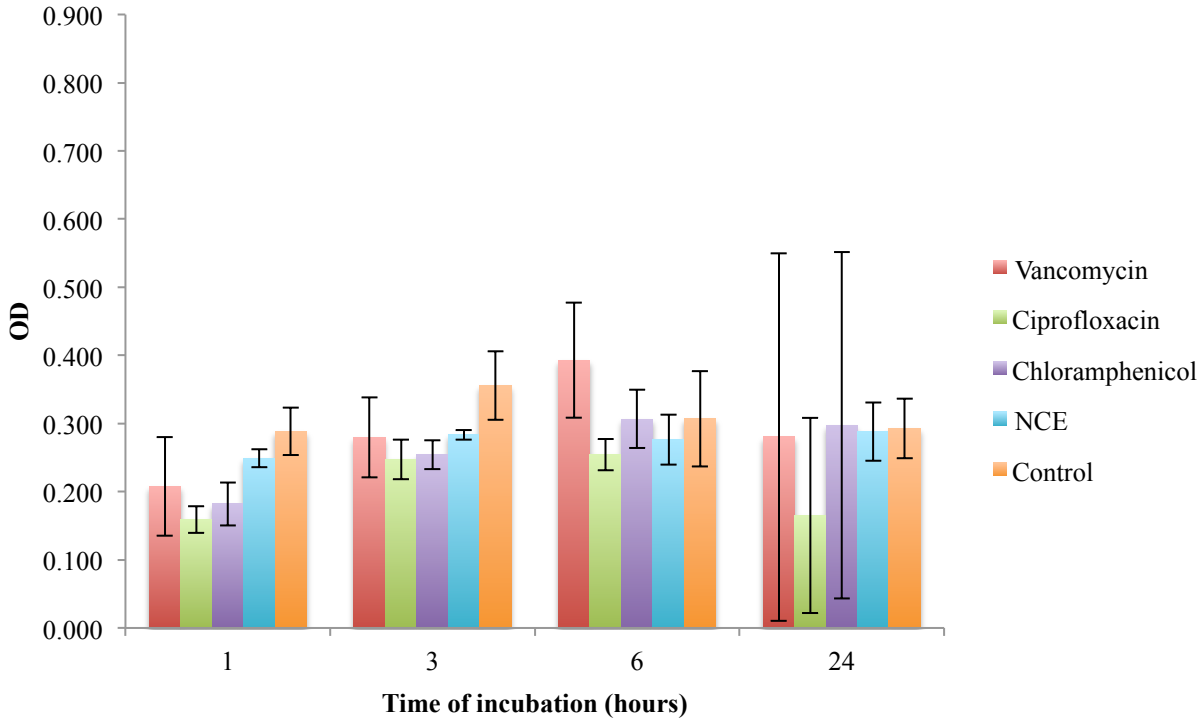

Figure 34. The biofilm elimination of the strain RP62A (1) at 1x MIC of various antimicrobial substances. The NCE samples were exposed to light as described above. The values represent three replicates of three biological parallels.

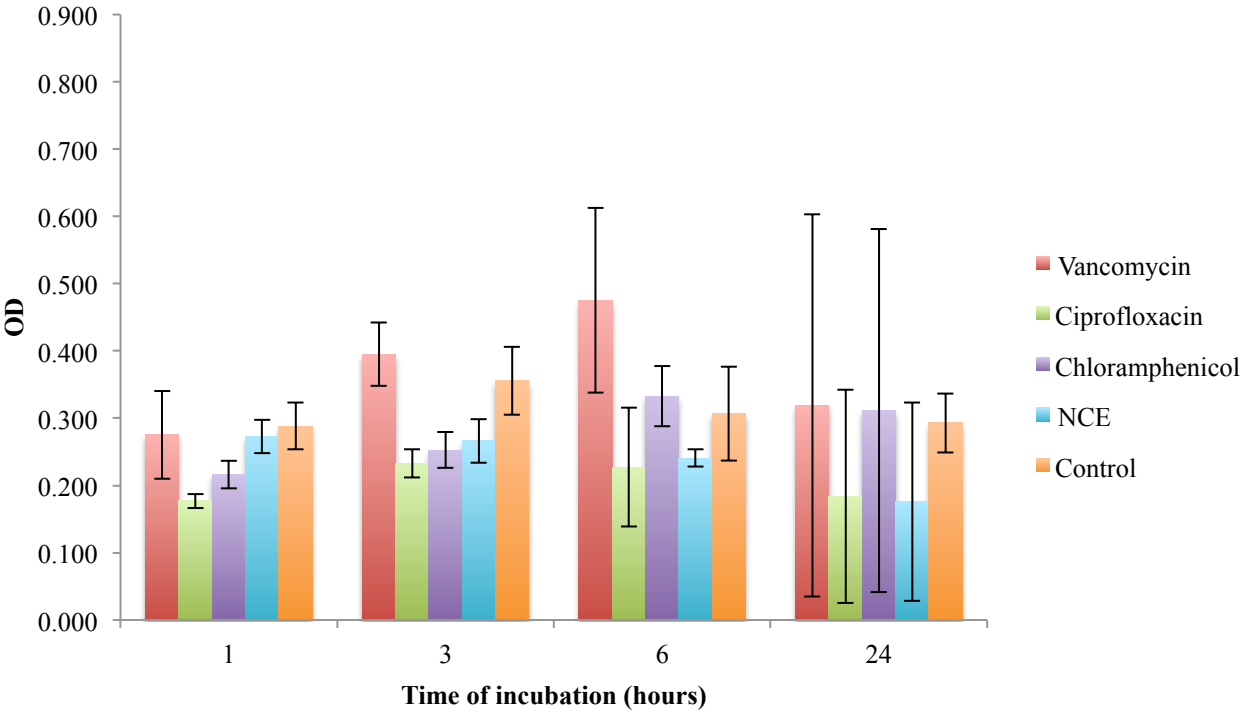

Figure 35. The biofilm elimination of the strain RP62A (1) at 2x MIC of various antimicrobial substances. The NCE samples were exposed to light as described above. The values represent three replicates of three biological parallels.

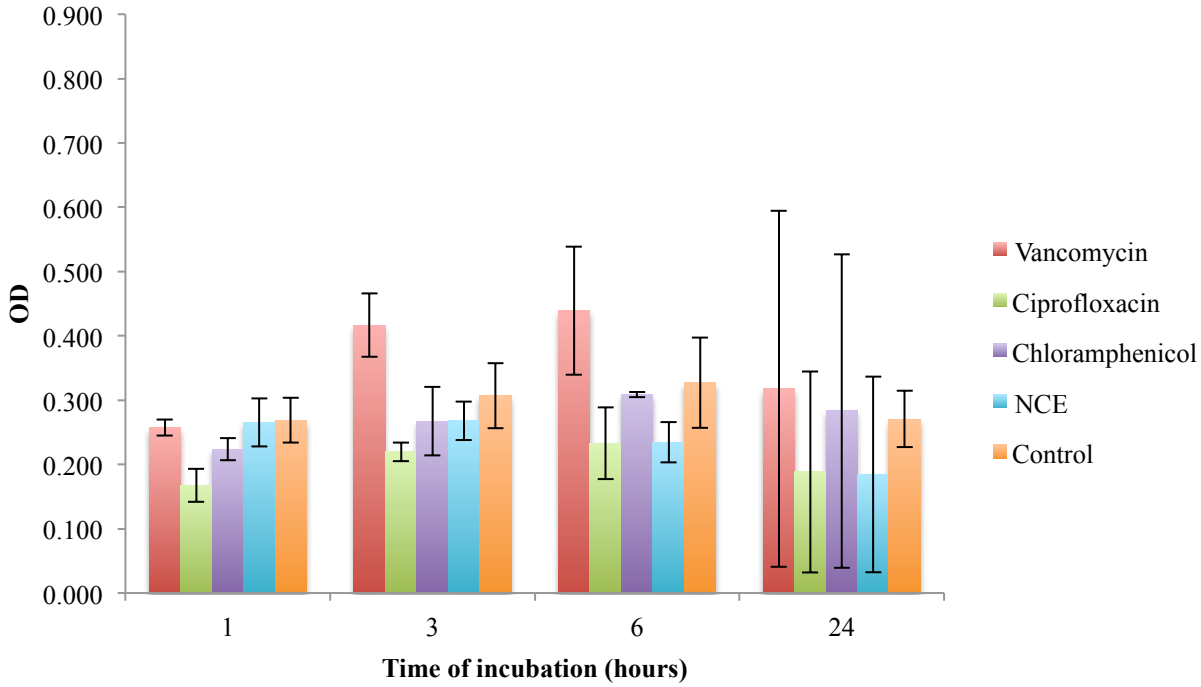

Figure 36. The biofilm elimination of the strain RP62A (1) at 3x MIC of various antimicrobial substances. The NCE samples were exposed to light as described above. The values represent three replicates of three biological parallels.

As mentioned earlier, the two variants of the strain RP62A performed differently in both MIC testing and biofilm formation in the initial testing, therefore we used both in the testing. After the biofilm elimination with the different antimicrobial substances, we were not able to show a statistical difference between RP62A (1) and RP62A (2) and in a *t*-test there were no differences either at a confidence level of 95 % or at even 90 % (data not shown). Considering these results and the time limit, we continued the experiments with one of the strains, strain nr. 2 represented in **Figure 26**, **Figure 27** and **Figure 28** earlier.

5.2.4. Biofilm elimination with the NCE in solution and without exposure to light

We continued with the strains RH 6-65 and RP62A and the incubation time of 6 and 24 hours to test the effect of the NCE without the light exposure. The reason why we discontinued the negative control was the observed limited growth and effect of the antimicrobial substances. We chose the incubation time of 6 and 24 hours because the best effect of the NCE was determined under those incubation times. The results of testing on RH 6-65 are presented in **Figure 37**. None of the OD values were significantly different at a 95 % confidence level.

The biofilm formation seems to be stronger in the bacteria exposed to the NCE when observing **Figure 37**. This indicates that the NCE does not exhibit an anti-biofilm activity when not exposed to light, as expected.

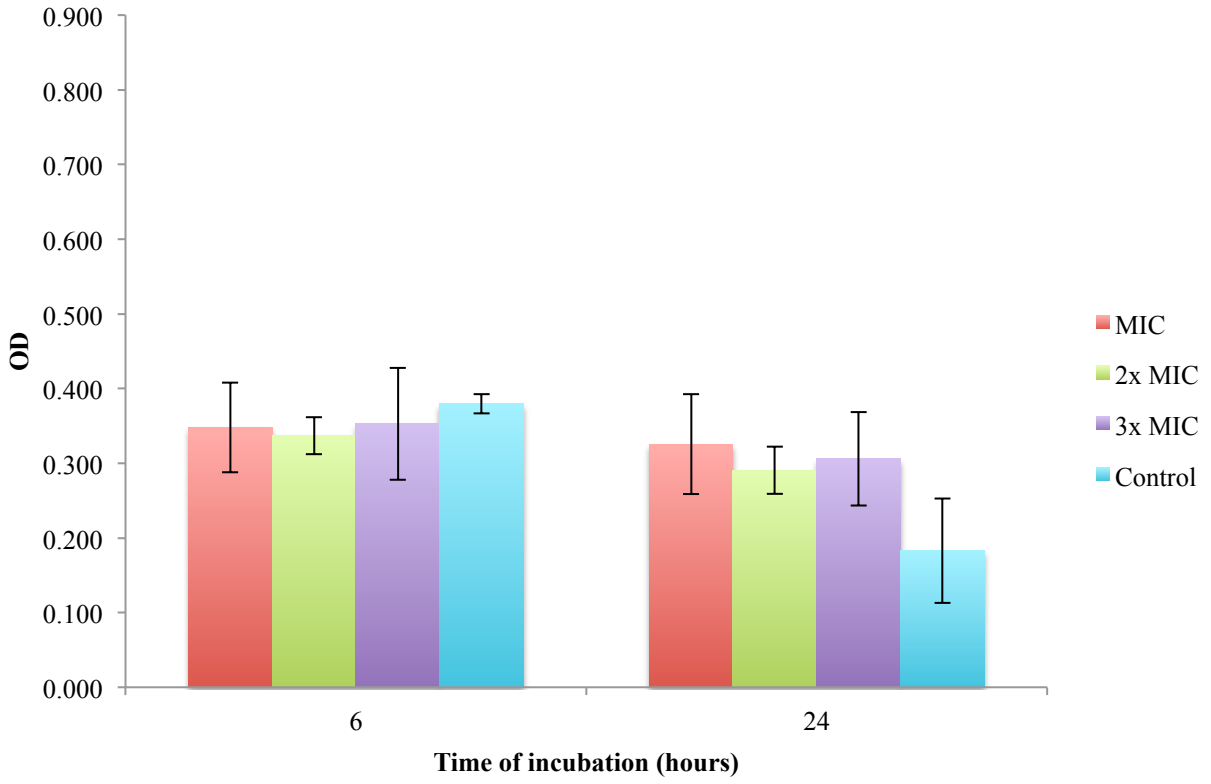

Figure 37. The impact of the NCE on the strain RH 6-65 without the exposure to light. Represented by two replicates of three biological parallels.

The strain RP62A (2) was also tested in the same manner and the results are presented in **Figure 38**. The biofilm formation was found to be weak for all the different concentrations and the control in both 6 and 24 hours of incubation and there was no statistical difference between any of the different concentrations or the control after an incubation of 6 hours. After 24 hours of incubation is seems that the inhibition of the biofilm is stronger with higher concentration of the NCE. As mentioned, the NCE is not expected to exhibit the effect when not exposed to light; however, based on these results it seems to have an effect by eliminating more of the biofilm. The preparation of plates was done in as dark conditions as possible; however it was not possible to prepare the plates in the total absence of light. This has to be investigated further.

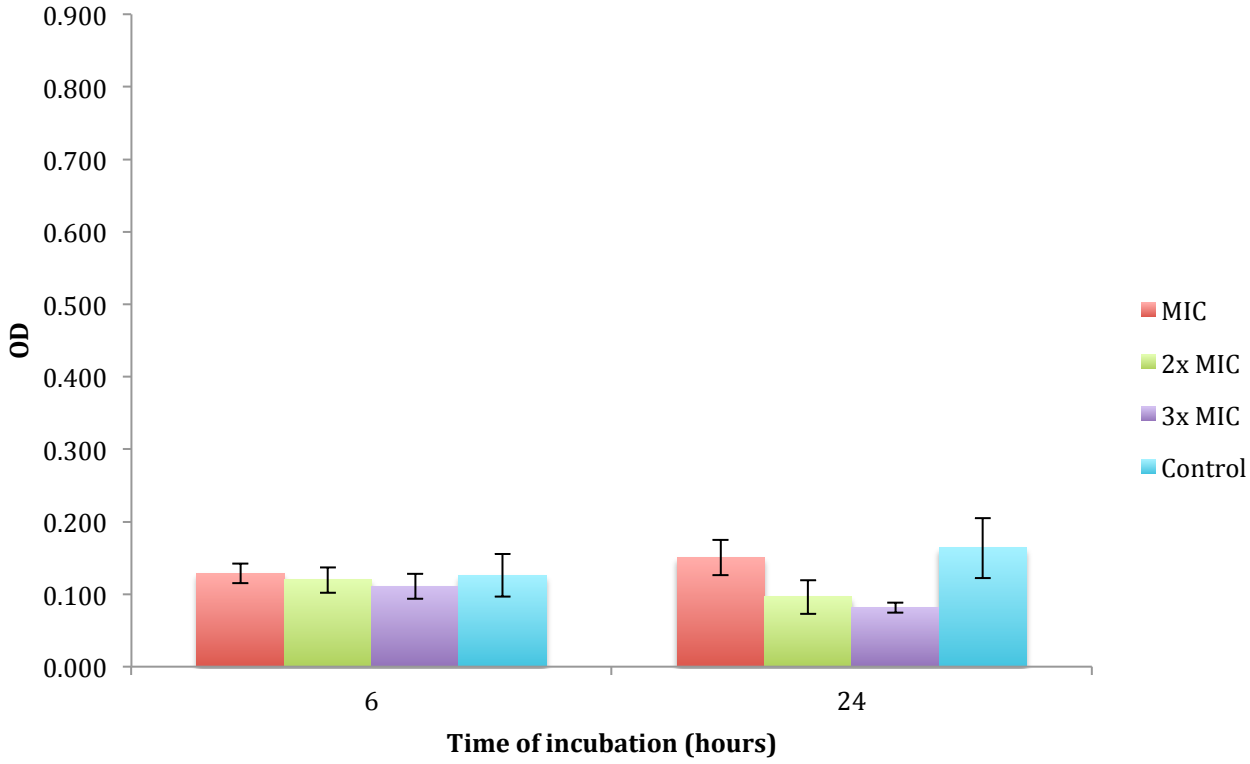

Figure 38. The impact of the NCE on the strain RP62A (2) without the exposure to light. Represented by two replicates of three biological parallels.

5.2.5. Biofilm elimination by NCE-containing NPs

When the testing of the NCE in solution was done, we started the testing of the NCE-containing NPs. The concentration of the NCE was changed from the originally determined MIC to concentrations of 0.01, 0.1 and 1 mM to this test due to the low entrapment and because the volume of NPs suspension needed to carry out the test at the previously described concentrations would be too large due to low entrapment. The concentrations of 0.01, 0.1 and 1 mM were used last year by Thoresen and we decided to test them again to investigate if they had an impact on the biofilm (Thoresen, 2014). The strains RH 6-65 and RP62A (2) were also used for biofilm elimination with NCE-containing NPs. Again, we started with the strain RH 6-65 and the results are presented in **Figure 39**. The standard deviations were quite large for these OD values too. Due to the wide standard deviations, there were no statistical differences between any of the concentrations. The biofilm formation is seemingly stronger in the bacteria exposed to the NCE than in the control, suggesting that we were not able to eliminate the biofilm in this strain (**Figure 39**).

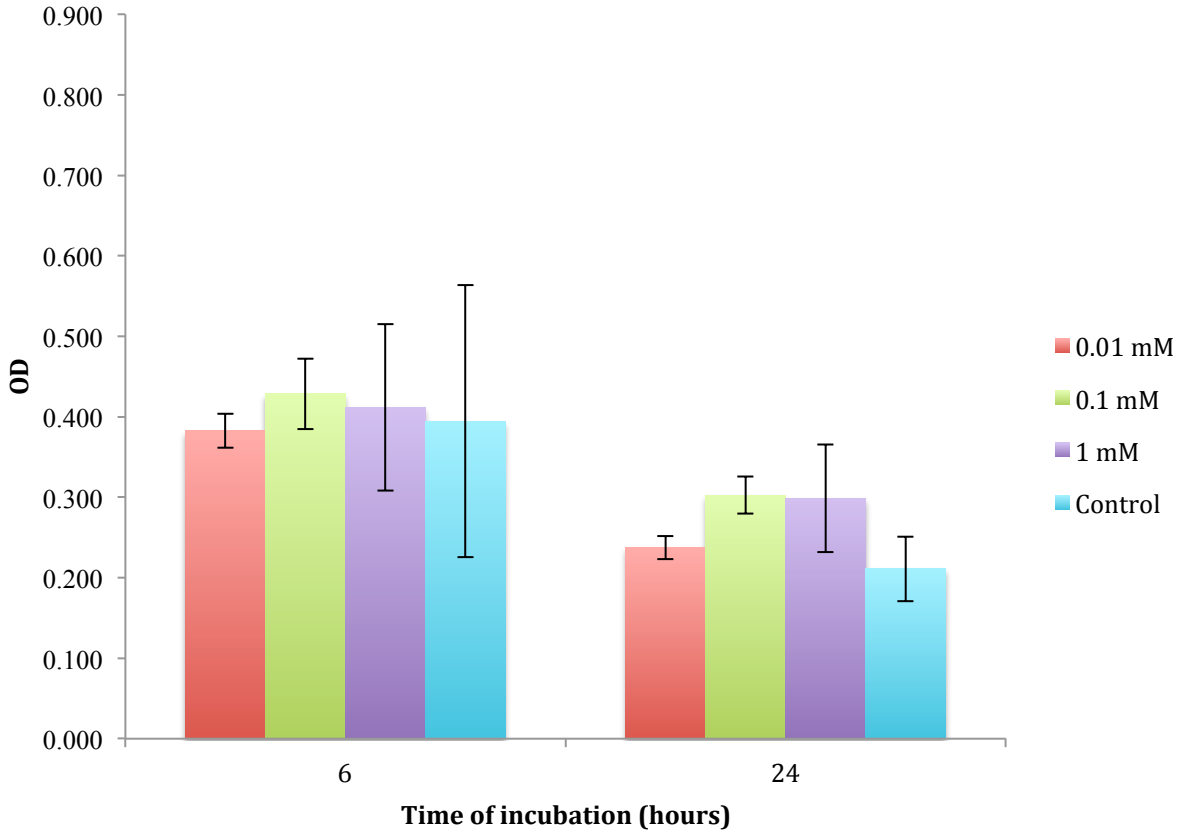

Figure 39. The effect of NCE-containing NPs on the biofilm elimination of the strain RH 6-65. Represented by four replicates of three biological parallels.

The data collected from the strain RP62A (2) are presented in **Figure 40**. In contrast to the strain RH 6-65, RP62A (2) seemingly demonstrates a weakening biofilm formation when exposed to the NCE, especially at concentrations of 0.1 and 1 mM, compared with the control. The differences between the bacteria exposed to the NCE and the control were not statistically significant, but a trend is indicated. The standard deviations were large for this strain as well, but there was a statistical difference between 0.1 and 1 mM after 24 hours of incubation; bacteria exposed to 1 mM NCE formed a weaker biofilm than when exposed to a concentration of 0.1 mM (**Figure 40**). This difference between the two concentrations indicates a decline in biofilm with increased concentrations of the NCE. Seemingly the NCE-containing NPs have the potential to eliminate biofilm in this strain, but more data is needed to prove the effect.

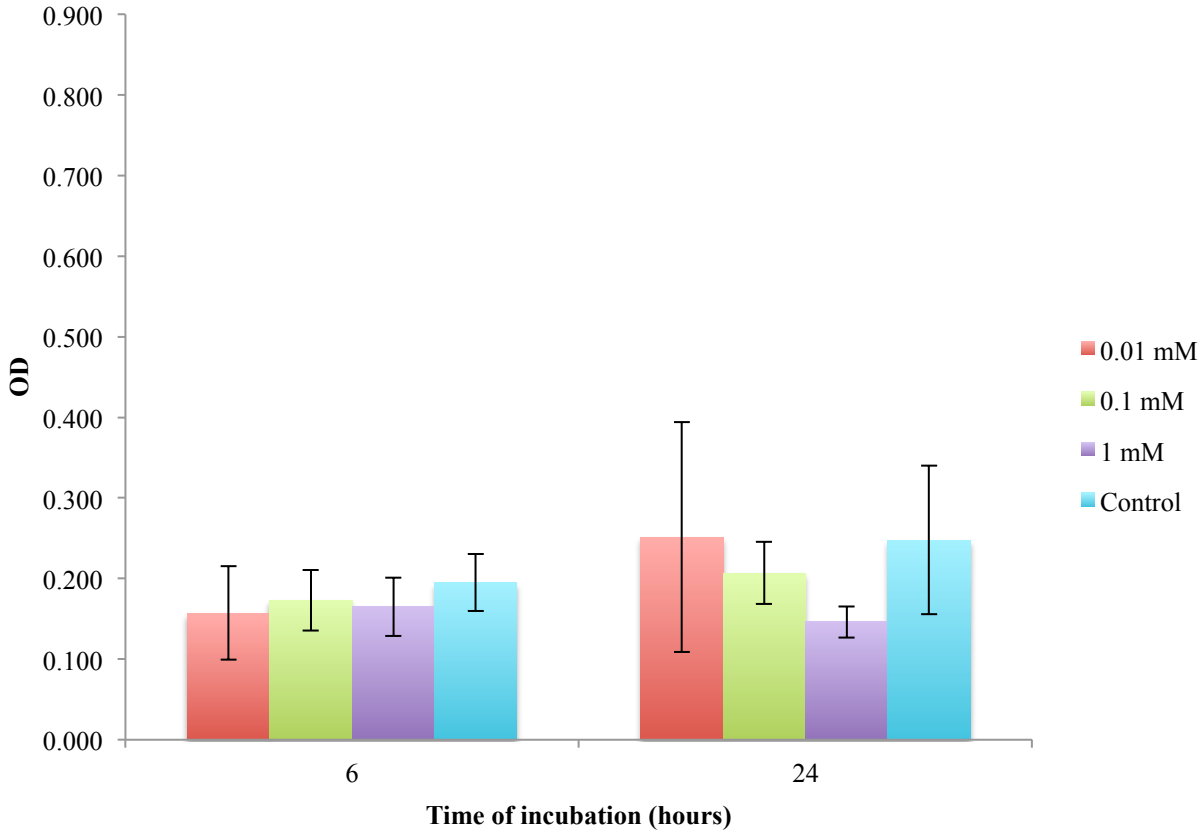

Figure 40. The effect of NCE-containing NPs on the biofilm elimination of the strain RP62A (2). Represented by four replicates of three biological parallels.

5.2.6. Biofilm elimination by empty NPs

The NPs are expected to exhibit an antimicrobial effect due to chitosan present in the vesicles. To compare with the previous work of Thoresen (Thoresen, 2014), we also used the concentration of 35 mg/mL of the empty NPs, but included the concentration of 17.5 mg/mL as well, as we tried to see if the effect was dose-dependent. In addition, the NPs concentration of 17.5 mg/mL was included as it might be possible to increase the entrapment of the NCE, as explained in the section 5.1.3. If it is possible to increase the entrapment in later studies, the concentration of the NPs would decrease accordingly, that is if the same concentrations of the NCE (0.01, 0.1 and 1 mM) were to be investigated. The effects of the empty NPs on the strain RH 6-65 are presented in **Figure 41**. Most of the results are according to what was expected based on the previous findings. The OD values were seemingly reduced after 24 hours of incubation compared to the OD values at 6 hours of incubation, except for the OD value for the concentration of 35 mg/mL after 24 hours of incubation. At this concentration, the value is

very high indicating a stronger biofilm formation. The biofilm formation differs significantly from 17.5 mg/mL at the same incubation time (**Figure 41**). At this concentration (24 hours) NPs failed to improve the activity as compared to 6 hours, and the only reasonable explanation for this discrepancy could be the experimental error. At the concentration of 17.5 mg/mL (**Figure 41**), it seems as there might be higher biofilm elimination after 24 hours of incubation compared with 6 hours of incubation. This is an indication of an anti-biofilm activity of the NPs, but this is not a statistically significant result and so different from the control. The incompatibility between the results of 17.5 and 35 mg/mL is another indication that there might be an experimental error present. The testing of anti-biofilm activity of the empty NPs on RH 6-65 needs to be repeated, and more replicates are necessary to provide enough data to draw a conclusion.

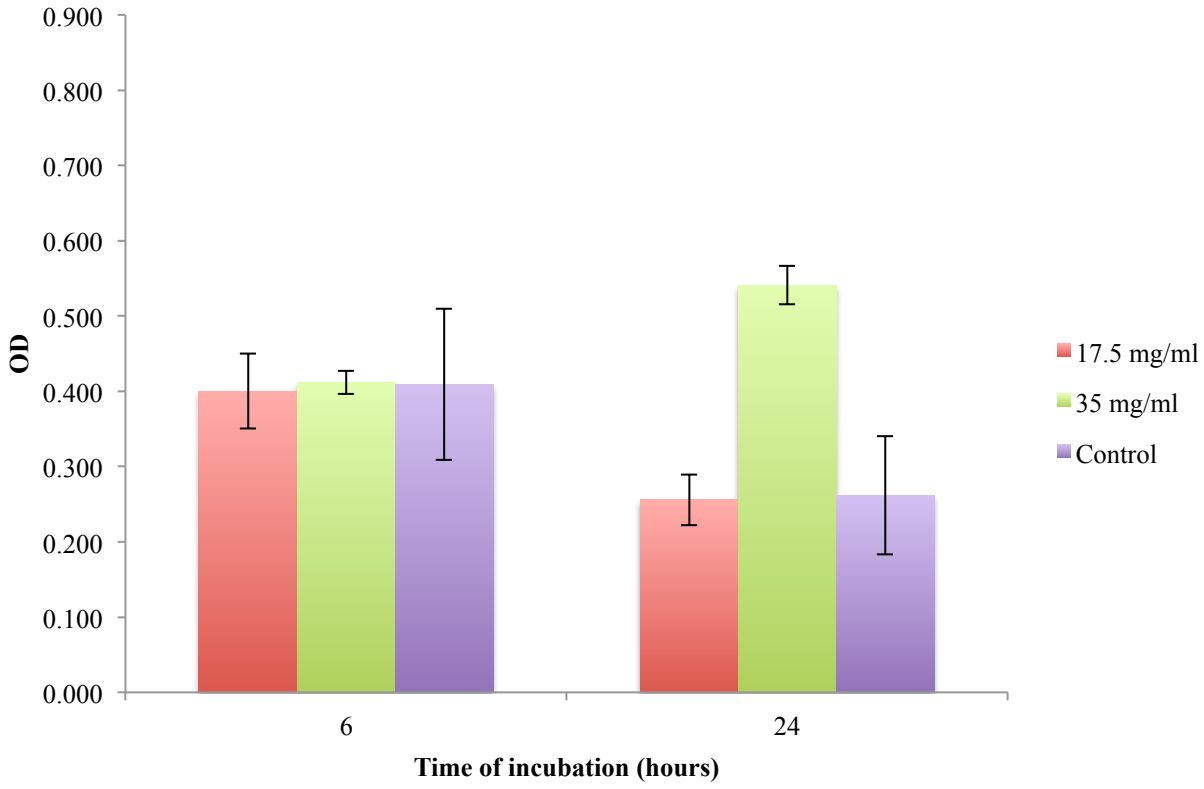

Figure 41. The effect of the empty NPs on biofilm elimination of the strain RH 6-65. Represented by two replicates of three biological parallels.

The findings for the strain RP62A are presented in **Figure 42** and these findings indicate that NPs have no anti-biofilm effect on their own. These results were rather unexpected. The OD value for the NPs concentration of 35 mg/mL after 24 hours of incubation remains to be very

high. The number of replicates in this test was only two and these two deviated from each other, which could be one of the reasons for this result (**Figure 42**). Unfortunately, due to the time limitations, the experiment could not be repeated, and remains to be further investigated. We have considered that one reason for this failure of chitosan-based NPs to exhibit the effect may be the precipitation of the NPs applied in rather high concentration and the incubation time. By naked eye, we were not able to detect the precipitation of NPs. Thoresen (Thoresen, 2014) reported that empty NPs caused the reduction of the biofilm as compared to untreated biofilm, but the standard deviations were quite high in their experiment and they also failed to prove the significance. Their method of biofilm preparation was different from ours. They had amongst other an incubation time of 24 hours in the biofilm formation and they resuspended the bacteria in NaCl as they made the initial bacterial suspension, whereas we incubated for 14 hours and diluted the bacteria in TSB with glucose in the initial bacterial suspension. The only statistically different values (confidence level of 95 %) in our results exist between the control and 35 mg/mL NPs after 6 hours incubation time (**Figure 42**). The OD values were higher for the NPs than the control suggesting that empty NPs do not have anti-biofilm potential on their own in this strain.

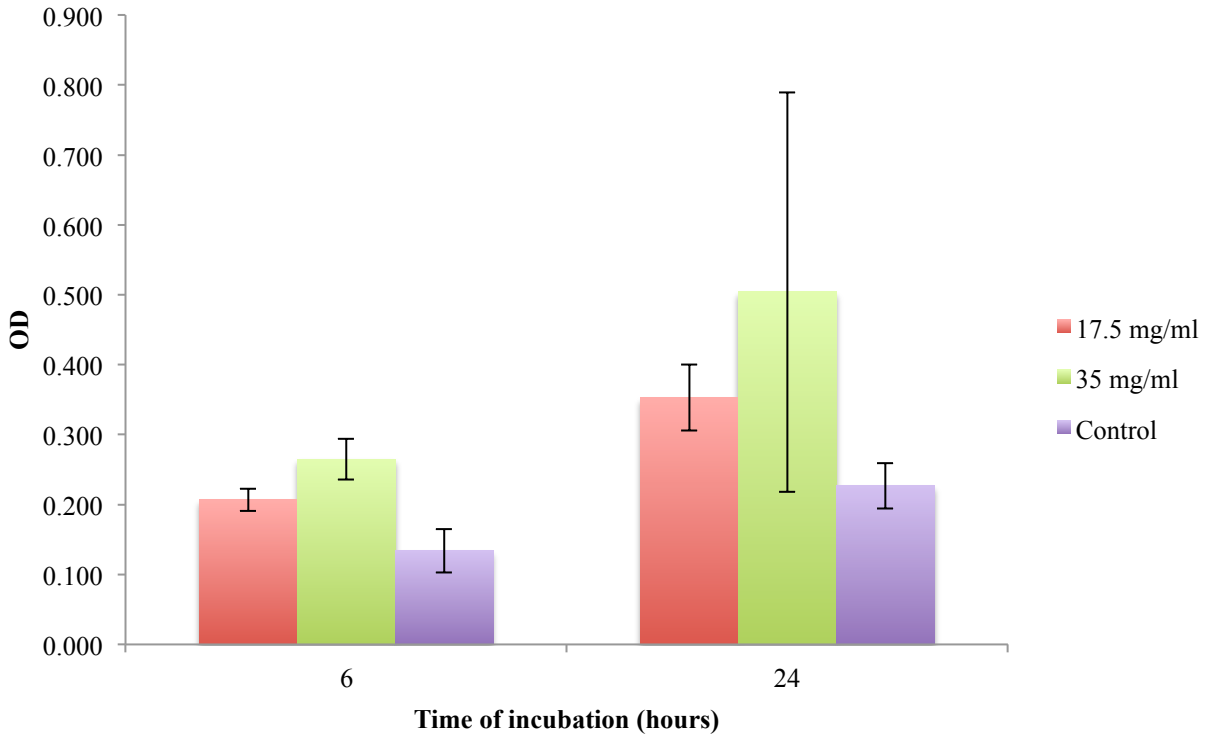

Figure 42. The effect of empty NPs on the biofilm elimination of the strain RP62A (2). Represented by two replicates of three biological parallels.

5.2.7. General observations in biofilm formation and elimination testing

We can state that the NCE has an effect on the biofilm; however, the significant effect of the NCE in solution or in NPs has not been proven. More testing is needed to solve this problem. The results in **Figure 40** suggest that the use of NPs as delivery system for NCE might offer a solution to this problem as chitosan can provide synergistic anti-biofilm effect to the NCE. It would be interesting to try to expand the time of incubation to investigate if the effect increased when the growth time is increased or if there would be a regrowth or stagnation of the effect indicated (**Figure 40**). Hopefully the NPs enable the NCE ability to eliminate more of the biofilm and potentially make the effect longer lasting to provide the immune system enough time to eliminate the rest of the bacteria. We were planning to conduct the NCE release studies but due to constrain of time could not complete those studies in this project. If a biofilm regrowth is indeed taking place, one possible solution could be to use a double or multiple exposures of the NCE-containing NPs as photodynamic treatment. If multiple exposures are necessary, the NPs might be able to reduce the potential adverse effects of the substance, linked to the use of NCE in a free form. This line of research should be further investigated.

More extensive optimization of the light dose is required. In this project we only used a pre-set light dose of 37 J/cm^2 at a distance of 5 cm for 8 minutes and 49 seconds to be able to compare our findings with the previous results of Thoresen (Thoresen, 2014). It would be beneficial to invest more time in optimizing the light doses to see if the effect of the NCE might change/improve. The lamp has a pre-setting of light dose versus time; thereof the time frame of the exposure in this project was pre-set. The distance between the light source and the plates should also be further investigated as we have indications that it affects the treatment efficiency.

The effect of the empty NPs was not found to be as expected as we hoped for the stronger effect of carrier particles. As mentioned earlier, the response of RP62A (2) to the empty NPs were unexpected (**Figure 42**). We expected this strain to be more affected by the empty NPs; the more prominent effect of chitosan, a constituent of NPs was expected and it remains to be seen whether the growth conditions of only 16-18 hours might be the reason for such a week response.

We used two types of bacteria from the same stain, the RP62A. In the initial MIC test and the biofilm formation without exposure to any antimicrobial substances we saw a difference between RP62A (1) and (2) and decided to used both in the experiments. However, throughout the testing, the difference between the RP62A (1) and (2) was not on a significant level when the biofilms were exposed to the different antimicrobial substances in the biofilm elimination test; the last part of the antimicrobial testing was carried out with only the RP62A (2).

Even though RP62A (1) and (2) appear at the final stage of the project to be identical, the difference they exhibited in the initial testing was interesting. Phenotypic shift or switching have been described in literature and might be a possible explanation of this phenomenon (Sousa *et al.*, 2011, Corona and Martinez, 2013). It is a known fact that bacteria may change according to the stress factors, as their survival technique. Phenotypic switching, also called the phase variation, is described as a switch between two phenotypic states and this switch is reversible. These changes occurs only in small parts of the bacterial population (Sousa *et al.*, 2011). It might be possible that these bacteria exhibit different phenotypic characters depending on the growth conditions, but to explain this and to confirm that the phenotypic switch indeed occurred in our conditions more investigation is needed. Phenotypic resistance to antibiotics has also been reported. Corona and Martinez summarized the different strategies to address and deal with this type of resistance. They described four events: i) the biofilm formation, ii) the persistent cells that are not killed easily by the antimicrobial substances, iii) the changes in permeability when the bacteria e.g. have a reduced amount of transporters or an increased amount of efflux pumps in the cell wall and iv) when physiological condition in the bacteria causes drug indifference e.g. when the bacteria is not responding to the antimicrobial substance because they are not dividing or are in a metabolic resting period (Corona and Martinez, 2013). Biofilm formation is often explained as a phenotypic resistance therefore it might be possible that two types of the same strain are actually exhibiting different characters.

6. Conclusions

In this project we evaluated the anti-biofilm effect of NCE-containing NPs with the intent that this might be the new approach in treatment of chronic biofilm-infected skin wounds. Although the anti-biofilm effect observed in this study was minimal, the results indicate that NCE bears certain potential in respect to anti-biofilm activity. We realized that the optimization of the bacterial biofilm growth is needed in addition to a better understanding of the ideal concentrations of the NCE for biofilm elimination. We believe that the results can serve as a strong base for further formulation development. In addition, the reliable and reproducible methods for the biofilm formation and evaluation are necessary to provide enough data to conduct a proper evaluation of the potential of the photodynamic therapy. In this respect, the light exposure conditions need to be closer optimized

The potential of both the NCE and the NPs needs to be further investigated. The optimization process of the NPs needs to continue. It might be possible to increase the entrapment of NCE and this will have an effect on the biofilm elimination. The need for more stability studies are also needed, even though it seemed that the stability of the NCE increased when entrapped in the NP. The stability of the NPs also needs an evaluation to ensure the optimal drug delivery system.

The findings in this project are promising and should be of high interest for further utilization of a novel field of nanoparticle-based photodynamic therapy.

7. Perspectives

Short-term perspectives

- Optimize the preparation of the NPs including:
    - Find the optimal amount of NCE to entrap in the particles.
    - Optimize the entrapment of the NCE, possibly by using different preparation method.
    - Investigate both the short and long-term stability of the NCE-containing NPs.
    - Evaluation of the analytical methods to ensure reliable results. Investigate if implementing a standard for the degradation product might increase the precision and reliability of the HPLC method.
    - Investigate the NCE release profile.
- Find the most appropriate antimicrobial control, that is; a control that have the potential to work in the formed biofilm. This might be achieved through the time-kill studies of different antimicrobial substances and their effect on the specific strains included in the project.
- Optimization of the biofilm formation and elimination, including:
    - Ensure a stable and large, viable biomass in the biofilm. This might be achieved through the optimization of the method described in this thesis or by applying the alternative method for the biofilm formation.
    - Evaluate the concentration needed to reach the optimal NCE effect.
    - Evaluate the light dose, exposure time and exposure distance to ensure optimal photodynamic therapy.
    - Evaluate the staining and plate reading conditions.
    - Evaluate and optimize the biofilm elimination by the NPs, especially the method used to evaluate the empty NPs, for example potential precipitation of NPs.

- The effects of the NCE in free form on the negative control need to be further investigated. Evaluation and validation of the method to assure that no methodical error is introduced during the measurements, which might contribute to the lower observed activity of the NCE.
- Investigate the possibility for regrowth after NCE exposure. If there is a regrowth, consider the possibility for double or multiple exposures. The NPs might reduce the possibilities for adverse effect if this is necessary.

Long-term perspectives

- Evaluate the anti-biofilm effect of NCE-containing NPs in other biofilm-forming bacteria and in polymicrobial biofilms.
- Investigate if the tested strains exhibit different phenotypic characters. If they do, investigate if this has an influence on the anti-biofilm effect of the NCE.
- *In vivo* studies of the effect and safety in suitable animal model.

8. References

ACKROYD, R., KELTY, C., BROWN, N. & REED, M. 2001. The History of Photodetection and Photodynamic Therapy. *Photochem. Photobiol. ,* 74 (5), 656-69.

AGOSTINIS, P., BERG, K., CENGEL, K. A., FOSTER, T. H., GIROTTI, A. W., GOLLNICK, S. O., HAHN, S. M., HAMBLIN, M. R., JUZENIENE, A., KESSEL, D., KORBELIK, M., MOAN, J., MROZ, P., NOWIS, D., PIETTE, J., WILSON, B. C. & GOLAB, J. 2011. Photodynamic therapy of cancer: an update. *CA Cancer J Clin,* 61 (4), 250-81.

AJIOKA, R. S., PHILLIPS, J. D. & KUSHNER, J. P. 2006. Biosynthesis of heme in mammals. *Biochim. Biophys. Acta (BBA) - Molecular Cell Research,* 1763 (7), 723-36.

AKSELSEN, P. E. 2012. Nasjonale faglige retningslinjer for antibiotikabruk i primærhelsetjenesten. *Diabetisk fotsår* Oslo: Helsedirektoratet.

ALVARENGA, L. H., PRATES, R. A., YOSHIMURA, T. M., KATO, I. T., SUZUKI, L. C., RIBEIRO, M. S., FERREIRA, L. R., PEREIRA, S. A., MARTINEZ, E. & SABA-CHUJFI, E. 2015. Aggregatibacter actinomycetemcomitans biofilm can be inactivated by methylene blue-mediated photodynamic therapy. *Photodiagnosis Photodyn Ther,* 12 (1), 131-5

AMRITKAR, A. S., CHAUDHARI, H. S., NARKHEDE, D. A., JAIN, D. K. & BAVISKAR, D. T. 2011. Nanotechnology for biomedical application. *Int. J Pharm Sci Rev Res,* 8 (2), 45-53.

ANDERSON, R. J., GROUNDWATER, P. W., TODD, A. & WORSLEY, A. J. 2012a. Chloramphenicol. *Antibacterial agents: chemistry, mode of action, mechanisms of resistance and clinical applications.* 231-42. Chichester, UK: John Wiley & Sons, Ltd

ANDERSON, R. J., GROUNDWATER, P. W., TODD, A. & WORSLEY, A. J. 2012b. Quinolone Antibacterial Agents. *Antibacterial agents: chemistry, mode of action, mechanisms of resistance and clinical applications.* 35-61. John Wiley & Sons, Ltd

ARTHUR, M. 2010. Antibiotics: vancomycin sensing. *Nat Chem Biol,* 6 (5), 313-5.

AUERBACH, R., LEWIS, R., SHINNERS, B., KUBAI, L. & AKHTAR, N. 2003. Angiogenesis assays: a critical overview. *Clin Chem,* 49 (1), 32-40.

BALDRICK, P. 2010. The safety of chitosan as a pharmaceutical excipient. *Regul Toxicol Pharmacol,* 56 (3), 290-9.

BARBIERI, S., SONVICO, F., COMO, C., COLOMBO, G., ZANI, F., BUTTINI, F., BETTINI, R., ROSSI, A. & COLOMBO, P. 2013. Lecithin/chitosan controlled release nanopreparations of tamoxifen citrate: loading, enzyme-trigger release and cell uptake. *J Control Release,* 167 (3), 276-83.

BAROLI, B. 2010. Penetration of nanoparticles and nanomaterials in the skin: fiction or reality? *J Pharm Sci,* 99 (1), 21-50.

BARONI, A., BUOMMINO, E., DE GREGORIO, V., RUOCCO, E., RUOCCO, V. & WOLF, R. 2012. Structure and function of the epidermis related to barrier properties. *Clin Dermatol,* 30 (3), 257-62.

BARRY, B. W. 1991. Lipid-Protein-Partitioning theory of skin penetration enhancement. *J Control Release,* 15 (3), 237-48.

BELDON, P. 2010. Basic science of wound healing. *Surgery (Oxford),* 28 (9), 409-12.

BERNKOP-SCHNURCH, A. 2013. Nanocarrier systems for oral drug delivery: do we really need them? *Eur J Pharm Sci,* 49 (2), 272-7.

BLECHER, K., NASIR, A. & FRIEDMAN, A. 2011. The growing role of nanotechnology in combating infectious disease. *Virulence,* 2 (5), 395-401.

BOATENG, J. S., MATTHEWS, K. H., STEVENS, H. N. & ECCLESTON, G. M. 2008. Wound healing dressings and drug delivery systems: a review. *J Pharm Sci,* 97 (8), 2892-923.

BOMBELLI, C., BORDI, F., FERRO, S., GIANSANTI, L., JORI, G., MANCINI, G., MAZZUCA, C., MONTI, D., RICCHELLI, F., SENNATO, S. & VENANZI, M. 2008. New cationic liposomes as vehicles of m-tetrahydroxyphenylchlorin in photodynamic therapy of infectious diseases. *Mol Pharm,* 5 (4), 672-9.

BOONCHIANGMA, S., NGEONTAE, W. & SRIJARANAI, S. 2012. Determination of six pyrethroid insecticides in fruit juice samples using dispersive liquid–liquid microextraction combined with high performance liquid chromatography. *Talanta,* 88 209-15.

BOUYARMANE, H., EL HANBALI, I., EL KARBANE, M., RAMI, A., SAOIABI, A., SAOIABI, S., MASSE, S., CORADIN, T. & LAGHZIZIL, A. 2015. Parameters influencing ciprofloxacin, ofloxacin, amoxicillin and sulfamethoxazole retention by natural and converted calcium phosphates. *J Hazard Mater,* 291 38-44.

BOWLER, P. G., DUERDEN, B. I. & ARMSTRONG, D. G. 2001. Wound microbiology and associated approaches to wound management. *Clin Microbiol Rev,* 14 (2), 244-69.

CANGELOSI, G. A., PALERMO, C. O., LAURENT, J. P., HAMLIN, A. M. & BRABANT, W. H. 1999. Colony morphotypes on Congo red agar segregate along species and drug susceptibility lines in the Mycobacterium avium-intracellulare complex. *Microbiology,* 145 (Pt 6), 1317-24.

CHADHA, R., GUPTA, S. & PATHAK, N. 2012. Artesunate-loaded chitosan/lecithin nanoparticles: preparation, characterization, and in vivo studies. *Drug Dev Ind Pharm,* 38 (12), 1538-46.

CHHONKER, Y. S., PRASAD, Y. D., CHANDASANA, H., VISHVKARMA, A., MITRA, K., SHUKLA, P. K. & BHATTA, R. S. 2015. Amphotericin-B entrapped lecithin/chitosan nanoparticles for prolonged ocular application. *Int J Biol Macromol,* 72 1451-8.

CHO, J. Y., CHUNG, B. Y. & HWANG, S. A. 2015. Detoxification of the veterinary antibiotic chloramphenicol using electron beam irradiation. *Environ Sci Pollut Res Int*.

CHRISTENSEN, G. D., SIMPSON, W. A., BISNO, A. L. & BEACHEY, E. H. 1982. Adherence of slime-producing strains of Staphylococcus epidermidis to smooth surfaces. *Infect Immun,* 37 (1), 318-26.

CHRISTENSEN, G. D., SIMPSON, W. A., YOUNGER, J. J., BADDOUR, L. M., BARRETT, F. F., MELTON, D. M. & BEACHEY, E. H. 1985. Adherence of coagulase-negative staphylococci to plastic tissue culture plates: a quantitative model for the adherence of staphylococci to medical devices. *J Clin Microbiol,* 22 (6), 996-1006.

CIEPLIK, F., TABENSKI, L., BUCHALLA, W. & MAISCH, T. 2014. Antimicrobial photodynamic therapy for inactivation of biofilms formed by oral key pathogens. *Front Microbiol,* 5 405.

COOPER, R., BJARNSHOLT, T. & ALHEDE, M. 2014. Biofilms in wounds: a review of present knowledge. *J. Wound Care,* 23 (11), 570-82.

CORONA, F. & MARTINEZ, J. L. 2013. Phenotypic resistance to antibiotics. *Antibiotics (Basel, Switz.),* 2 (2), 237-55.

CRAMTON, S. E. & GÖTZ, F. 2004. *Biofilm Development in Staphylococcus, 64-84.* Washington, D.C, ASM Press.

DANHIER, F., FERON, O. & PREAT, V. 2010. To exploit the tumor microenvironment: Passive and active tumor targeting of nanocarriers for anti-cancer drug delivery. *J Control Release,* 148 (2), 135-46.

DANIELL, W. E., STOCKBRIDGE, H. L., LABBE, R. F., WOODS, J. S., ANDERSON, K. E., BISSELL, D. M., BLOOMER, J. R., ELLEFSON, R. D., MOORE, M. R., PIERACH, C. A., SCHREIBER, W. E., TEFFERI, A. & FRANKLIN, G. M. 1997. Environmental chemical exposures and disturbances of heme synthesis. *Environ Health Perspect,* 105 Suppl 1 37-53.

DAROUICHE, R. O. 2001. Device-associated infections: a macroproblem that starts with microadherence. *Clin Infect Dis,* 33 (9), 1567-72.

DESAI, N. 2012. Challenges in development of nanoparticle-based therapeutics. *The AAPS journal,* 14 (2), 282-95.

DIAS RIBEIRO, A. P., ANDRADE, M. C., BAGNATO, V. S., VERGANI, C. E., PRIMO, F. L., TEDESCO, A. C. & PAVARINA, A. C. 2015. Antimicrobial photodynamic therapy against pathogenic bacterial suspensions and biofilms using chloro-aluminum phthalocyanine encapsulated in nanoemulsions. *Lasers Med Sci,* 30 (2), 549-559.

DIEKEMA, D. J., COFFMAN, S. L., MARSHALL, S. A., BEACH, M. L., ROLSTON, K. V. & JONES, R. N. 1999. Comparison of activities of broad-spectrum beta-lactam compounds against 1,128 gram-positive cocci recently isolated in cancer treatment centers. *Antimicrob Agents Chemother,* 43 (4), 940-3.

DONNELLY, R. F., MORROW, D. I., MCCARRON, P. A., JUZENAS, P. & WOOLFSON, A. D. 2006. Pharmaceutical analysis of 5-aminolevulinic acid in solution and in tissues. *J Photochem Photobiol B,* 82 (1), 59-71.

DOUGHERTY, T. J. 1996. A brief history of clinical photodynamic therapy development at Roswell Park Cancer Institute. *J Clin Laser Med Sur* 14 (5), 219-21.

EHRLICH, J., BARTZ, Q. R., SMITH, R. M., JOSLYN, D. A. & BURKHOLDER, P. R. 1947. Chloromycetin, a new antibiotic from a soil actinomycete. *Science,* 106 (2757), 417.

EL MAGHRABY, G. M., BARRY, B. W. & WILLIAMS, A. C. 2008. Liposomes and skin: from drug delivery to model membranes. *Eur J Pharm Sci,* 34 (4-5), 203-22.

ENOCH, S. & LEAPER, D. J. 2008. Basic science of wound healing. *Surgery (Oxford),* 26 (2), 31-7.

FEI LIU, X., LIN GUAN, Y., ZHI YANG, D., LI, Z. & DE YAO, K. 2001. Antibacterial action of chitosan and carboxymethylated chitosan. *J. Appl. Polym. Sci.,* 79 (7), 1324-35.

FERREIRA, M. C., TUMA, P., JR., CARVALHO, V. F. & KAMAMOTO, F. 2006. Complex wounds. *Clinics (Sao Paulo),* 61 (6), 571-8.

FERRO, S., JORI, G., SORTINO, S., STANCANELLI, R., NIKOLOV, P., TOGNON, G., RICCHELLI, F. & MAZZAGLIA, A. 2009. Inclusion of 5-[4-(1-dodecanoylpyridinium)]-10,15,20-triphenylporphine in supramolecular aggregates of cationic amphiphilic cyclodextrins: physicochemical characterization of the complexes and strengthening of the antimicrobial photosensitizing activity. *Biomacromolecules,* 10 (9), 2592-600.

FILIPOVIC-GRCIC, J., SKALKO-BASNET, N. & JALSENJAK, I. 2001. Mucoadhesive chitosan-coated liposomes: characteristics and stability. *J Microencapsul,* 18 (1), 3-12.

FOTINOS, N., CAMPO, M. A., POPOWYCZ, F., GURNY, R. & LANGE, N. 2006. 5‐Aminolevulinic Acid Derivatives in Photomedicine: Characteristics, Application and Perspectives. *Photochem. Photobiol.,* 82 (4), 994-1015.

FRANK, C., BAYOUMI, I. & WESTENDORP, C. 2005. Approach to infected skin ulcers. *Can Fam Physician,* 51 1352-9.

FRANTZEN, C. B., INGEBRIGTSEN, L., SKAR, M. & BRANDL, M. 2003. Assessing the accuracy of routine photon correlation spectroscopy analysis of heterogeneous size distributions. *AAPS PharmSciTech,* 4 (3), 36.

FREEMAN, D. J., FALKINER, F. R. & KEANE, C. T. 1989. New method for detecting slime production by coagulase negative staphylococci. *J Clin Pathol,* 42 (8), 872-4.
GADES, M. D. & STERN, J. S. 2003. Chitosan supplementation and fecal fat excretion in men. *Obes Res,* 11 (5), 683-8.
GARCIA, L. S. & ISENBERG, H. D. 2010. Preparation of Routine Media and Reagents Used in Antimicrobial Susceptibility Testing. *Clinical microbiology procedures handbook.* 3rd ed. 181-201. Washington, D.C: ASM Press
GARDNER, S. E. & FRANTZ, R. A. 2008. Wound bioburden and infection-related complications in diabetic foot ulcers. *Biol Res Nurs,* 10 (1), 44-53.
GARRETT, D., JOCHIMSEN, E., MURFITT, K., HILL, B., MCALLISTER, S., NELSON, P., SPERA, R., SALL, R., TENOVER, F., JOHNSTON, J., ZIMMER, B. & JARVIS, W. 1999. The emergence of decreased susceptibility to vancomycin in Staphylococcus epidermidis. *Infect. Control Hosp. Epidemiol.,* 20 (3), 167-70.
GEORGE, M. W. 2003. The 'right' size in nanobiotechnology. *Nat. Biotechnol.,* 21 (10), 1161-5.
GILMORE, B. F., MCCARRON, P. A., MORROW, D. I., MURPHY, D. J., WOOLFSON, A. D. & DONNELLY, R. F. 2006. In vitro phototoxicity of 5-aminolevulinic acid and its methyl ester and the influence of barrier properties on their release from a bioadhesive patch. *Eur J Pharm Biopharm,* 63 (3), 295-309.
GRICE, E. A. & SEGRE, J. A. 2011. The skin microbiome. *Nat Rev Microbiol,* 9 (4), 244-53.
GRINHOLC, M., NAKONIECZNA, J., FILA, G., TARASZKIEWICZ, A., KAWIAK, A., SZEWCZYK, G., SARNA, T., LILGE, L. & BIELAWSKI, K. P. 2015. Antimicrobial photodynamic therapy with fulleropyrrolidine: photoinactivation mechanism of Staphylococcus aureus, in vitro and in vivo studies. *Appl Microbiol Biotechnol,* 99 (9), 4031-43.
GUGGENHEIM, B., GIERTSEN, E., SCHUPBACH, P. & SHAPIRO, S. 2001. Validation of an in vitro biofilm model of supragingival plaque. *J Dent Res,* 80 (1), 363-70.
HADAFOW, M. A. 2014. *Chitosan-based Drug Delivery Dystem for a New Chemical Entity for Photodynamic Wound Therapy.* The degree master of pharmacy, Not-open access, The University of Tromsø The Arctic University of Norway.
HAFNER, A., DURRIGL, M., PEPIC, I. & FILIPOVIC-GRCIC, J. 2011. Short- and long-term stability of lyophilised melatonin-loaded lecithin/chitosan nanoparticles. *Chem Pharm Bull (Tokyo),* 59 (9), 1117-23.
HAFNER, A., LOVRIC, J., VOINOVICH, D. & FILIPOVIC-GRCIC, J. 2009. Melatonin-loaded lecithin/chitosan nanoparticles: physicochemical characterisation and permeability through Caco-2 cell monolayers. *Int J Pharm,* 381 (2), 205-13.
HANNIGAN, G. D. & GRICE, E. A. 2013. Microbial ecology of the skin in the era of metagenomics and molecular microbiology. *Cold Spring Harb Perspect Med,* 3 (12), a015362.
HANSON, B. R. & NEELY, M. N. 2012. Coordinate regulation of Gram-positive cell surface components. *Curr Opin Microbiol,* 15 (2), 204-10.
HE, H. J., SUN, F. J., WANG, Q., LIU, Y., XIONG, L. R. & XIA, P. Y. 2014. Erythromycin resistance features and biofilm formation affected by subinhibitory erythromycin in clinical isolates of Staphylococcus epidermidis. *J Microbiol Immunol Infect,* S1684-1182(14)00034-6.
HE, P., DAVIS, S. S. & ILLUM, L. 1998. In vitro evaluation of the mucoadhesive properties of chitosan microspheres. *Int. J. Pharm. ,* 166 (1), 75-88.
HEURTAULT, B., SAULNIER, P., PECH, B., PROUST, J. E. & BENOIT, J. P. 2003. Physico-chemical stability of colloidal lipid particles. *Biomaterials,* 24 (23), 4283-300.

HIRAMATSU, K. 1998. Vancomycin resistance in staphylococci. *Drug Resist Updat,* 1 (2), 135-50.
HIRAMATSU, K., HANAKI, H., INO, T., YABUTA, K., OGURI, T. & TENOVER, F. C. 1997. Methicillin-resistant Staphylococcus aureus clinical strain with reduced vancomycin susceptibility. *J Antimicrob Chemother,* 40 (1), 135-6.
HUEBNER, J. & GOLDMANN, D. A. 1999. Coagulase-negative staphylococci: role as pathogens. *Annu Rev Med,* 50 223-36.
HUPFELD, S., HOLSÆTER, A. M., SKAR, M., FRANTZEN, C. B. & BRANDL, M. 2006. Liposome size analysis by dynamic/static light scattering upon size exclusion-/field flow-fractionation. *J Nanosci Nanotechnol,* 6 (9-10), 3025-31.
HURLER, J., BERG, O. A., SKAR, M., CONRADI, A. H., JOHNSEN, P. J. & ŠKALKO-BASNET, N. 2012. Improved burns therapy: liposomes-in-hydrogel delivery system for mupirocin. *J Pharm Sci,* 101 (10), 3906-15.
HURLER, J. & ŠKALKO-BASNET, N. 2012. Potentials of chitosan-based delivery systems in wound therapy: bioadhesion study. *J Funct Biomater,* 3 (1), 37-48.
HØIBY, N., BJARNSHOLT, T., MOSER, C., BASSI, G. L., COENYE, T., DONELLI, G., HALL-STOODLEY, L., HOLA, V., IMBERT, C., KIRKETERP-MOLLER, K., LEBEAUX, D., OLIVER, A., ULLMANN, A. J. & WILLIAMS, C. 2015. ESCMID guideline for the diagnosis and treatment of biofilm infections 2014. *Clin Microbiol Infect,* S1198-743X(14)00090-1.
IRVINE, C. 1991. 'Skin failure'--a real entity: discussion paper. *J R Soc Med,* 84 (7), 412-3.
JAYAKUMAR, R., PRABAHARAN, M., NAIR, S. V., TOKURA, S., TAMURA, H. & SELVAMURUGAN, N. 2010. Novel carboxymethyl derivatives of chitin and chitosan materials and their biomedical applications. *Prog. Mater Sci.,* 55 (7), 675-709.
JENKINS, G. W., KEMNITZ, C. P. & TORTORA, G. J. 2006. *Anatomy and physiology: from science to life.* New York, John Wiley & Sons Inc.
JORI, G., FABRIS, C., SONCIN, M., FERRO, S., COPPELLOTTI, O., DEI, D., FANTETTI, L., CHITI, G. & RONCUCCI, G. 2006. Photodynamic therapy in the treatment of microbial infections: basic principles and perspective applications. *Lasers Surg Med,* 38 (5), 468-81.
JUZENIENE, A., IANI, V. & MOAN, J. 2013. Clearance mechanism of protoporphyrin IX from mouse skin after application of 5-aminolevulinic acid. *Photodiagnosis Photodyn Ther,* 10 (4), 538-45.
KIRBY, B. J. & HASSELBRINK, E. F., JR. 2004. Zeta potential of microfluidic substrates: 1. Theory, experimental techniques, and effects on separations. *Electrophoresis,* 25 (2), 187-202.
KONG, H. H. & SEGRE, J. A. 2012. Skin microbiome: looking back to move forward. *J Invest Dermatol,* 132 (3), 933-9.
LAI-CHEONG, J. E. & MCGRATH, J. A. 2013. Structure and function of skin, hair and nails. *Medicine,* 41 (6), 317-20.
LECLERCQ, R., DERLOT, E., DUVAL, J. & COURVALIN, P. 1988. Plasmid-mediated resistance to vancomycin and teicoplanin in Enterococcus faecium. *N Engl J Med,* 319 (3), 157-61.
LI Q., D. E. T., GRANDMAISON E.W., GOOSEN M.F.A., 1992. Applications and Properties of Chitosan. *J Bioact Compat Pol* 7(4), 370-97.
LIM, C. K., RAZZAQUE, M. A., LUO, J. & FARMER, P. B. 2000. Isolation and characterization of protoporphyrin glycoconjugates from rat harderian gland by HPLC, capillary electrophoresis and HPLC/electrospray ionization MS. *Biochem J,* 347 (Pt 3), 757-61.

LIU, C., ZHOU, Y., WANG, L., HAN, L., LEI, J., ISHAQ, H. M. & XU, J. 2014. Mechanistic Aspects of the Photodynamic Inactivation of Vancomycin-Resistant Enterococci Mediated by 5-Aminolevulinic Acid and 5-Aminolevulinic Acid Methyl Ester. *Curr Microbiol,* 70 (4), 528-35

LIU, X., MA, L., MAO, Z. & GAO, C. 2011. Chitosan-Based Biomaterials for Tissue Repair and Regeneration. *In:* JAYAKUMAR, R., PRABAHARAN, M. & MUZZARELLI, R. A. A. (eds.) *Chitosan for Biomaterials II.* 81-127. Heidelberg Berlin: Springer Berlin Heidelberg

MAH, T. F. & O'TOOLE, G. A. 2001. Mechanisms of biofilm resistance to antimicrobial agents. *Trends Microbiol,* 9 (1), 34-9.

MAHAPATRO, A. & SINGH, D. K. 2011. Biodegradable nanoparticles are excellent vehicle for site directed in-vivo delivery of drugs and vaccines. *J Nanobiotechnology,* 9 (1), 55-65.

MAISCH, T., HACKBARTH, S., REGENSBURGER, J., FELGENTRAGER, A., BAUMLER, W., LANDTHALER, M. & RODER, B. 2011. Photodynamic inactivation of multi-resistant bacteria (PIB) - a new approach to treat superficial infections in the 21st century. *J Dtsch Dermatol Ges,* 9 (5), 360-6.

MATHUR, T., SINGHAL, S., KHAN, S., UPADHYAY, D. J., FATMA, T. & RATTAN, A. 2006. Detection of biofilm formation among the clinical isolates of Staphylococci: an evaluation of three different screening methods. *Indian J Med Microbiol,* 24 (1), 25-9.

MCBAIN, A. J. 2009. Chapter 4: In vitro biofilm models: an overview. *Adv Appl Microbiol,* 69 99-132.

MISHRA, S. K., BASUKALA, P., BASUKALA, O., PARAJULI, K., POKHREL, B. M. & RIJAL, B. P. 2015. Detection of biofilm production and antibiotic resistance pattern in clinical isolates from indwelling medical devices. *Curr Microbiol,* 70 (1), 128-34.

MITCHELL, C. R., BAO, Y., BENZ, N. J. & ZHANG, S. 2009. Comparison of the sensitivity of evaporative universal detectors and LC/MS in the HILIC and the reversed-phase HPLC modes. *J. Chromatogr. B,* 877 (32), 4133-9.

MOHANRAJ, V. J. & CHEN, Y. 2006. Nanoparticles - A Review. *Trop J Pharm Res,* 5 (1), 561-73.

MORTON, C. A. 2003. Methyl aminolevulinate (Metvix) photodynamic therapy - practical pearls. *J Dermatolog Treat,* 14 (3), 23-6.

MORTON, C. A., MCKENNA, K. E. & RHODES, L. E. 2008. Guidelines for topical photodynamic therapy: update. *Br J Dermatol,* 159 (6), 1245-66.

MULLER, P., GUGGENHEIM, B. & SCHMIDLIN, P. R. 2007. Efficacy of gasiform ozone and photodynamic therapy on a multispecies oral biofilm in vitro. *Eur J Oral Sci,* 115 (1), 77-80.

MUZZARELLI, R. A. A. 1977. *Chitin.* Oxford, Pergamon Press.

MUZZARELLI, R. A. A. 2009. Chitins and chitosans for the repair of wounded skin, nerve, cartilage and bone. *Carbohydr. Polym.,* 76 (2), 167-82.

NORWOOD, D. E. & GILMOUR, A. 2000. The growth and resistance to sodium hypochlorite of Listeria monocytogenes in a steady-state multispecies biofilm. *J Appl Microbiol,* 88 (3), 512-20.

OLIVEIRA, A. & CUNHA M. DE, L. 2010. Comparison of methods for the detection of biofilm production in coagulase-negative staphylococci. *BMC Res Notes,* 3 260.

OTTO, M. 2009. Staphylococcus epidermidis--the 'accidental' pathogen. *Nat Rev Microbiol,* 7 (8), 555-67.

PARVEEN, S., MISRA, R. & SAHOO, S. K. 2012. Nanoparticles: a boon to drug delivery, therapeutics, diagnostics and imaging. *Nanomed Nanotech Biol Med,* 8 (2), 147-66.

PENG, Q., BERG, K., MOAN, J., KONGSHAUG, M. & NESLAND, J. M. 1997. 5‐Aminolevulinic Acid‐Based Photodynamic Therapy: Principles and Experimental Research. *Photochem. Photobiol. ,* 65 (2), 235-51.

PERCIVAL, S. L., HILL, K. E., WILLIAMS, D. W., HOOPER, S. J., THOMAS, D. W. & COSTERTON, J. W. 2012. A review of the scientific evidence for biofilms in wounds. *Wound Repair Regen,* 20 (5), 647-57.

PLANAS, O., BRESOLI-OBACH, R., NOS, J., GALLAVARDIN, T., RUIZ-GONZALEZ, R., AGUT, M. & NONELL, S. 2015. Synthesis, Photophysical Characterization, and Photoinduced Antibacterial Activity of Methylene Blue-loaded Amino- and Mannose-Targeted Mesoporous Silica Nanoparticles. *Molecules,* 20 (4), 6284-98.

PRATTEN, J. & READY, D. 2010. Use of biofilm model systems to study antimicrobial susceptibility. *Methods Mol Biol,* 642 203-15.

PRICE, L. B., LIU, C. M., FRANKEL, Y. M., MELENDEZ, J. H., AZIZ, M., BUCHHAGEN, J., CONTENTE-CUOMO, T., ENGELTHALER, D. M., KEIM, P. S., RAVEL, J., LAZARUS, G. S. & ZENILMAN, J. M. 2011. Macroscale spatial variation in chronic wound microbiota: a cross-sectional study. *Wound Repair Regen,* 19 (1), 80-8.

PROW, T. W., GRICE, J. E., LIN, L. L., FAYE, R., BUTLER, M., BECKER, W., WURM, E. M., YOONG, C., ROBERTSON, T. A., SOYER, H. P. & ROBERTS, M. S. 2011. Nanoparticles and microparticles for skin drug delivery. *Adv Drug Deliv Rev,* 63 (6), 470-91.

QINGYI XU, M. N., ZENGSHE LIU AND TAKEO SHIINA 2011. *Soybean - Applications and Technology, Soybean-based Surfactants and Their Applications, 341-364.* Tzi-Bun Ng, InTech.

RABEA, E. I., BADAWY, M. E., STEVENS, C. V., SMAGGHE, G. & STEURBAUT, W. 2003. Chitosan as antimicrobial agent: applications and mode of action. *Biomacromolecules,* 4 (6), 1457-65.

RAFTERY, R., O'BRIEN, F. J. & CRYAN, S. A. 2013. Chitosan for gene delivery and orthopedic tissue engineering applications. *Molecules,* 18 (5), 5611-47.

REDMOND, R. W. & GAMLIN, J. N. 1999. A compilation of singlet oxygen yields from biologically relevant molecules. *Photochem Photobiol,* 70 (4), 391-475.

RIPOLLES, C., PITARCH, E., SANCHO, J. V., LOPEZ, F. J. & HERNANDEZ, F. 2011. Determination of eight nitrosamines in water at the ng L(-1) levels by liquid chromatography coupled to atmospheric pressure chemical ionization tandem mass spectrometry. *Anal Chim Acta,* 702 (1), 62-71.

ROSENTHAL, M., GOLDBERG, D., AIELLO, A., LARSON, E. & FOXMAN, B. 2011. Skin microbiota: microbial community structure and its potential association with health and disease. *Infect Genet Evol,* 11 (5), 839-48.

SAMBROOK, J. & RUSSELL, D. W. 2001. *Molecular cloning : a laboratory manual.* 3rd. ed., Cold Spring Harbor, NY, Cold Spring Harbor Laboratory Press.

SCHWALBE, R. S., STAPLETON, J. T. & GILLIGAN, P. H. 1987. Emergence of vancomycin resistance in coagulase-negative staphylococci. *N Engl J Med,* 316 (15), 927-31.

SEN, C. K., GORDILLO, G. M., ROY, S., KIRSNER, R., LAMBERT, L., HUNT, T. K., GOTTRUP, F., GURTNER, G. C. & LONGAKER, M. T. 2009. Human skin wounds: a major and snowballing threat to public health and the economy. *Wound Repair Regen,* 17 (6), 763-71.

SENYIĞIT, T., SONVICO, F., BARBIERI, S., OZER, O., SANTI, P. & COLOMBO, P. 2010. Lecithin/chitosan nanoparticles of clobetasol-17-propionate capable of accumulation in pig skin. *J Control Release,* 142 (3), 368-73.

SHAH, H. & SINGH, K. 2014. *Lecithin* [Online]. Pharmaceutical Press and American Pharmacists Association 2015: MedicinesComplete © 2015 Royal Pharmaceutical Society Available: https://www.medicinescomplete.com/mc/excipients/2012/1001940783.htm [Accessed April 20 2015].

SHAH, P. M. 1991. Ciprofloxacin. *Int J Antimicrob Ag,* 1 (2), 75-96.

SHARMA, S. K., MROZ, P., DAI, T., HUANG, Y. Y., ST DENIS, T. G. & HAMBLIN, M. R. 2012. Photodynamic Therapy for Cancer and for Infections: What Is the Difference? *Isr J Chem,* 52 (8-9), 691-705.

SHAW, T. J. & MARTIN, P. 2009. Wound repair at a glance. *J Cell Sci,* 122 (Pt 18), 3209-13.

SHEN, S. C., LEE, W. R., FANG, Y. P., HU, C. H. & FANG, J. Y. 2006. In vitro percutaneous absorption and in vivo protoporphyrin IX accumulation in skin and tumors after topical 5 - aminolevulinic acid application with enhancement using an erbium: YAG laser. *J. Pharm. Sci. ,* 95 (4), 929-38.

SHERWOOD, L. 2010. *Human physiology: from cells to systems, 453-6.* 7th ed., Australia, Brooks/Cole.

SILHAVY, T. J., KAHNE, D. & WALKER, S. 2010. The bacterial cell envelope. *Cold Spring Harb Perspect Biol,* 2 (5), a000414.

SIMONETTI, O., CIRIONI, O., ORLANDO, F., ALONGI, C., LUCARINI, G., SILVESTRI, C., ZIZZI, A., FANTETTI, L., RONCUCCI, G., GIACOMETTI, A., OFFIDANI, A. & PROVINCIALI, M. 2011. Effectiveness of antimicrobial photodynamic therapy with a single treatment of RLP068/Cl in an experimental model of Staphylococcus aureus wound infection. *Br J Dermatol,* 164 (5), 987-95.

SINGH, M. R., SARAF, S., VYAS, A., JAIN, V. & SINGH, D. 2013. Innovative approaches in wound healing: trajectory and advances. *Artif Cells Nanomed Biotechnol,* 41 (3), 202-12.

SINGH, R., RAY, P., DAS, A. & SHARMA, M. 2010. Penetration of antibiotics through Staphylococcus aureus and Staphylococcus epidermidis biofilms. *J. Antimicrob. Chemother. ,* 65 (9), 1955-8.

SITHISARANKUL, P., VIRGINIA, M. W., CECILIA, T. D. & STRICKLAND, P. T. 1999. Urinary 5-aminolevulinic acid in lead-exposed children. *Biomarkers,* 4 (4), 281-9.

SONVICO, F., CAGNANI, A., ROSSI, A., MOTTA, S., DI BARI, M. T., CAVATORTA, F., ALONSO, M. J., DERIU, A. & COLOMBO, P. 2006. Formation of self-organized nanoparticles by lecithin/chitosan ionic interaction. *Int J Pharm,* 324 (1), 67-73.

SOUSA, A. M., MACHADO, I. & PEREIRA, M. 2011. Phenotypic switching: an opportunity to bacteria thrive. *In:* MÉNDEZ-VILAS, A. (ed.) *Science against microbial pathogens: communicating current research and technological advances.* 252-62. Badajoz, Spain: Formatex Research Center

SPELLBERG, B. 2000. The cutaneous citadel: a holistic view of skin and immunity. *Life Sci,* 67 (5), 477-502.

STRODTBECK, F. 2001. Physiology of wound healing. *Newborn Infant Nurs Rev,* 1 (1), 43-52.

SWOBODA, J. G., CAMPBELL, J., MEREDITH, T. C. & WALKER, S. 2010. Wall teichoic acid function, biosynthesis, and inhibition. *Chembiochem,* 11 (1), 35-45.

SZEIMIESA, R. M., KARRERA, S., RADAKOVIC-FIJANB, S., TANEWB, A., CALZAVARA-PINTONC, P. G., ZANEC, C., SIDOROFFD, A., HEMPELE, M., ULRICHF, J., PROEBSTLEG, T., MEFFERTH, H., MULDERI, M., SALOMONJ, D., DITTMARK, H. C., BAUERL, J. W., KERNLANDM, K. & BRAATHENM, L. 2002. Photodynamic therapy using topical methyl 5-aminolevulinate compared with

cryotherapy for actinic keratosis: A prospective, randomized study. *J Am Acad Dermatol,* 47 (2), 258-62.
SZUHAJ, B. F. 1983. Lecithin production and utilization. *J Am Oil Chem Soc,* 60 (2), 306-9.
TAKAHASHI, M., INOUE, K., YOSHIDA, M., MORIKAWA, T., SHIBUTANI, M. & NISHIKAWA, A. 2009. Lack of chronic toxicity or carcinogenicity of dietary N-acetylglucosamine in F344 rats. *Food Chem Toxicol,* 47 (2), 462-71.
TAN, Q., LIU, W., GUO, C. & ZHAI, G. 2011. Preparation and evaluation of quercetin-loaded lecithin-chitosan nanoparticles for topical delivery. *Int J Nanomedicine,* 6 1621-30.
TANER, G., YEŞILÖZ, R., ÖZKAN VARDAR, D., ŞENYIĞIT, T., ÖZER, Ö., DEGEN, G. H. & BAŞARAN, N. 2014. Evaluation of the cytotoxic and genotoxic potential of lecithin/chitosan nanoparticles. *J Nanopart Res,* 16 (2), 2220.
TARASZKIEWICZ, A., FILA, G., GRINHOLC, M. & NAKONIECZNA, J. 2013. Innovative strategies to overcome biofilm resistance. *Biomed Res Int,* 2013 ID: 150653.
TEIXEIRA, A. H., PEREIRA, E. S., RODRIGUES, L. K., SAXENA, D., DUARTE, S. & ZANIN, I. C. 2012. Effect of photodynamic antimicrobial chemotherapy on in vitro and in situ biofilms. *Caries Res,* 46 (6), 549-54.
THE EUROPEAN COMMITTEE ON ANTIMICROBIAL SUSCEPTIBILITY TESTING. 2015. Breakpoint tables for interpretation of MICs and zone diameters, Version 5.0,. Available from: http://www.eucast.org [Accessed April 26 2015].
THORESEN, I. E. 2014. *Advanced Drug Delivery System for New Chemical Entity Destined for Wound Therapy: Anti-biofilm Potential of Novel Drug Delivery System.* The degree master of pharmacy, Not-open access, The University of Tromsø The Arctic University of Norway.
TOPALOGLU, N., GULSOY, M. & YUKSEL, S. 2013. Antimicrobial photodynamic therapy of resistant bacterial strains by indocyanine green and 809-nm diode laser. *Photomed Laser Surg,* 31 (4), 155-62.
UENO, H., MORI, T. & FUJINAGA, T. 2001. Topical formulations and wound healing applications of chitosan. *Adv Drug Deliv Rev,* 52 (2), 105-15.
VANYSACKER, L., BOERJAN, B., DECLERCK, P. & VANKELECOM, I. F. 2014. Biofouling ecology as a means to better understand membrane biofouling. *Appl Microbiol Biotechnol,* 98 (19), 8047-72.
VATANSEVER, F., DE MELO, W. C., AVCI, P., VECCHIO, D., SADASIVAM, M., GUPTA, A., CHANDRAN, R., KARIMI, M., PARIZOTTO, N. A., YIN, R., TEGOS, G. P. & HAMBLIN, M. R. 2013. Antimicrobial strategies centered around reactive oxygen species--bactericidal antibiotics, photodynamic therapy, and beyond. *FEMS Microbiol Rev,* 37 (6), 955-89.
WACHOWSKA, M., MUCHOWICZ, A., FIRCZUK, M., GABRYSIAK, M., WINIARSKA, M., WAŃCZYK, M., BOJARCZUK, K. & GOLAB, J. 2011. Aminolevulinic acid (ala) as a prodrug in photodynamic therapy of cancer. *Molecules,* 16 (12), 4140-64.
WAGNER, V., DULLAART, A., BOCK, A.-K. & ZWECK, A. 2006. The emerging nanomedicine landscape. *Nat. Biotechnol.,* 24 (10), 1211-1217.
WHO 1974. Toxicological evaluation of some food additives including anticaking agents, antimicrobials, antioxidants, emulsifiers and thickening agents. *FAO Nutrition Meetings Report Series.* 1974/01/01 ed.
WICKETT, R. R. & VISSCHER, M. O. 2006. Structure and function of the epidermal barrier. *Am J Infect Control,* 34 (10), S98-S110.
WIKENE, K. O., HEGGE, A. B., BRUZELL, E. & TONNESEN, H. H. 2014. Formulation and characterization of lyophilized curcumin solid dispersions for antimicrobial

photodynamic therapy (aPDT): studies on curcumin and curcuminoids LII. *Drug Dev Ind Pharm,* 1-9.
WILCZEWSKA, A. Z., NIEMIROWICZ, K., MARKIEWICZ, K. H. & CAR, H. 2012. Nanoparticles as drug delivery systems. *Pharmacol Rep,* 64 (5), 1020-37.
WILHELM, M. & ESTES, L. 1999. Vancomycin. *Mayo Clin Proc,* 74 (9), 928-35.
WOJTYCZKA, R. D., ORLEWSKA, K., KEPA, M., IDZIK, D., DZIEDZIC, A., MULARZ, T., KRAWCZYK, M., MIKLASINSKA, M. & WASIK, T. J. 2014. Biofilm formation and antimicrobial susceptibility of Staphylococcus epidermidis strains from a hospital environment. *Int J Environ Res Public Health,* 11 (5), 4619-33.
WYSOCKI, A. B. 2002. Evaluating and managing open skin wounds: colonization versus infection. *AACN Clin Issues,* 13 (3), 382-97.
YAZDANKHAH, S. P., SORUM, H., LARSEN, H. J. & GOGSTAD, G. 2001. Use of magnetic beads for Gram staining of bacteria in aqueous suspension. *J Microbiol Methods,* 47 (3), 369-71.
ZHAO, G., USUI, M. L., LIPPMAN, S. I., JAMES, G. A., STEWART, P. S., FLECKMAN, P. & OLERUD, J. E. 2013. Biofilms and Inflammation in Chronic Wounds. *Adv Wound Care (New Rochelle),* 2 (7), 389-99.
ZIEGELHOFFER, E. C. & DONOHUE, T. J. 2009. Bacterial responses to photo-oxidative stress. *Nat Rev Microbiol,* 7 (12), 856-63.
ZOLNIK, B. S., SADRIEH, N., GONZÁLEZ-FERNÁNDEZ, Á. & DOBROVOLSKAIA, M. A. 2010. Minireview: Nanoparticles and the immune system. *Endocrinology,* 151 (2), 458-465.
ÖZCAN, I., AZIZOGLU, E., SENYIGIT, T., OZYAZICI, M. & OZER, O. 2013. Comparison of PLGA and lecithin/chitosan nanoparticles for dermal targeting of betamethasone valerate. *J Drug Target,* 21 (6), 542-50.

Appendices

Appendix I

As mentioned above, NICOMP fit exhibited an uneven size distribution relative to the assumed real size. The biases of the measurements are detectable when considering the other parameters of the measurements. The residual, shown in **Appendix Table 1** indicates a large number of larger particles or aggregates. These do not appear in the peaks of the measurement. The residual is very different in the group were the chitosan lipid ratio is 1:20 (w/w) compared to the other groups as indicated in **Appendix Table 1** and **Appendix Figure 1**. The chi-square is also large considering the peaks of the measurement and the differences between the chitosan lipid ratios of the NPs. This effect is indicated in **Appendix Table 1** and in **Appendix Figure 2**.

Appendix Table 1. Characteristics of the size of empty NPs. The values are presented as the mean of each of the groups (1:5 n = 12, 1:10 n = 3, 1:20 n = 3).

Chitosan lipid ratio	Residual	Chi-square	Baseline adj.	Fit error
1:5	42.077 ± 6.485	239.81 ± 50.77	0.08 ± 0.06	2.484 ± 1.089
1:10	41.274 ± 6.473	185.00 ± 103.33	0.16 ± 0.02	2.222 ± 0.546
1:20	23.624 ± 7.079	17.11 ± 5.72	0.03 ± 0.05	2.203 ± 0.508

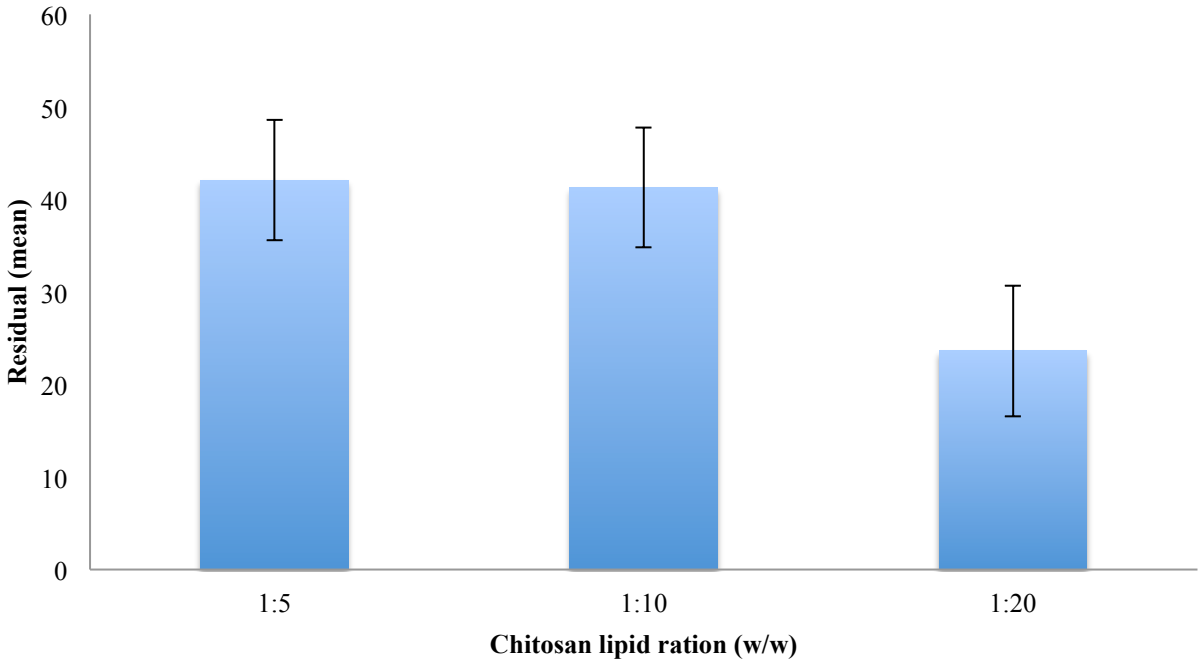

Appendix Figure 1. The difference in the residual (mean) between the different chitosan lipid ratios of empty NPs (1:5 n = 12, 1:10 n = 3, 1:20 n = 3).

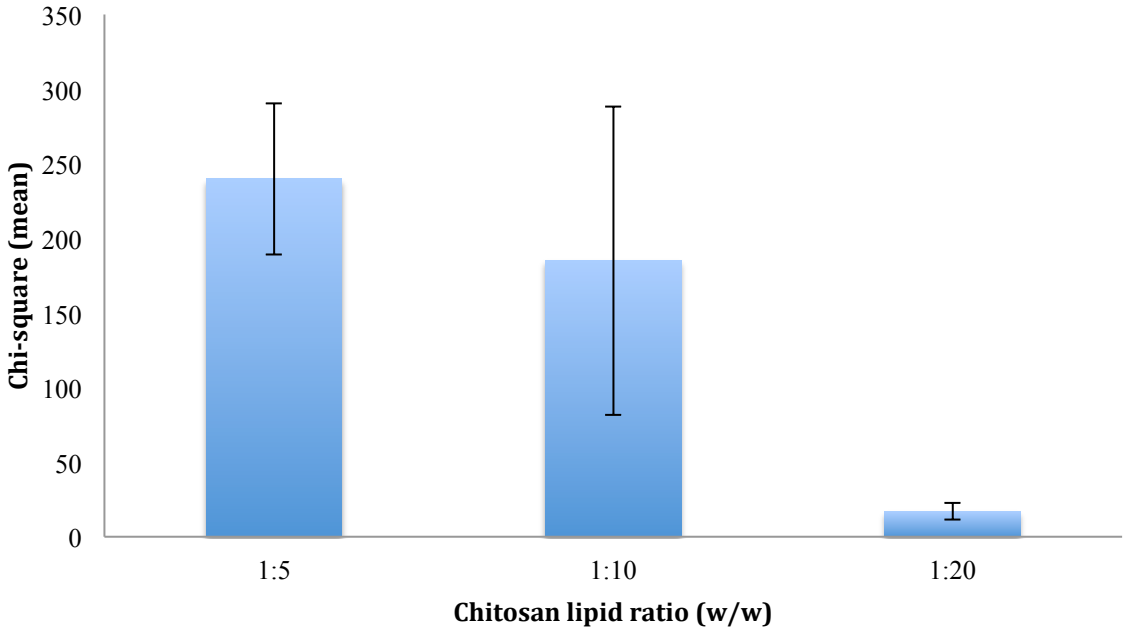

Appendix Figure 2. The difference in the chi-square (mean) between the different chitosan lipid ratios in empty NPs (1:5 n = 12, 1:10 n = 3, 1:20 n = 3).

The NICOMP fit of the PCS measurement looses some data due to the large particles present in the sample. As seen in **Appendix Table 2**, some of the values are far from the ones shown in **Table 5**. If we take the preparation 1 (**Appendix Table 2**) as an example, it looks like a

vesicle size fitting our aim, however we might we might oversee the particles due to the cut of line for the measurement. Data on some of the smaller particles might be lost too because the larger particles overshadows them.

Appendix Table 2. Size distributions represented as peaks of empty NPs (intensity) (n=3). The intensity states the intensity of the peak relative to the whole sample.

Peak 1		Peak 2		Peak 3	
Mean (nm)	Intensity (%)	Mean (nm)	Intensity (%)	Mean (nm)	Intensity (%)
21.9 ± 7.3	6.03 ± 0.52	137.1 ± 1.2	42.23 ± 4.96	251.8 ± 100.5	51.74 ± 4.44
58.1 ± 65.5	3.27 ± 3.47	196.0*	4.33*	866.9 ± 32.8	92.39 ± 10.97
42.7 ±27.7	1.92 ± 0.97	203.6 ± 56.9	27.80 ± 11.55	780.4 ± 211.9	70.28 ± 12.34
113.8 ± 31.8	6.65 ± 2.53	190.3 ± 15.4	15.82 ± 7.67	691.7 ± 367.7	77.53 ± 5.14
56.3 ± 63.0	6.53 ± 0.57	152.1 ± 36.4	18.96 ± 7.06	429.6 ± 410.4	74.51 ± 7.62
10.5*	1.71*	135.9 ± 2.9	20.16 ± 14.72	624.1 ± 372.0	78.13 ± 17.68
15.9 ±6.7	1.51 ± 0.78	87.8 ± 12.3	12.07 ± 3.02	543.0 ± 325.4	86.42 ± 3.52
15.0 ± 5.5	0.79 ± 0.74	163.9 ± 9.4	17.69 ± 0.79	756.3 ± 33.7	81.52 ± 0.25
87.6 ± 66.4	6.10 ± 2.72	181.9 ± 26.2	10.45 ± 1.17	875.0 ± 48.0	83.45 ± 3.51
11.2 ± 0.4	2.59 ± 3.45	122.7 ± 12.1	17.48 ±16.60	605.9 ± 350.5	79.92 ± 19.87
21.2 ± 18.2	4.96 ± 3.38	128.5 ± 59.0	33.16 ±24.44	424.8 ± 349.6	61.88 ± 27.82
17.1 ± 7.4	8.10 ± 8.52	93.8 ± 39.5	22.32 ± 13.55	319.1 ± 323.4	69.58 ± 22.04
43.3 ± 35.0	2.61 ± 2.51	204.0 ± 85.3	26.47 ± 12.21	771.9 ± 211.8	70.93 ± 14.25
20.0 ± 8.3	0.84 ± 0.29	215.8 ± 127.3	19.91 ± 3.55	679.5 ± 190.4	79.26 ±3.80
46.0 ± 21.0	2.85 ± 1.53	219.7 ± 29.6	87.56 ± 12.84	870.6 ±58.1	9.59 ± 12.93
50.2 ± 13.0	3.04 ± 2.17	246.6 ± 63.7	54.99 ± 34.67	744.7 ± 222.0	41.97 ± 8.44
53.6 ± 55.2	4.14 ± 7.93	259.3 ± 98.3	74.87 ± 33.25	668.0*	20.99*
13.9 ± 4.7	2.28 ± 2.09	119.1 ±49.3	67.66 ± 50.11	292.9*	30.06*

* The peak did only appear in one of the cycles.

Appendix Figure 3 is representation of the same results as in **Figure 18**. The relationship between the size and the zeta potential is not seen here. In the figure we can see a clear indication of a large variation in the measurements.

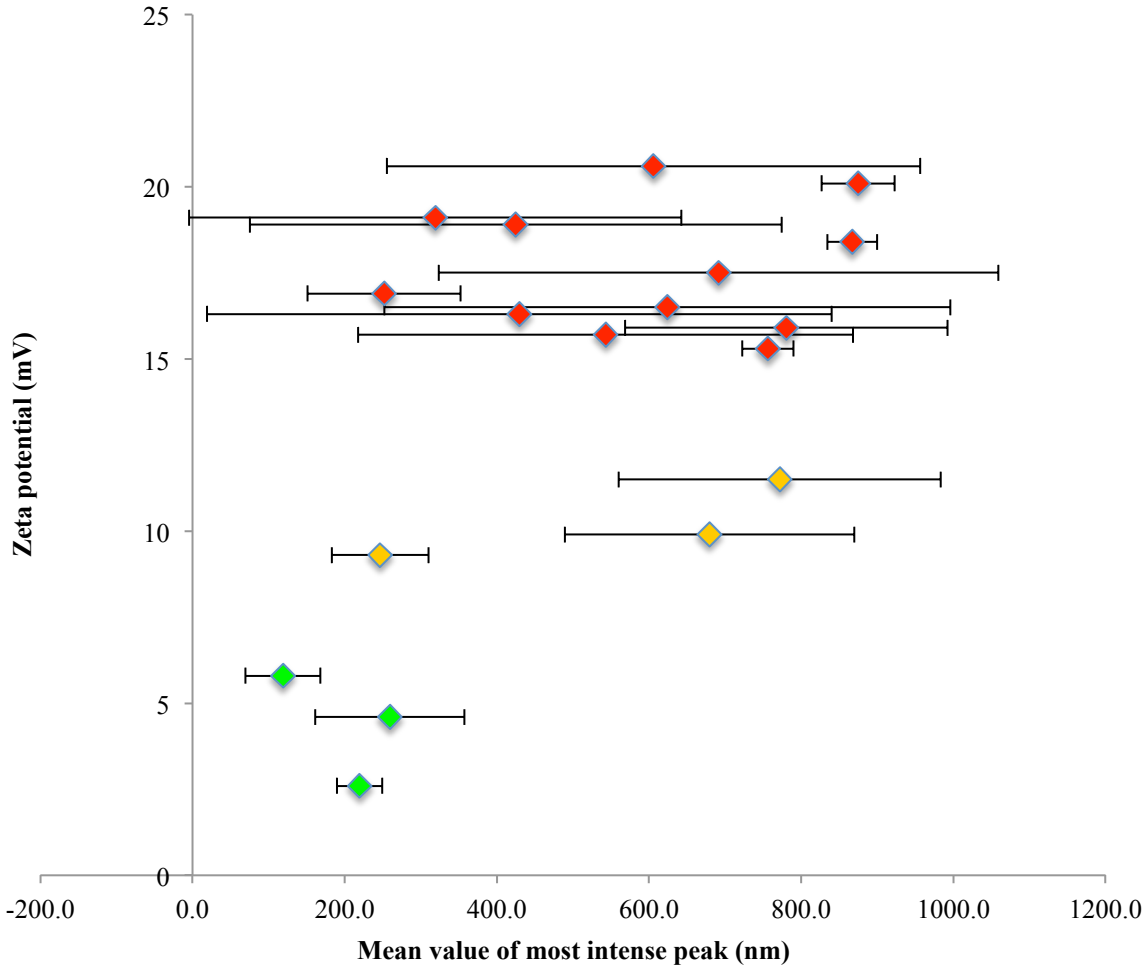

Appendix Figure 3. **Zeta potential of empty NPs.**

The green colour refers to NPs with chitosan lipid ratio of 1:20 (w/w), the yellow the chitosan lipid ratio of 1:10 (w/w) and the red the chitosan lipid ratio of 1:5 (w/w).

Appendix II

The limitation of the size determination and the absence of peaks was greater with the empty NPs, but to be able to compare the empty NPs and the NCE-containing NPs it is preferable to present them both in a similar manner. Considering **Appendix Table 3** the values are closer to the cumulative percentage displayed in **Table 6** than the values for the empty NPs and when viewing **Appendix Figure 4** the standard deviations are smaller. The residual (**Appendix Table 4**) is also smaller indicating less aggregation in these samples. It seems that the samples prepared with a 1:20 (w/w) chitosan lipid ratio deviate more from expected frequency due to a higher chi-square.

Appendix Table 3. Size distributions representing peaks of NCE-containing NPs (expressed as intensity) (n=3).

	Peak 1		Peak 2		Peak 3	
	Mean (nm)	Intensity (%)	Mean (nm)	Intensity (%)	Mean (nm)	Intensity (%)
1	162.5 ± 40.7	10.45 ± 3.25	811.8 ± 57.9	89.55 ± 3.22		
2	72.0 ± 19.8	8.88 ± 3.14	344.5 ± 28.2	91.12 ± 3.14		
3	66.1 ± 8.7	10.15 ± 5.35	300.0 ± 17.0	89.85 ± 5.35		
4	16.6 ± 5.5	6.26 ± 0.60	146.7 ± 8.4	71.54 ± 0.23	537.2*	22.21*
5	45.0 ± 10.1	6.58 ± 0.52	190.8*	30.13*	333.2 ± 13.4	63.28 ± 0.00
6	19.6*	0.23*	86.3 ± 25.6	8.98 ± 4.53	387.1 ± 49.4	90.79 ± 4.82
7	16.3 ± 4.9	0.82 ± 0.32	132.4 ± 26.3	20.10 ± 6.33	432.6 ± 37.9	79.08 ± 6.65
8	61.6 ± 12.6	7.48 ± 2.49	309.4 ± 70.4	76.53 ± 27.37	565.6*	17.24*
9	86.0 ± 23.2	7.48 ± 4.09	385.0 ± 48.8	92.52 ± 4.09		

* The peak did only appear in one of the cycles.

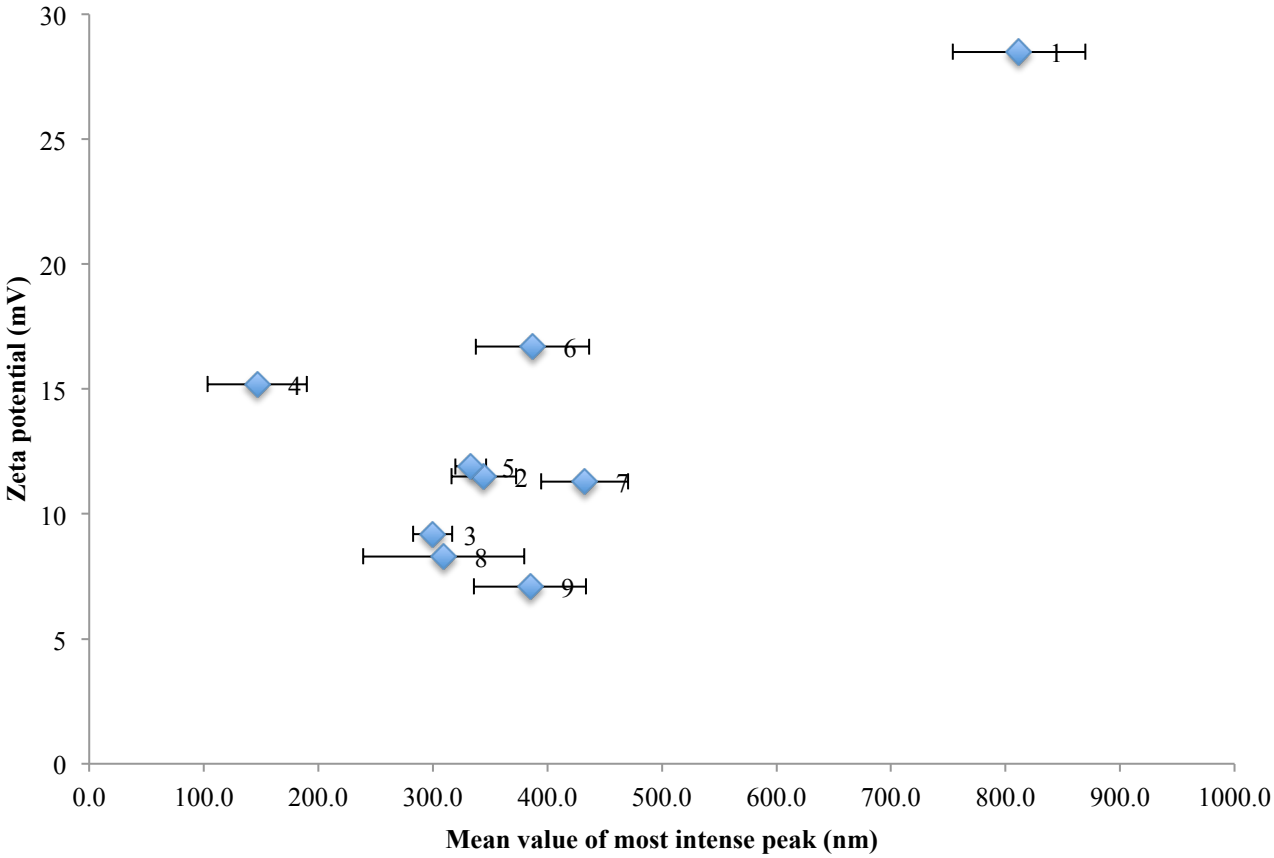

Appendix Figure 4. Zeta potential of NCE-containing NPs

The marks are presented with numbers according to the designation in **Appendix Table 3**.

Appendix Table 4. Other parameters for the size measurement of NCE-containing NPs. The values are presented as the mean of each of the groups. (1:20 n = 8)

Chitosan lipid ratio	Residual	Chi-square	Baseline adj.	Fit error
1:5*	21.844	108.37	0.00	2.732
1:20	7.424 ± 4.755	78.84 ± 15.71	0.00 ± 0.00	2.267 ± 0.623

* Only one NPs suspension